1972

Behavior of steel frames subjected to gravity load and reversed lateral load, Ph. D. dissertation, 1972

Lauren D. Carpenter

BEHAVIOR OF STEEL FRAMES SUBJECTED TO GRAVITY LOAD AND REVERSED LATERAL LOAD

by

Lauren D. Carpenter

A Dissertation

Presented to the Graduate Committee

of Lehigh University

in candidacy for the Degree of

Doctor of Philosophy

in

Civil Engineering

Lehigh University

1972

Approved and recommended for acceptance as a dissertation in partial fulfillment of the requirements for the degree of Doctor of Philosophy.

Dec 30 1971
(date)

Le-Wu Lu, Professor in Charge

Accepted May 23, 1972
(date)

Special committee directing
the doctoral work of
Mr. Lauren D. Carpenter.

George C. Driscoll Jr.
Prof. George C. Driscoll, Jr.
Chairman

Prof. Le-Wu Lu, Thesis Advisor

George C.M. Sih
Prof. George C.M. Sih, Member

Ben T. Yen
Prof. Ben T. Yen, Member

David A. VanHorn
Prof. David A. VanHorn,
Ex-Officio

ACKNOWLEDGMENTS

The experimental portion of this study is a part of the research project on "Behavior of Steel Frames Subjected to Repeated Loading" sponsored by the American Iron and Steel Institute. Technical guidance is provided by a special Task Force organized by the Institute whose membership includes: I. M. Viest (Chairman), G. V. Berg, H. J. Degenkolb, G. C. Driscoll, Jr., T. V. Galambos, C. W. Pinkham, E. P. Popov, and J. L. Stratta. The writer gratefully acknowledges the support given by the Institute and the advice received from the members of the Task Force.

The experimental work was conducted at the Fritz Engineering Laboratory which is directed by Professor Lynn S. Beedle. The academic guidance of the members of the faculty of the Department of Civil Engineering which is chaired by Professor David A. VanHorn is appreciatively acknowledged. The assistance of Dr. Fazlur R. Khan, Partner and Chief Structural Engineer of Skidmore, Owings and Merrill in making computer time available for the theoretical work is gratefully acknowledged.

The author acknowledges the guidance of the members of the special committee who directed his doctoral work and in particular Professor Le-Wu Lu under whose guidance the work leading to this dissertation was developed.

Appreciation is also extended to the author's many associates at Fritz Laboratory for their day and night assistance during the many

phases of the experiments. Particular long term assistance was provided by Basil Kattula, Richard A. Schmidt, and Robert J. Kirchberger in the data reduction and experimental portions of the study. The assistance of Mr. Kenneth R. Harpel and the technicians in the preparations for and carrying out of the experiments, and Mr. Richard Sopko for photographically recording the various portions of the experiments and the results generated, is gratefully acknowledged. The final typing of the dissertation was performed by Ms. Karen Philbin and the tracing of the figures was done by Mr. Jack Gera and Ms. Sharon Balogh.

TABLE OF CONTENTS

TABLE OF CONTENTS (Cont'd)

TABLE OF CONTENTS (Cont'd)

LIST OF TABLE

LIST OF FIGURES

LIST OF FIGURES (Cont'd)

LIST OF FIGURES (Cont'd)

ABSTRACT

An analytical method was presented to determine the behavior of single-bay, low multi-story frames subjected to combined gravity and lateral loads. The types of analysis that are performed by using this method are:

(a) Second-order elastic analysis of frames subjected to gravity and/or monotonic lateral load.

(b) Second-order elastic-perfectly plastic analysis of frames subjected to gravity and monotonic lateral load.

(c) Second-order elastic-perfectly plastic analysis of frames subjected to reversed and repeated cycles of lateral load (or displacement) with constant gravity loads applied to the beams.

(d) Second-order elastic analysis of frames subjected to monotonic loading with the beam represented by a series of segments. Each segment has moment versus curvature characteristics in a Ramberg-Osgood type formulation. The column behavior is elastic-perfectly plastic.

(e) Second-order elastic-plastic analysis of frames subjected to reversed and repeated cycles of lateral loading (or displacement) with constant gravity loads. The beam and column behavior is as presented in item (d).

The effects of the various parameters utilized in the Ramberg-Osgood formulation were examined for the sensitivity on the calculated results. Variations in the significant increment and control parameters

in the numerical solution were also observed. The effects of the finite size of the beam-to-column intersection on the calculated results were evaluated.

A portion of an experimental investigation during which three full-scale multi-story frame assemblages were subjected to constant gravity loads and reversed and repeated cycles of lateral load or displacement was presented. The significant results of the tests were summarized.

The effects on the experimental behavior of a frame with a non-compact beam with $b/t = 21$ were evaluated. In addition the effects of having the beam web welded or bolted to the column flange were evaluated during the tests. Portions of one test indicated the effect of having shear stiffening in the panel zones present or absent.

The experimental behavior of the frames was compared to:

(a) The original design for the frames

(b) The second-order elastic-perfectly plastic behavior during monotonically increasing lateral loading.

(c) The second-order elastic-perfectly plastic analysis during reversed and repeated lateral loading.

(d) The second-order elastic-plastic behavior with the beam represented by the Ramberg-Osgood function during reversed and repeated lateral loading.

Some design implications of the experimental and analytical evaluations and areas for continuing research which are generic to the reversed loading problem were described.

1. INTRODUCTION

The design of buildings in areas of high seismic activity is based on past experience of concerned designers. The current code provisions[1] tacitly assume inelastic behavior of the building's frames and non-structural components. The values of story shear based on an elastic analysis of a building frame subjected to earthquake motions indicate larger shear forces than the shears in the frame resulting from the aseismic code lateral forces. Various damping percentages have been utilized to bring the elastic analysis into closer agreement with the behavior of actual buildings subjected to earthquakes. However, older structures are considerably more rigid than just their steel framing would indicate due to a large amount of masonry used in the construction. Due to cracking of the large quantity of masonry walls, considerable dissipation of the energy imparted to the building by an earthquake is possible. In newer steel framed construction the energy dissipation is due primarily to the inelastic behavior of the steel framing during severe earthquakes.

Therefore, designers in seismic areas of modern steel framed structures must be able to estimate the capacity of the building frame to resist the effects of the seismic disturbance.

The following chapters describe analytical techniques for evaluating the behavior of steel frames subjected to gravity loads and reversed and repeated lateral loads. The design of steel frames subjected to aseismic code lateral forces, the behavior and strength of the

frames subjected to gravity loads and monotonically increasing lateral loads, and the results of a series of laboratory experiments on full size frames under constant gravity loads and simulated lateral earthquake forces are described. The later chapters compare the analytical and experimental behavior of the frames, and describe some design implications as well as indicating areas for continuing research.

1.1 Dynamic Versus Static Response

Dynamic analyses of multi-story steel buildings are performed to evaluate the behavior of buildings for:

1. Comfort of the inhabitants of the building during frequently occurring winds or earthquake shocks of relatively small magnitude.
2. Bending moment and axial force distributions in the building's frames subjected to conditions for use with the "allowable stress" provisions of Part 1 of the AISC Specification for the buildings subjected to mean design wind plus gusts, or design earthquakes.
3. Maximum strength of the building's frames subjected to various types of assumed inelastic conditions existing throughout the frames when the building is subjected to overloading (for example, when earthquakes exceed the design earthquakes).

Normally items 1 and 2 above require selection of a basic set of damping mechanisms in the building. The damping is a function of the assumed structural representation of the building and the commensurate degree of analytical sophistication. The damping is represented typically

in elastic cases as a percentage of the critical damping of the first mode of vibration (for example, by interfloor dash pots in a shear building model).

When the building is subjected to moderate to severe conditions as implied in item 3 above, a similar percentage of critical damping is assumed to exist in the structural representation of the building to govern the response when the amplitudes are small and elastic. When the amplitudes are large the inelastic behavior of the building's components are assumed to govern the response by absorbing the energy imparted to the structure.[2] This inelastic behavior could be initiated also by heavy winds or aeroelastic instability as well as moderate to severe earthquakes. In either case the lateral loads must be considered in in combination with gravity loads. The dynamic analysis remains essentially the same for all cases once the loading function has been suitably defined. Therefore, the essential elements in the analyses are the dynamic lateral load versus deformation characteristics of the building since lateral motions are predominant.

Preliminary experimental load versus deflection hysteresis loops obtained from static and dynamic tests on simple specimens have nearly duplicate shapes.[3,4] In addition, the effects of strain rate in structural steel are considered to be small during earthquake loadings.[5] Therefore, a small increase in yield stress of the steel could be used to account for the dynamic effects.[6]

In conclusion, the static load versus deformation characteristics of the structural elements and of the structure subjected to combined

lateral and gravity loads are the basic information necessary to perform the dynamic analyses.

1.2 Previous Research

The following articles review the previous experimental and theoretical research on the behavior of members and frames subjected to reversed lateral loads.

1.2.1 Experimental Behavior of Steel Members and Frames

Steel members in building frames may be subjected to repeated loading of large magnitudes such that inelastic strains occur at various times during the loading history. For example, due to the vibration of a building caused by the ground motions of an earthquake, several excursions into the inelastic range have been analytically predicted to occur in members of the frame.[7]

Test results show that, as a material experiences reversed inelastic strains, hysteresis loops of characteristic load versus deformation parameters develop during each cycle.[8,9] The area enclosed by the hysteresis loop is a measure of the energy dissipated by the specimen. The characteristics of the hysteresis loops obtained for individual members can be utilized to determine the energy dissipated by an entire structure which is then compared to the energy imparted to the structure by the actions of the external loading.

A considerable number of tests have been performed on structural components and simple structures subjected to repeated and reversed loads.[10] These studies have resulted in a better understanding of the

response of structural members and frames subjected to reversed and repeated loadings.

In one series of tests, cantilever beams were tested to study the basic behavior of these beams subjected to reversed loads.[11] Further studies in the series included welded and bolted beam-to-column connections for moment and shear typical of building connections used in earthquake resistant design subjected to similar loadings.[12,13,14,15,16] These cantilever beam tests showed a remarable stability of the hysteresis loops for very high strain amplitudes. Significant local buckling did not signal immediate loss of capacity for these beams which had "compact" flanges and relatively close bracing spacing. Low cycle fatigue and attention to welding details were indicated as necessary design parameters since most of the tests were terminated by fractures. Other recent cantilever beam tests have indicated a proper lateral bracing spacing is required to ensure stable hysteretic behavior of the beam.[17] Since both the moment versus curvature and the load versus deflection hysteresis loops have remarkably stable shapes, the cantilever beam test results imply that a practically constant amount of energy dissipation per cycle can be depended upon at each level of strain.[18,19,20] The test results also show that the areas enclosed by the hysteresis loops increased with increasing load magnitude.[13] Similar behavior has been exhibited during reversed bending tests of different types of beams.[21,22,23]

Beam-columns bent in double and single curvature have been tested subjected to constant axial loads and alternating end moments.[24,25] More comprehensive experiments including interaction of beams subjected

to repeated and reversed loading with axially loaded columns have been carried out[26,27] and several reversed load tests of model frames and small frames with wide flange cross sections have been reported.[28,29,30,31] The results of these tests showed that for columns with small and nearly constant axial loads stable hysteretic behavior is generated.

As an adjunct to tests of multi-story frames designed to study the static behavior of the frames subjected to monotonic lateral load applications, these full scale frames were subjected to reversed loading after very large inelastic deformations had occurred due to the initial loading.[32,33,34] These tests were all terminated after one or two cycles and gave an indication of the possible lateral load carrying capacity of the full scale frames subjected to reversed loading. Approximate analysis using an elastic and perfectly plastic moment versus curvature relationship was carried out for some of these frames, but no satisfactory agreement between the analytical and test results was found.

1.2.2 Moment Versus Curvature Relationships

The tests described in Article 1.2.1 exhibited a curvilinear response to the applied loading whereas the predictions for the test results were usually based on linear or bilinear approximations. For all of these test conditions better agreement could have resulted if a curvilinear moment versus curvature relationship had been used for analytical comparisons. Most analytical methods are concerned with the behavior of steel frames subjected to proportional or monotonically increasing loadings rather than reversed loadings. Reasonably good agreement with test results was observed by employing in the analysis an

elastic and perfectly plastic moment versus curvature relationship for the cross section. However, these analyses are concerned only with the first loading of the member cross sections.[35, 36,37] The "rounding" near the knee in the moment versus curvature relationship is found to have small effect and it is satisfactory to assume that the shape factor of the cross section is equal to unity in the analysis.

The previous experimental results show a marked "rounding" at the knee especially during reversed loading. This pronounced rounding during reversed loading is due, in part, to the Bauschinger effect in the material.[38] Therefore, the most appropriate moment versus curvature relationship to be used to analyze frames subjected to reversed loading is a curvilinear one.[39]

The results mentioned for the cantilever beam tests given in Article 1.2.1 may be used as being typical of the moment versus curvature curves of steel members subjected to reversed bending. The cantilever beam test represents a situation of high moment gradient and therefore only a short length of the beam is yielded which corresponds to the conditions existing at a concentrated plastic hinge or yielded zone. Therefore, care should be exercised before applying these results to a uniform moment zone.

Simple analytical techniques can be used to compute the moment versus curvature characteristics by integration across the cross section of an inelastic member including the residual stresses. Any number of representations of the stress versus strain curve for the material could be pieced together including a digital representation of the actual stress versus strain curve. However, a simple representation of the

initial stress (σ) versus strain (ε) curve can be used which was presented originally by Ramberg and Osgood as

$$\varepsilon = \frac{\sigma}{E} + K \left(\frac{\sigma}{E}\right)^{n}, \text{ for } \sigma > 0, \tag{1.1}$$

where K, E and n are determined experimentally.[40] Optionally, the analysis could utilize a bilinear elastic and perfectly plastic[41] or a trilinear elastic and perfectly plastic with strain hardening relationship[33] to define the stress versus strain behavior. The integration can be performed on a given section in a piecewise manner. The resulting moment (M) versus curvature (ϕ) curve would be similar in shape to the stress versus strain curve and may be represented by

$$\phi = M \frac{\phi_y}{M_y} \left(1 + \alpha \left(\frac{M}{M_y}\right)^{R-1}\right), \text{for } M > 0, \tag{1.2}$$

where ϕ_y is a characteristic positive curvature, M_y a characteristic positive moment, α an appropriate positive factor, and R is an appropriate positive exponent. The particular values of ϕ_y, M_y, α and R can be determined by a least square fitting of the integrated moment versus curvature relationship.

Several optional forms of equations similar to Eq. 1.2 and equations derived from fatigue considerations have been utilized by Tanabashi, et al,[42] Davidenkov,[43] Jennings,[44] Berg,[7] Kaldjian,[38] Goel[45] and Popov.[19] The Ramberg-Osgood type of function represented above with $\alpha = 1.0$ has been used analytically to define the moment versus curvature relationship for a wide-range of steel beams and typical values of the parameters of the stress versus strain and moment versus curvature functions.[38]

Analytical work has indicated that the longitudinal strains may not vary linearly from the neutral axis of a steel beam of wide flange cross section for all conditions of plasticity of the cross section.[32] Such non-linear strain behavior leads to a non-linear moment versus curvature relationship.

The cyclic stress versus strain behavior of small axially loaded pieces of steel has been investigated for the usual purpose of studying the fatigue characteristics of the material rather than the basic load carrying properties of the materials. Benham and Ford[9] and Tavernelli and Coffin[46] considering the fatigue aspects alone are primarily concerned with relating the stress versus plastic strain results to fatigue behavior. Although fatigue behavior is recognized as a possible governing factor in the overall behavior of the frames, emphasis should be placed on the load versus deformation behavior of the frames subjected to alternating loads. These loadings in no way imply equal amplitude strain cycling throughout each "fiber" of each cross section of the members of the frame. In fact only in the simplified experiments by Popov,[11-16] Tanabashi, et al,[42] Kurobane,[47] Chipman,[48] and Sherbourne, et al[21,22] were the strains alternating at approximately equal amplitudes throughout the various portions of the tests. However, the value of such tests and correlations cannot be overlooked since the basic shape and characteristic parameters obtained determine the basic stress versus strain behavior during reversed loading from which the required moment versus curvature relationship can be derived. Similar to the comparison given earlier in this article for

monotonic loading conditions, the basic moment versus curvature relationships can be derived for reversed loading situations.

The essential observation to be made from inspection of these tests is that a similar type of hysteresis loop is generated for a rolled steel member in bending as for a short specimen subjected alternately to tensile and compressive loading or straining.(11)

The Ramberg-Osgood function has been used analytically to define the moment versus curvature relationship for a wide range of steel beams and typical values of the exponential factor.(38) However, extensive experiments have not yet been performed to establish the values of the factors and their variations associated with this function for the structural steels.

1.2.3 Predictions of Behavior of Simple Frames

Even though nonlinearities are generally expected, researchers and designers have concentrated on the linear and bilinear approaches to the earthquake problem. The linear and bilinear approaches are quite justified from the points of view of computational convenience and since basic test data are limited to monotonic response. Bilinear analyses may include a linear strain hardening modulus for the second slope. Strain hardening can also be considered by having two beams of different stiffnesses in parallel between each pair of joints in the frame.(49)

The curvilinear representations become more feasible for fast large-frame computational equipment wherein a moment versus curvature relationship or a moment versus rotation relationship is linearized over appropriately small increments. Although the Ramberg-Osgood function

has been used in a multi-story frame dynamic analysis program,[45] the structure and loading have been simplified to one half of a single bay "equivalent" frame having gravity loads only at the joints. Experimental results have shown a significant influence of gravity moments in the beams on the behavior of the frame subjected to reversed loading.[50,51] The effects of the additional moments, known as the PΔ moments, caused by the gravity loads acting through the sway displacement have also been shown to be significant to define properly the actual behavior of frames.[52]

Therefore, an appropriate analytical technique to study the behavior of frames subjected to gravity loads and reversed lateral loading should include a curvilinear moment versus curvature relationship, the effects of gravity loads on the beam, and the additional PΔ moments.

1.3 Scope of the Investigation

An analytical technique will be described in Chapters 2 and 3 which will utilize the Ramberg-Osgood functional relationship to represent the moment versus curvature relationship for the beams. The method includes the effect of gravity loads on the beam, the PΔ effects and axial load effects on the strength and stiffness of the columns. The technique generally is an elastic and perfectly plastic analysis of steel frames subjected to gravity loads and reversed lateral loads with options to specify beams having an elastic and perfectly plastic or a Ramberg-Osgood moment versus curvature relationship.

In the experimental portion of the current investigation,

several full scale frames have been designed and tested to study in particular the behavior of steel frames subjected to constant gravity loads and cyclic lateral displacements of the top of the frame.[50,51] The design and the experimental behavior of three of these frames will be examined in Chapters 4 and 5.

Comparisons between analytical and experimental results for the frames will be described in Chapter 6. Several design implications for frames subjected to reversed loadings based on the analytical and experimental results are discussed in Chapter 7. Chapter 8 indicates areas of research which are generic to the problem and should be the subjects of continuing research and development.

2. PREDICTIONS OF BEHAVIOR OF NON-SYMMETRIC RAMBERG-OSGOOD BEAMS

2.1 Introduction

The most complete inelastic response computations reported in the literature[45] for the general behavior of multi-story buildings subjected to gravity loads plus the earthquake motions of the base of the structure were performed with the gravity loads concentrated at the joints of the structure. Since the completely symmetrical single-bay frame was used, the end moment versus end rotation relationships were the same at both ends of the beams. However, the gravity loads should be more realistically placed on the beams rather than at the joints.

Therefore, for the more general case the initial gravity moments when combined with the moments developed during the earthquake motion result in the end moment versus end rotation behavior of each end of the beam being different. The term "non-symmetric" will be used to denote this more general case.

The term "Ramberg-Osgood" will be used to denote the type of nonlinear moment versus curvature behavior which is assumed to exist at each cross section of the beam. The formulation of the particular Ramberg-Osgood function parameters may vary, but those used in this investigation represent typical values for the frame geometries and member sizes selected for the correlative experimental study. In general, the complete nonlinear inelastic frame analysis technique as developed may be

altered for other parameters. In addition, other functional representations of the moment versus curvature relationships may be incorporated in the analysis by small variations in a computational subroutine.

The following articles will describe the basic nonsymmetric Ramberg-Osgood relationship and illustrate the end moment versus end rotation behavior of the beam with and without gravity loads on the beams.

2.2 The Non-Symmetric Ramberg-Osgood Beam

2.2.1 Basic Definitions

The basic Ramberg-Osgood beam is defined as a beam where the relationship between the moment and curvature existing at every cross section in the beam is represented by a suitably defined Ramberg-Osgood type functional relation as described in Chapter 1. Therefore, the curvature ϕ_{xi} at the point a distance x_i along the beam as a function of the moment M_{xi} at the cross section can be represented by

$$\phi_{xi} = \frac{\phi_y}{M_y} M_{xi} \left(1 + \alpha \left(\frac{M_{xi}}{M_y}\right)^{R-1}\right), \text{ for } M_{xi} > 0 \qquad (2.1)$$

where ϕ_y, M_y, α and R are defined as for Eq. 1.2.

The combination of the four characteristic parameters ϕ_y, M_y, α and R may be determined by a least square curve fitting of experimental moment versus curvature curves based on simple conditions of restraint, cross-section geometry or lateral support. Alternatively, these basic constants can be evaluated from an analytical or a numerical integration of a cross section's individual fibers during a given loading. With a significant increase in computational effort, the appropriate stress

versus strain parameters may be used directly in the analysis of the frame.(41)

From the basic stress versus strain relationship given by

$$\epsilon = \frac{\sigma}{E} + K \left(\frac{\sigma}{E}\right)^n, \text{ for } \sigma > 0, \tag{1.1}$$

and since $E = \sigma_y/\epsilon_y$,

$$\frac{\epsilon}{\epsilon_y} = \frac{\sigma}{\sigma_y} \left(1 + K\, \epsilon_y^{n-1} \left(\frac{\sigma}{\sigma_y}\right)^{n-1}\right), \text{ for } \sigma > 0, \tag{2.2}$$

For A36 steel, the value of ϵ_y is more likely to be determined from static yield level of the material and a typical value of the modulus of elasticity. For a typical three plate cross section without residual stresses, the latter equation can be integrated across the cross section to give a moment versus curvature expression. For example, assume that the web contribution is small and the area of each flange, A_f, is concentrated at a distance d/2 from the bending axis of the beam. Then the moment is given by

$$M = 2\, A_f \frac{d}{2}\, \sigma \quad \text{or conversely} \quad \sigma = \frac{M}{A_f d} \tag{2.3}$$

The corresponding curvature is

$$\phi = \epsilon\, \frac{2}{d} \tag{2.4}$$

which is subjected to the assumption that plane sections remain plane throughout the loading program. Therefore,

$$\phi = \frac{2}{d} \left[\frac{M}{A_f d} \frac{\epsilon_y}{\sigma_y} \left(1 + K\, \epsilon_y^{n-1} \left(\frac{M}{A_f d\, \sigma_y}\right)^{n-1}\right)\right], \text{for } M > 0 \tag{2.5}$$

Since $\sigma_y = M_y/A_f d$ and $\phi_y = \epsilon_y\, 2/d$, the equation reduces to

$$\phi = M \frac{\phi_y}{M_y} \left(1 + K \left(\frac{d\, \phi_y}{2}\right)^{n-1} \left(\frac{M}{M_y}\right)^{n-1}\right), \text{ for } M > 0 \tag{2.6}$$

Comparing Eq. 2.6 with Eq. 2.1, the value of the exponent n is the same as the exponent R. Similarly, the value of

$$\alpha = K \left(\frac{d}{2} \phi_y\right)^{n-1} \quad \text{or} \quad \alpha = K \left(\epsilon_y\right)^{R-1} \tag{2.7}$$

The purpose of the preceeding example was to indicate the significant similarities between the form of the representations of the stress versus strain curve and the moment versus curvature curve, Although the example was simplified from the expected behavior of actual members, the effects of residual stresses, axial loading, the contribution of the web, fatigue, and strain reversal can be accounted for by numerically integrating across the cross section for incremental curvatures.

For the case where

$$K \epsilon_y^{n-1} = 1.0, \tag{2.8}$$

or

$$\frac{\epsilon}{\epsilon_y} = \frac{\sigma}{\sigma_y} \left(1 + \left(\frac{\sigma}{\sigma_y}\right)^{n-1}\right), \text{ for } \sigma > 0, \tag{2.9}$$

representative values for use with the moment versus curvature relationship with $\alpha = 1.0$, or

$$\frac{\phi}{\phi_y} = \frac{M}{M_y} \left(1 + \left(\frac{M}{M_y}\right)^{R-1}\right), \text{ for } M > 0, \tag{2.10}$$

have been computed for a wide range of typical beam sections.[38]

Therefore for beams a simple integration can be performed as desired for any assumed (or actual) residual strain or stress distribution for various values of monotonically increasing curvatures in order to evaluate the corresponding moments.

Therefore in the subsequent discussion, the characteristic parameters will have the following definitions unless noted otherwise. The characteristic moment, M_y, is the value of moment at the cross section at first yielding in an initially unstressed bending member. This moment is assumed to be applied to a section symmetric about the bending axis such that the value is the same for both directions of applied moment. Similarly, the characteristic curvature, ϕ_y, is the value of curvature which corresponds to M_y. The values of the exponent, R and the coefficient α can be selected based on a best fit of an experimental stress versus strain curve (to find K and n) and the numerical evaluation of a given loading program at the cross section. However, Jennings,[44] Popov,[19] Berg,[7] and Goel[45] have utilized the fully plastic load capacity instead of the load at first yield. Kaldjian's analytical study[38] using a Ramberg-Osgood stress versus strain relationship produced least squares determinations of R for $\alpha = 1.0$ by utilizing values of ϕ_y and M_y between the first yield and fully plastic values as a function of the ductility ratio. In addition, Al Muti studied[4] the behavior of beams utilizing an elastic and perfectly plastic stress versus strain relationship with strain hardening. Al Muti concluded that the resulting deformations computed should be increased by 20 percent for better correlation with his experimental results. The effects of variations in the above Ramberg-Osgood parameters on the behavior of frames subjected to reversed loading will be delineated further in Chapter 3 and compared to the experiments in the current investigation in Chapter 6.

Two most significant and related questions now arise. What are the values of K and n appropriate to the conditions under study here?

And, what is an appropraite description of the hysteresis behavior during reversed and repeated loading?

First, for a monotonic condition, the values of K and n can be selected directly from the monotonic stress versus strain curve obtained in a tensile test. However, since the monotonic condition is not typical during even a simplified nonproportional loading of a frame first with gravity loads and then adding a monotonically increasing lateral load, a more general examination must be made.

Secondly, therefore, an appropriate question at this time is the basic formulation of the expression for ϕ during curvature reversals after the first monotonic curvature has been applied at a given cross section. Experimental evidence observed during cycling tests of small axially loaded specimens gives an indication of the basic hysteretic behavior.[53] The test series on cantilever beams and connections referred to in Chapter 1 gives experimental confirmation of the type of hysteretic behavior expected adjacent to a clamped cross section and at various beam-to-column moment connections. The curve which connects the tips of the various curves produced during equal amplitude curvature cycling has been denoted as the skeleton or locus curve or in the stress-strain sense, the cyclic stress-strain curve. Various investigators have shown that the hysteresis loop and skeleton curve can have the same formulation but varying by a factor of approximately 2 based on an original hypothesis by Masing.[53,54,46,42,19,7,8,9,38,43,44,45] Therefore, the general form of the hysteretic equation is:

$$\phi = \frac{\phi_y}{M_y}(M - M_o)\left[1 + \alpha\left(\frac{M - M_o}{2\,M_y}\right)^{R-1}\right] + \phi_o, \text{for } (M - M_o) > 0, \quad (2.11)$$

where M_o and ϕ_o are respectively the moment and curvature at the point of curvature reversal as shown in Fig. 2.1. Since the bracketed sum in the previous equation must be greater than one, a more general form is

$$\phi = \frac{\phi_y}{M_y} (M - M_o) \left[1 + \alpha \left| \frac{M - M_o}{2 M_y} \right|^{R-1} \right] + \phi_o \qquad (2.12)$$

where the vertical bars indicate an absolute value function. Similarly for both positive and negative moments the original curve given by Eq. 1.1 is more generally stated as

$$\phi = \frac{\phi_y}{M_y} M \left(1 + \alpha \left| \frac{M}{M_y} \right|^{R-1} \right) \qquad (2.13)$$

Since experimental evidence[42] and intuition support the possibility of α and R being different for the locus or skeleton curve as compared to the hysteretic curves, the numerical procedure permits the specification of two values of α and R. In addition, since the factor of 2 between the skeleton and hysteretic curves is only approximate, the value of α can be easily adjusted in the equation of the hysteresis loop.

The method of advancing therough a series of random curvature reversals is a procedure based on intuition and mathematical convenience.[7] The basic procedure which was used by Berg[7] and Goel[45] is outlined in the Appendix of Reference 45. The procedure is based on knowing the four following items at each cross section; namely,

1. M_o and ϕ_o which correspond to the most recent reversal or turning point.
2. M_{old} and ϕ_{old} which correspond to the beginning of the current curvature increment.

3. M_{new} and $\emptyset_{new}$ which correspond to the end of the current curvature increment, and

4. $\emptyset_{max}$ which corresponds to the maximum curvature already attained in either direction during the response.

The procedure presumes that when $\emptyset_{max}$ is exceeded the response follows the skeleton curve again to the next curvature reversal.

As in each case of theoretical determination of structural behavior using nonlinear behavioral characteristics in bending members, the basic moment versus curvature parameters are assumed to be unchanged during the analysis. The distinct possibilities of deteriorating overall member behavior caused by local or lateral, elastic or inelastic instability effects are also neglected. These comments are relative to the often tacit assumption of non-deteriorating hysteretic behavior of the member.

Therefore, the moment versus curvature behavior of the member is assumed to be representable by a Ramberg-Osgood function and the hysteretic behavior is assumed to be of the non-deteriorating type (i.e. adequate lateral bracing must be provided and sectional geometry must be such that local conditions as well as fatigue do not affect member behavior).

2.2.2 Sign Conventions

For purposes of relating moments and corresponding curves along the beam, positive moments and the corresponding positive curvatures are produced by moments causing compression stresses in the top portion of the beam member. For purposes of inserting such Ramberg-Osgood beams into a frame analysis program, the slope deflection method's sign

convention for end moments and rotations of the beam will be utilized (i.e. clockwise moments or rotations at the ends of the member are considered as positive).

2.2.3 Additional Assumptions

1. Since the basic problem to which the proposed analytical technique will be applied is one with constant gravity loads, the effects of vertical displacements of the ends of the beam member on its strength and stiffness will be neglected.
2. Any axial load effect on the moment versus curvature behavior of the beam has been considered negligible.
3. Any residual stresses (strains) due to cooling, welding or erection which are present at the beginning of the loadings are also considered negligible.

2.2.4 Basic Ramberg-Osgood Beam Behavior

Since the moment versus curvature representation of the beam behavior is curvilinear rather than bilinear (either elastic-perfectly plastic or elasto-plastic), the moment versus rotation relations at the ends of the beam are also curvilinear.

For a beam without gravity loads, the incremental horizontal load moment diagram (Fig. 2.2a) produces the corresponding incremental curvature distribution throughout the beam (Fig. 2.2b). The moment-versus rotation curves for the ends of the beam are shown schematically in Fig. 2.2c. For a beam with two symmetrically positioned equal constant gravity loads and then subjected to the incremental horizontal load moments, the initial curvature diagrams for gravity loads alone

would change as shown in Fig. 2.2d. The moment versus rotation relationships at the ends of the beam are similar to the curves shown in Fig. 2.2e.

To find the incremental stiffnesses of the beam, successive values of moments and the corresponding end rotations must be found for the member. The following two articles illustrate the evaluations required for a simplified case of the general Ramberg-Osgood functional relationship for a beam with and without concurrent lateral loads. The computations give the end rotations corresponding to a given set of end moments. During the incremental stiffness computations the current values of the angles will be computed before and after the stiffness moments are applied in turn at each end of the member.

2.3 Ramberg-Osgood Beam without Intermediate Lateral Loads

For example, for the beam shown in Fig 2.3 and letting α = 1.0 and R = N, an odd positive integer to simplify the integrations, the monotonic moment at any point i at a distance x_i along the beam is

$$M_{x_i} = M_A - V_A \, x_i \tag{2.14}$$

The curvature at point i is represented by

$$\phi_{x_i} = (M_A - V_A \, x_i) \left(\frac{\phi_y}{M_y}\right) \left[1 + \left(\frac{M_A - V_A \, x_i}{M_y}\right)^{N-1}\right] \tag{2.15}$$

where the basic curvature relationship is given by Eq. 2.1. The curvature relation can be reduced to the following form.

$$\phi_{x_i} = \frac{\phi_y}{M_y} (M_A - V_A \, x_i) + \frac{\phi_y}{M_y^N} (M_A - V_A \, x_i)^N \tag{2.16}$$

Two standard equations are available to evaluate the beam. The

first equation relates the slopes of tangents to the deformed shape of the beam along its length and the second equation relates displacements of the beam relative to a tangent placed at one point on the beam. The first equation is

$$- \theta_A + \int_o^L \phi_{xi} \, dx_i = \theta_B \tag{2.17}$$

Inserting ϕ_{xi} from Eq. 2.16 gives

$$-\theta_A + \frac{\theta_y}{M_y} \int_o^L (M_A - V_A x_i) \, dx_i + \frac{\theta_y}{M_y^N} \int_o^L (M_A - V_A x_i)^N \, dx_i = \theta_B \tag{2.18}$$

which, when integrated, gives the following equation

$$- \theta_A + \frac{\theta_y}{M_y} \left(M_A L - \frac{V_A L^2}{2}\right)$$

$$- \frac{\theta_y}{M_y^N} \left[\frac{1}{V_A (N+1)}\right] \left[(M_A - V_A L)^{N+1} - M_A^{N+1}\right] = \theta_B \tag{2.19}$$

The second equation is

$$- \theta_A L + \int_o^L \phi_{xi} (L - x_i) \, dx_i = 0 \tag{2.20}$$

After inserting and integrating, the equation reduces to the following:

$$- \theta_A L + \frac{\theta_y}{M_y} \left(L^2 \frac{M_A}{2} - \frac{V_A L^3}{6}\right) + \frac{\phi_y}{M_y^N} \left\{\frac{L}{-V_A} \left[\frac{(M_A - V_A L)^{N+1} - M_A^{N+1}}{N+1}\right]\right.$$

$$\left. - \left(\frac{L}{-V_A}\right) \left(\frac{M_A - V_A L}{N+1}\right)^{N+1} + \left(\frac{1}{-V_A}\right)^2 \frac{1}{(N+1)(N+2)} \left[(M_A - V_A L)^{N+2} - M_A^{N+2}\right]\right\} = 0 \tag{2.21}$$

The solution for the end rotations which correspond to the given end moments follows by solving for θ_A from the second equation and then finding θ_B from the first equation.

2.4 Ramberg-Osgood Beam with Two Intermediate Lateral Loads

Similarly, for the beam with lateral loads (the loads may be of unequal magnitude) as shown in Fig. 2.4, the moments for each of the three segments of the beam are as follows:

$$M_{x_{1i}} = M_A - V_A x_{1i} \qquad 0 < x_{1i} < L_1 \qquad (2.22)$$

$$M_{x_{2i}} = (M_A - V_A L_1) - (V_A + P_L) x_{2i} \qquad 0 < x_{2i} < L_2 \qquad (2.23)$$

$$M_{x_{3i}} = [M_A - V_A(L_1+L_2) - P_L L_2] - (V_A+P_L+P_R) x_{3i} \qquad 0 < x_{3i} < L_3 \qquad (2.24)$$

In a similar way to the case without intermediate loads, the moment versus rotation behavior of the ends of the beam can be found for the case with loads on the beams by evaluating three integrals for each of the following two equations.

$$\theta_A = \int_o^L \theta_{x_i} \, dx_i - \theta_B = \int_o^{L_1} \phi_{x_{1i}} \, dx_{1i} + \int_o^{L_2} \phi_{x_{2i}} \, dx_{2i} + \int_o^{L_3} \phi_{x_{3i}} \, dx_{3i} - \theta_B \qquad (2.25)$$

$$\theta_A L = \int_o^{L_1} \phi_{x_{1i}} (L - x_{1i}) \, dx_{1i} + \int_o^{L_2} \phi_{x_{2i}} (L - x_{2i}) \, dx_{2i} + \int_o^{L_3} \phi_{x_{3i}} (L - x_{3i}) \, dx_{3i} \qquad (2.26)$$

These two equations can be solved for the end rotations corresponding to given moments by first solving for θ_A from the second equation and then substituting into the first equation and solving for θ_B. However, to evaluate the Eqs. 2.25 and 2.26, the effects of gravity loads alone can be added to the effects of the additional end moments as

a two-step loading. The gravity portion utilizes Eq. 2.13 since the initial moments and curvatures are zero throughout the beam. The added end moments portion (which may be due to lateral loading of the overall frame) utilizes Eq. 2.12 since the initial moments and curvatures are not zero throughout the beam when the additional end moments are added.

2.5 Numerical Evaluation of Moment Versus Rotation Relationships

Since computers are available to perform accurate repetitive calculations, the previous derivations need not actually be performed for each condition occurring during the loading history. The alternative is a segmental approach wherein the beam is considered as a lumped flexibility model as shown in Fig. 2.5. The two basic equations then may be replaced by the following summations which are equivalent in the limit. The two equations are:

$$- \theta_A + \sum_{i=1}^{N} \phi_{x_i} \Delta_{x_i} = \theta_B \tag{2.27}$$

and

$$- \theta_A L + \sum_{i=1}^{N} \phi_{x_i} (L - x_i) \Delta_{x_i} = 0 \tag{2.28}$$

With the numerical formulation, the curvature ϕ_{x_i} at the points x_i can be computed directly for the corresponding moment at the point for fractional values of the exponent R and the coefficient α. The numerical formulation also does not necessarily require a single moment curvature relationship but permits a piecewise definition or actual experimental curves suitably defined by closely spaced points.

Utilizing larger computing facilities the stress versus strain history can be kept incrementally for a suitable number of elements at

each cross section from which the current moment versus curvature can be derived. However, for the purposes of the current method of calculation, the moment versus curvature relationships are defined or refined prior to execution of the program by using a separate smaller program which computes moment versus curvature relationships including residual stresses.

Therefore, for a given beam having initial values of moment and curvature at each point x_i, the end rotations of the beam after incremental changes in the end moments can be computed. During the numerical evaluation of the frame, the stiffnesses of the beams are computed for an increment by fixing alternately one end of the beam against further rotation and applying a moment to the other end. After the gravity loads have been applied, the stiffnesses of the beam for an increment of moment on the left end of the beam produces a different curvature diagram than the diagram for moment applied on the right end of the beam. In a portion near the center of the beam the curvatures found during the stiffness computations at each nodal point do not always correspond in sign with the curvature for the total horizontal load moments. Fortunately, for a large portion of the beam the incremental moments and corresponding curvatures used during the two stiffness computations are of the same sign as the incremental moments and curvatures for the increment of horizontal load moments.

However, to evaluate this problem, an alternate procedure was formulated. The anticipated moments for the increment are computed. Incremental stiffnesses of each segment are computed as a ratio of the anticipated increment of moment to the corresponding increment of curvature.

The corresponding beam stiffnesses are computed using these ratios. After the complete results for the frame for the increment have been computed, the anticipated incremental moments are checked against the final incremental moments. Both methods compare closely for the sizes of the increments used.

In summary, during the numerical evaluation of the beam member's stiffness and strength, the beam is assumed to be adequately represented by individual segments whose moment versus curvature characteristics can be represented by suitable Ramberg-Osgood type functions. This representation is basically a lumped flexibility approach with idealized rigid links between the points of flexibility. During the numerical evaluation, the resulting member stiffnesses are assumed to be linearized during each suitable sized increment of moment.

3. PREDICTIONS OF BEHAVIOR OF FRAMES

3.1 Second-Order Elastic-Perfectly Plastic Analysis of Frames Subjected to Gravity and Monotonic Lateral Loads

Basic elastic-plastic analyses have been performed to determine the deflections of frames under the assumptions of simple plastic theory.[10] Second-order elastic-plastic analysis has been used to obtain a better estimate of the maximum load and general load deflection behavior of frames subjected to proportional or monotonic loading conditions.[32,37,38,39] The second-order analysis includes the additional moments existing in the frame due to the gravity loads acting at the sway displacement of the frame. This analysis may also include the effects of axial load on the strength and stiffness of the members of the frame, particularly, the columns. The analysis may also account partially or fully for the differential vertical movement of the ends of the beam members due to differential axial deformations of the ends of the adjoining columns. The effects of residual stresses and strain hardening have also been included in an approximate manner.[33]

Although the basic procedure of analysis has been thoroughly explained in the literature cited above, the following assumptions should be noted with respect to this type of analysis.

Since an elastic-perfectly plastic stress-strain curve and a shape factor of unity are typically assumed and strain hardening is

usually not considered, the moment-curvature diagram is also elastic-perfectly plastic. In addition, the yielding is assumed concentrated at the cross section of the plastic hinge.

Within the current plastic design techniques, failure in the panel zone of the connection is assumed to be prevented. Therefore, the ultimate load behavior of the frame is controlled by the behavior of the members outside of the connected zone. However, the checks against the plastic moment being reached or not, and stiffnesses are computed based on member centerlines and member properties. In addition, the panel zone and the connections are assumed to be rigid in the respect that no relative rotation of the ends of connected members occurs.

Member behavior is restricted to exclude lateral or lateral-torsional buckling or excessive deformations in the planar mode. Also the cross sectional shape of the members is assumed to remain unaltered throughout the various deformations applied to the planar member.

The vertical displacement of the joints of the frames are assumed negligible. This assumption has been examined in considerable detail by Parikh[37] and Korn.[39] Their studies show that proper maximum strength analyses of larger and taller building frames should include the effects of axial deformations. However, for the frames studied in the experimental portion of the current investigation, the maximum differential settlement of the columns produced less than one kip per square inch of bending stress in the beams. This maximum settlement was produced when the maximum second-order elastic-plastic lateral load was applied to the frame which was analytically constrained

to remain elastic.

The effects of the finite size of the panel zone at the beam-to-column intersection have not been included in previous analyses. However, the effective center of rotation of the plastic hinges occurring at the ends of the members may extend a distance D or D/2 from the face of the adjoining member. The shift of the plastic hinge locations tends to alter the stiffness and strength of the frames.[32] Furthermore, finite size of the panel zone reduces the effective lengths of the members with a resulting increase in the effective stiffnesses of the members. For example, the combined effects can be observed in Fig. 3.1 where the elastic-plastic and Ramberg-Osgood behavior with the end portions of the beam remaining several times as stiff as the basic elastic beam throughout the beam's inelastic behavior are shown. Therefore, the conditions assumed at the beam-to-column intersection have a significant influence on the load-deflection behavior.

3.2 Second-Order Elastic-Plastic Analysis of Frames Subjected to Reversed Loading

The basis for the analysis of the frame subjected to reversed loading is incremental second-order elastic-plastic analysis of the frame subjected to monotonic increments of applied lateral load. At each step of the analysis an increment of lateral load may be applied in either direction to follow a given loading or displacement program.

Since the effect of the vertical loads acting through sway displacement (the P-Δ effect) is included in the second-order analysis, the effect is to decrease the magnitude of the maximum lateral loading on

the frame for the typical monotonic loading from an initially vertical position of the frame.

However, after a given displacement is reached in one direction and the lateral load is decreased to zero, a residual deflection remains in the frame if the frame had undergone inelastic deformations. For further lateral loading in the reversed dirction, the P-Δ moment existing at the residual deflection must also be overcome. Consequently, a somewhat larger lateral load is required than if the second order effect was not considered. However, after the frame passes through the vertical position during the reversed loading, the net P-Δ effect again decreases the lateral loading.

3.3 Second-Order Elastic-Plastic Analysis of Frames with Ramberg-Osgood Beams

Beams having nonlinear moment-curvature characteristics may be included in a multi-story frame analysis by using a suitably sized increment of deformation over which these nonlinearities may be assumed as linear. Such a linearizing technique has a distinct advantage over analytical derivation of the slope-deflection equations. Since the nonlinear moment versus rotation behavior is usually selected as the best fit to a given curve or curves, any number of empirical representations can result depending on the type and parameters selected. In such cases the slope-deflection equations would have to be rederived and reprogrammed from expressions similar to the simple examples given in Articles 2.3 and 2.4. The basic techniques of numerically obtaining the stiffness could accommodate various moment versus curvature subroutines.

The basic moment versus curvature relationship used in the proposed method of analysis is based in part on the experimental behavior to be described in Chapter 5. The moment versus curvature expressions may also be derived by dividing the member cross section into small elements or by curve fitting the data from the cantilever beam tests mentioned in Chapter 1. If experimental evidence is not available, the effects of strain hardening can be accounted for by a suitable change in the moment-curvature expressions selected.

From a least square fit of the experimental data to a Ramberg-Osgood function, the end moment versus end rotation behavior of the beam members is developed by summing the curvatures in the manner described in Article 2.5. Partial derivatives of the end moment versus end rotation expressions give the member stiffnesses. The member stiffnesses are incrementally found and inserted into the basic second-order elastic analysis to compute the overall frame behavior.

3.4 Evaluation of Lateral Load Versus Deflection Behavior of a Frame

The proposed method of analysis has been developed and applied specifically to analyze single-bay multi-story planar frames having beams with Ramberg-Osgood moment-curvature characteristics and elastic columns. The frame analysis is based on second order elastic behavior of the frame with the axial load effect altering the strength and stiffness of the columns. The beam stiffness and strength is based on a lumped flexibility model utilizing the Ramberg-Osgood function in moment versus curvature terms to define the basic behavior of the beam cross sections.

The general procedure followed in the numerical computations is based on linearizing over small increments and may be summarized in the

following steps:

a. Compute the gravity loading conditions assuming second-order elastic behavior throughout the frame. The corresponding Ramberg-Osgood curvatures are computed for each segment of the beam. The above computations require that the gravity loading is elastic to the extent that all moments are less than about one-half of the yield moment. The continuing steps assume the gravity load remains constant throughout the analysis.

b. Compute the beam stiffness for a given increment of end moment.

   1. Assume a given set of incremental end moments which are typical of the incremental end moments to be found in the beam at the completion of the frame loading increment.

   2. Compute the moment diagram for the given change in one of the end moments alone and compute the total moments at each beam segment. Compute the corresponding curvatures.

   3. Compute the slopes at each end of the beam. Since the values of curvature are known at each segment along the axis of the beam, the standard equations for the beam (one relating rotations along the beam and the other relating displacements) can be integrated piecewise and solved to obtain the end rotations of the beam.

   4. Apply an increment of moment at the opposite end of the beam to return the rotation at that end to its initial

value prior to application of the stiffness moment.

5. Compute the incremental stiffness and cross stiffness for the beam from the previously applied stiffness moment.

6. Repeat steps 2 through 5 for an incremental stiffness moment applied at the opposite end of the beam. The resulting stiffnesses of the beam as computed in steps 1 through 6 are:

$$\begin{bmatrix} \frac{\partial M_A}{\partial \theta_A} & \frac{\partial M_A}{\partial \theta_B} \\ \frac{\partial M_B}{\partial \theta_A} & \frac{\partial M_B}{\partial \theta_B} \end{bmatrix} = \begin{bmatrix} \frac{M_A - M_{A_o}}{\theta_A - \theta_{A_o}} & \frac{C_A M_A - M_{A_o}}{\theta_B - \theta_{B_o}} \\ \frac{C_B M_B - M_{B_o}}{\theta_A - \theta_{A_o}} & \frac{M_B - M_{B_o}}{\theta_B - \theta_{B_o}} \end{bmatrix}$$

c. Insert the resulting beam stiffness into the slope-deflection frame analysis program.

d. Assume an increase (or decrease) in the lateral shear load applied to the frame.

e. Analyze the frame with the given stiffnesses and loads to find the incremental and total moments, rotations and deflections throughout the frame.

f. Compare the incremental moments at each end of the beam with values used during the stiffness computations. If the incremental moment values exceed the stiffness moments, the increment of horizontal shear applied to the frame is reduced. If the ratio of end moments for the increment does not compare with the ratio of end moment defined in Step 1, return to step 1 with a new ratio.

g. Repeat steps b through g as required by the displacement program.

3.5 General Computational Logic and Selection of Control Parameters

The general computational logic for the computer solutions to both the elastic-plastic and Ramberg-Osgood type of analysis is indicated in Figs. 3.2 and 3.3.

Several evaluations of the proposed numerical technique were performed in the development of the procedure as applied to frames similar to those tested in the experimental portion of the study.

The size of the incremental lateral load was maintained at one kip throughout the analysis unless the following deformation control prevailed. The incremental deflections at the story level were controlled such that the story chord rotations did not exceed 0.0010 radians. The effect of variation in chord rotation may be observed by noting the divergence of the curves shown in Fig. 3.4. For the case shown the increment through 9 kips of total lateral load is one kip. Thereafter, relative lateral deformations of each half-story do not exceed 0.09 or 0.06 inches corresponding to the maximum chord rotations of 0.015 and 0.010 respectively.

Several trial segmentations of the beams were tried with the most success for the number and positions indicated in Fig. 3.5. The amount of computer time involved was also a factor in this determination. Comparison of the effects of the number of elements can be made by observation of the curves indicated in the Fig. 3.6. The comparison between the 56 more realistically spaced elements and the 74 realis-

tically spaced elements indicate that 56 elements are adequate to represent the given beam. The more realistic spacings of the segments imply a closer spacing in regions of high values of curvature as compared to a uniform spacing along the beam. The quality of the numerical results for a given number of segments should be better for the case with the more realistic spacings.

Several methods for approximating the nonlinear beam stiffnesses are possible such as a tangent at the beginning or some approximate midpoint of the increment, or a chord stiffness for the approximated increment. Either of the tangent methods may be refined by iteration between the approximation and the results at the end of the increment of frame behavior. However, these methods also imply increased computational time which may be justified for larger problems or with the use of larger computational facilities. The method used herein is a chord type of stiffness computation with the size of the incremental moment used during the stiffness computations being the critical parameter. The size of the incremental moment used for the current stiffness computation is equal to the increment of moment for the last increment of loading of the frame with a minimum value of 50 kip-inches for the computational scheme used herein. Figure 3.7 shows the small effect on the horizontal load between using 100 kip-inches and 200 kip-inches for the minimum value of the incremental stiffness moments. For the first increment after reversal of load and also for the initial stiffness, 300 kip-inches for both incremental moments were used.

In order to account for the finite size of the panel zone at the beam-to-column intersection, the stiffnesses of the beam segments

included within the half-depth of the column were adjusted The stiffnesses of these segments were linearized to remain at 1, 5 and 10 times the basic elastic stiffnesses of the segment. The effect of the change is shown in Fig. 3.8 and a value of 10 was selected to be used.

As described in Article 2.2.1, Al Muti proposed a 20 percent increase in theoretical deformations to permit a better correlation between his beam tests and theory. The effect of the variation of the Ramberg-Osgood parameter, $\emptyset_y$, on the reversed load behavior of frames can be observed in Fig. 3.9.

4. DESIGN AND ANALYSIS OF TEST FRAMES SUBJECTED TO COMBINED GRAVITY AND LATERAL LOADS

4.1 Scope of the Experimental Program

The earthquake problem is essentially one of constant gravity loads at the working value and variable displacements of the base of the structure. In the study of the effects of earthquakes on building frames, the resulting inertia forces are often assumed to be concentrated at the floor levels. Therefore, the basic static behavior of the building subjected to constant gravity loads and reversed and repeated lateral loads at the floor levels must be determined before the dynamic analysis of an inelastic frame can properly proceed. For this reason, the experimental portion of the research program was initiated as a continuation of the maximum strength evaluation of full scale frames from the static and monotonic loading condition to the repeated loading condition.

In general, the overall investigation was restricted to problems dealing with the behavior during an earthquake of low multi-story steel frames loaded as described.

Two frames were tested initially. Both frames had the same members and bay width. The main test, Frame B was a three-story assemblage and the first test, Frame A was a single story frame loaded as the lowest level of the main test frame. These frames had their columns and beams oriented for major axis bending. The beam-to-

column connections were designed as typical fully moment-resisting welded connections in earthquake zones. The frames were designed for aseismic design conditions with typical member stiffnesses, working load strength and drift. In addition, the columns had significant but typical proportions of gravity load.

A third frame was tested for the purpose of investigating the effect of cross sectional instability in the beam member (local buckling) on the behavior of the frame subjected to reversed and repeated loads. This problem was evaluated in Frame C which was a duplicate of Frame A except that a non-compact section (in the context of plastic design) was used for the beam. The beam section had nearly the same moment of inertia and fully plastic moment as the beam section used in Frame A, but its flange width-to-thickness ratio was about 21.

4.2 Design Parameters

The design of the frames was based on current aseismic design practice as applied to an eight-story single-bay prototype structure shown in Fig. 4.1. The columns of the prototype frame are likely to be bent in double curvature and have points of inflection near their mid heights when lateral loads are applied. Therefore, assemblages can be formed by subdividing the prototype frame at the mid-heights of the columns. A three-story assemblage that would represent levels 5, 6 and 7 of the prototype frame is shown in Fig. 4.1. A single-story frame, Frame A, was then selected as the lowest story of the three-story frame, Frame B and loaded accordingly. Frame C was subjected to the same conditions as Frame A.

Eighty pounds per square foot were selected for full dead loads and also for full live loads with an average live load reduction of forty percent applied to both beams and columns. The gravity loads applied to the frames were based on an eighteen foot spacing between each frame in the prototype building. The total tributary floor loading was placed as two equal concentrated loads at approximately the quarter points of the beam span.

Since the portion of the building selected for design, analysis and testing is in a region of small variation in the total aseismic design shear, the working design shear was selected as the summation of the aseismic shears through level 5 for Frame B as shown in Fig. 4.2. The working shear is equal to approximately 3-1/2 percent of the sum of the dead loads through level 7. The geometry of the frame and the member sizes were selected to have ratios of column-to-beam stiffnesses which are representative of buildings designed for seismic areas based on current design practice.

4.3 Plastic Design of Three-Story Frame B

The test frames were designed plastically by initially assuming no frame instability or P-Δ effect and a likely-to-occur mechanism. A plastic moment balancing analysis was then performed to check that all moments were less than or equal to their fully plastic values or reduced values for columns. Using the moment diagram which resulted from the analysis and the preliminary member sizes, the deflections were calculated. The frame was redesigned including the P-Δ moments and the preliminary member sizes were altered if

necessary. The previous combined load analysis and design were based on the working load times a load factor of 1.30. The resulting design was then checked with gravity load acting alone with a load factor of 1.70. As previously described, Frame A was then selected as the lowest story of Frame B, and Frame C was selected to duplicate Frame A. However, all the frames could have been individually designed and analyzed in the same manner as described for the three-story frame.

The beam-to-column connections were designed as fully moment resisting and are similar to those tested by Popov.[13] In addition, the panel zones were provided with shear stiffening (diagonal or doubler plates) in accordance with the requirements of plastic design.[52]

4.4 Second-Order Elastic Analyses of the Test Frames

The test frames were then analyzed for their second-order elastic behavior. The analyses were carried out on the frames subjected to working gravity load alone and after the working value of the monotonically increasing horizontal load was added. The results obtained permitted comparing the adequacy of the beams and columns with the allowable stresses specified in the AISC (American Institute of Steel Construction) Specification. The final member sizes selected for the test frames are shown in Fig. 4.3.

4.5 Second-Order Elastic-Plastic Analyses of the Test Frames

To find the complete load versus deflection curve for each frame subjected to a monotonically increasing horizontal force and

constant gravity loads at the working value as shown in Fig. 4.4, the second-order elastic combined load analyses were continued into the inelastic range past the point of frame instability. In these analyses, the material was assumed to be elastic and perfectly-plastic.

The load versus deflection curve for Frame A, Fig. 4.5, indicates that the frame instability load[36] and the plastic mechanism load coincide at a lateral load of 14.8 kips. However, the behavior of the three-story frame, Frame B, Fig. 4.6, shows the frame to be unstable at a load of 15.3 kips before a mechanism is formed. The behavior of Frame C would be expected to be approximately the same as Frame A if local buckling of the beam flanges would not have an effect on the lateral load capacity of the frame.

All of the previous analyses were based on handbook values for cross sectional properties and on an assumed static yield stress level for ASTM-A36 steel of 36 kips per square inch. The basic assumptions of elastic perfectly plastic member and second-order frame behavior were used for the above analyses.

Comparing the working value of lateral load of 5.2 kips with the maximum capacity of all frames shows a considerable reserve of strength and a source of possible material savings.

Additional calculations indicate that a design involving W8x35 columns and W10x25 beams would be satisfactory to resist the same design loads. Figure 4.7 gives the lateral load versus deflection

relationship of the plastically designed alternate frame. At the factored gravity load, the maximum lateral load that can be sustained by the alternate frame is about 8 kips which is higher than the factored lateral load (the design lateral load) of 6.75 kips. The total weight of the alternate frame is about 13 percent less than the total weight of the test frames which were checked by the allowable-stress method. The potential savings that can be achieved by recognizing the inelastic strength of the structure in design is appreciable.

5. EXPERIMENTAL BEHAVIOR OF TEST FRAMES

5.1 Introduction

The frames were tested by subjecting them to constant gravity loads at the working value and a program of statically applied cyclic lateral displacements of the top of the frames.[60] The lateral displacement programs were similar to those used by Popov[12-16,18-20] on cantilevered beams.

Initially the gravity loads were applied to the frames and then sets of lateral displacements of increasing amplitudes were applied to the frames in a cyclic manner. In each case the amplitudes to be cycled were selected to bracket the plastic hinge occurrences based on elastic-plastic analyses and other intermediate points on the respective load-deflection curves. For displacements in the elastic range the frames were subjected to three cycles at each amplitude and for inelastic range displacements five cycles were imposed. The number of repetitions of each cycle amplitude were set to observe the stability of the hysteresis loops at the various amplitudes of deflection and inelastic conditions of the frames. The amplitudes selected for Frame A and the resulting displacement program are shown in Fig. 5.1.

5.2 Testing Technique

5.2.1 Basic Testing Schedule

Each frame was commercially bid on and fabricated by structural fabricators from working drawings supplied by the writer. The

shop fabricated members were erected in the basic testing arrangement and aligned by transits to be vertical in two directions. The beams were leveled and aligned. The frame was instrumented and initial readings were taken. The beam-to-column connections were then field welded in the laboratory by the structural fabricator. The gravity loads were then added incrementally to the columns to verify and adjust the column stresses to "alignment under load" conditions. The gravity loads were increased to the dead load portion of the total load on all members.

At this point in the test several cycles at different amplitudes of lateral displacement were applied for the purpose of making a complete checkout of the transducers and the experimental data generated. These amplitudes were selected such that the frame remained essentially elastic.

After completely unloading the frame the main portion of the testing program was started by applying the full gravity loads to the columns and to the beams incrementally. At this point sets of cycles of increasing lateral displacement amplitudes were applied to the top of the frame until the test was nearly completed. At the end of each test the frame was displaced in one direction to the maximum amount possible for the displacement apparatus used in the test.

5.2.2 Mechanical and Electrical Measurements

Various types of data were taken during the tests. Vertical loads were measured through the applied jack pressure and by means of load cells at the points where the jack loads were applied to the

frame. Horizontal loads were measured by load cells which were in series with the lateral displacement apparatus. Lateral deflections of several points on each column were measured by linear potentiometers, or surveyor's transits, or a combination of both methods. Vertical deflections along the beams were measured by surveyor's levels. Rotations at various points throughout the frame were measured mechanically, electrically or by both methods. Strains throughout the frame were measured by means of electrical resistance strain gages. The electrical measurements were digitized and automatically punched onto computer cards whereas various mechanical measurements were recorded by hand and then punched onto the cards. In addition, the progression of yielding and other pertinent data were logged throughout the tests by hand or photographically.

Preliminary data in each test series consisted of testing three coupons cut from each end of every member as well as the stiffener material.[60] These coupons were tested in tension at a very slow rate to observe the elastic, plastic, strain hardening, rupture and energy absorption characteristics of the as-delivered material. The as-delivered material was rolled steel members which were permitted to be straightened by gagging only and the welded steel beam used in Frame C was not straightened since careful fabrication techniques were used. Residual stresses were measured or considered for each member in order to position the strain gages used on the frame members properly at points of zero residual stresses due to rolling or welding of the individual members. The actual dimensions of each end of each

member were measured and the actual section area and section modulus were computed. In addition, from the actual dimensions and the static yield levels measured in the tension tests, the plastic moment values were computed.

5.2.3 General Testing Arrangement

Various pieces of hardware were procurred or fabricated and then assembled into the general arrangement for testing the frames in the manner previously described.[60] For example, the test of Frame B is shown in Fig. 5.2. Gravity loads were applied to each beam by utilizing gravity load simulators. Each simulator was attached to a load spreader beam which in turn applied load to two points on the beam through load cells and load hangers. Each load hanger was attached to a shaft passing through the beam at its mid-depth. The gravity load in each column was applied by two simulators. One simulator on each side of the column was attached through a load cell and load hanger to the ends of a large diameter shaft passing through the top of the column.

A common pressure source was used for the beam simulator jacks and another independent common source was used for the simulators applying loads to the columns. Each air-to-oil pump source was self regulating to hold the gravity loads essentially constant for all relative positions of the test and supporting frames.

The boundary conditions imposed on the frames required zero moments at the assumed points of inflection above and below the main portions of each frame as described in Chapter 4. Therefore, the base of each column was bolted to a specially designed hinged end fixture

which utilized a larger diameter shaft passing through roller bearings in adjacent pillow blocks. To distribute the applied lateral force, a link member was connected between the shafts passing through the top half story columns. Each end of the link member was attached to the shafts by means of roller bearing assemblies.

The lateral displacement of the top of the frame was accomplished by either turnbuckles on each side of the top of the frame pulling alternately or by a mechanical jack attached to the center of the link member. For either case, load cells were connected in series with the displacement apparatus to measure the corresponding lateral forces.

Special bracing linkages were used to brace the frame without offering any restraint to in plane movements. The top flange of each beam was supported laterally at each load point and at center span. In addition, the lower flange was effectively braced laterally by attaching the brace to the inside of the adjoining columns one inch below the beam flange. Braces were also added on the outside of each column opposite the interior braces.

5.3 Experimental Behavior of the Test Frames

The following articles describe the basic test results from the experimental portion of this investigation. The descriptions will be concerned primarily with:

1. The shapes of the lateral load versus deflection hysteresis curves.

2. The magnitudes of the lateral load attained during the test.
3. The stability of the size and shape of the load versus deflection hysteresis curves during repeated cycling at each constant deflection amplitude.
4. The local behavior of the members and their component plates as well as connections and fabrication details.

5.3.1 Single-Story Frame A

Sixty cycles at various amplitudes of lateral displacements were applied to Frame A with a maximum displacement amplitude of 5.2 inches. The largest cycled displacement is about 14 times the deflection at the working value of lateral load.

Initially, after alignment of the columns in the frame under gravity loads, the dead load portion of the total gravity load was applied to the beam and columns. Several cycles of elastic range displacements were applied to verify the complete testing arrangement.

The basic gravity loads applied to the test frame during the main portion of the test were 17.3 kips at each load point (at 0.275 L from the center of each column) and a total of 103.8 kips applied to the top of each column.

The nominal lateral displacement program was then applied to the top of the frame. The particular program consisted of three cycles at amplitudes of 0.2, 0.4, and 0.6 inches. Then five cycles were

applied at amplitudes of 0.8, 1.1, 1.4, 1.7, 1.9, 2.2, 2.8 and 5.2 inches and the test stopped.

The hysteresis loops for selected displacement amplitudes for Frame A are shown in Fig. 5.3. The maximum load obtained is about 40 percent greater than the maximum load indicated in Chapter 4.

As in the case of the hysteresis loops generated for the cantilever beam tests, the repetitions of the cycles at all amplitudes indicated stable hysteresis loops. However, for the frame the downward sloping portion of the curves between the deflection at the maximum load to the maximum deflection shown in Fig. 5.4 is important. In this portion of the curves, the instability effect governs the overall behavior of the frame yet Fig. 5.4 shows that during this instability of this single-story frame, the five large amplitude hysteresis loops remain stable.

The test shows the influence of strain-hardening when the frames were subjected to large lateral displacements. On each of the large amplitude cycles of the frame, once the deflection at the maximum lateral load had been exceeded, the lateral load-carrying capacity dropped off much slower, compared with the theoretical monotonic predictions that ignored strain hardening.

The curved shape of the hysteresis loops for frames subjected to reversed loading is caused not only by the Bauschinger effect in the material but also by the reduction in frame stiffness due to the spread of yielding at the plastic hinge locations as indicated in Fig. 5.5.

5.3.2 Three-Story Frame B

Fifty four cycles at various amplitudes of lateral displacements were applied to Frame B with a maximum cycled amplitude of ten inches. The largest cycled displacement is about 9 times the displacement at working load.

Initially, after alignment of the columns in the frame under full gravity loads alone, the dead load portion of the total working gravity load was applied to the beams and columns. Several cycles of displacement amplitudes in the elastic range were applied to check out the testing arrangement.

Then the gravity loads were increased to the full value of the gravity loads of 17.3 kips applied to the beam at each load point and a total of 69.1 kips applied to the top of each column.

The nominal lateral displacement program was then applied to the top of the three-story frame. The particular program consisted of three cycles at amplitudes of 1.0 and 2.0 inches. Then five cycles were applied at amplitudes of 3.0, 4.0, 5.0, 6.0, 7.0, 8.0, 9.0 and 10.0 inches.

Then, the gravity loads on beam and columns were reduced to the dead load portion of the total working gravity loads and two additional cycles were applied at an amplitude of 10.0 inches. The test was continued by re-establishing the full working gravity loads on the beams and columns. The test was stopped after displacing the top of the frame to about 13.5 inches to the east.

The hysteresis loops for selected displacement amplitudes for the three-story single-bay frame, Frame B are indicated in Fig. 5.6. In spite of the fact that the monotonic analysis given in Chapter 4 indicated that the maximum load was reached before formation of a mechanism, the maximum experimental lateral load is also about 40 percent greater.

In addition, the cycles when repeated at all the given displacement amplitudes were stable also for this taller frame. The downward sloping portion after maximum load is reached was also more gentle as was the case for Frame A.

Again, the yielding was not concentrated entirely at definite points in the frame but extended along the members as shown in Fig. 5.7.

5.3.3 Single-Story Frame C with Non-Compact Beam

Seventy five cycles at various amplitudes of lateral displacements were applied to Frame C with a maximum displacement amplitude of 5.2 inches. The largest cycled displacement was about 14 times the deflection at the working value of lateral load.

The basic gravity loads applied to the test frame during the main portion of the test were 17.3 kips at each load point (at 0.275 L from the center of each column) and a total of 103.8 kips applied to the top of each column.

The lateral displacement program consisted of three cycles at amplitudes of 0.2, 0.4, and 0.6 inches. Then five cycles were applied at amplitudes of 0.8, 1.1, 1.4, 1.7, 1.9, 2.2, 2.8, 3.3, 4.0, 4.6 and

5.2 inches. Eleven additional half-cycles were then applied to 5.2 inches to investigate various conditions in the beam-to-column connections and the panel zones. The test was stopped after displacing the frame to the west to 11.8 inches and then removing all loads.

Single-story Frame C is essentially a duplicate of Frame A except that the beam flanges have a b/t ratio of 21 as described in Art 4.1.

The W8x40 columns for both frames A and C were from the same piece of steel. The beam was welded from selected plate stock which had approximately the same static yield stress level as the flanges of the rolled beam used in Frame A. Keeping the depth of the welded beam equal to the depth of the W10x29 beam, the flange width of the welded section was adjusted to give nearly the same full plastic moment and elastic section modulus as the experimental properties of the W10x29 beam. The experimental properties for the beams used in Frames A and C show Frame C to be slightly stronger and stiffer as shown below.

	Plastic Moment M_p	Section Modulus S	Moment of Inertia I	Predicted Maximum Load H_{max}
Frame A	$1297^{k\text{-in}}$	$32.2\ in^3$	$165\ in^4$	15.5 kip
Frame C	$1349^{k\text{-in}}$	$34.3\ in^3$	$176\ in^4$	17.2 kip

The corresponding predicted maximum lateral loads using experimental properties show an increase of 1.7 kips for Frame C.

Selected load-deflection curves for Frame C are shown in Fig. 5.8 for amplitudes of 2.2, 2.8 and 5.2 inches. Local buckling did occur

in the beam flanges at relatively early stages of testing. However, the hysteresis loops are apparently unaltered by flange buckling. This is illustrated in Figs. 5.9 and 5.10 where hysteresis loops of Frame A and C are compared for two approximately equal lateral displacements. The maximum lateral loads obtained for similar amplitudes of displacement of the two frames are shown below.

Nominal Amplitudes	$\pm$ 2.2 in	$\pm$ 2.8 in	$\pm$ 5.2 in
Frame A	19.1 kip	20.0 kip	21.2 kip
Frame C	22.6 kip	23.2 kip	22.5 kip

The maximum loads are consistently higher for Frame C, even with extensive local buckling occurring in the beam. The relative differences between Frames A and C are slightly larger than the differences expected due to the differences in the beam properties.

Near the termination of the original test plan, fracture of the beam flange occurred. At this point, the frame was repaired and additional testing was planned to study the following two problems:

a. The necessity for placing shear stiffening in the panel zone of the beam-to-column connections.

b. The necessity for welding the beam web to the column flange.

Figure 5.11 shows the effect of removing the shear stiffeners. There is a definite drop in the maximum load, but the general shape of the hysteresis loops is not significantly changed.

The next step in the testing was to cut the web of the beam free of the column. The two erection bolts (3/4 in diameter) were inserted between the web and the erection clip angle. The resulting behavior, as shown by the solid line in Fig. 5.12, is essentially the same as when the web was fully welded.

For a more conclusive comparison, the shear stiffeners were replaced in the panel zone. Again the effect of having the web welded to the column flange or not is still apparently small, as shown by the dashed line in Fig. 5.13.

5.4 Conclusions Based on Observed Behavior of the Frames Tested

The experimental observations for Frames A, B and C are summarized below. However, these results should be considered with respect to the basic test conditions. The frames were single-bay in width with constant gravity loads applied to the beams at 0.275 L from each column centerline. Gravity loads were also applied to each column top, but the maximum ratio of applied axial load to yield load was about 0.30. The frames were braced to inhibit out-of-plane movements of the beams and columns. The horizontal displacement program should also be noted since other programs would change the resulting frame behavior.

The significant observations are as follows:

1. Hysteresis loops are stable for all deformations.
2. A considerable increase in lateral load capacity during reversed loading over that indicated by monotonic elastic-plastic analysis is possible.

3. A gradual unloading slope is available for displacements greater than those at the maximum load.
4. The presence of significant residual P-Δ moments existing in the frame when reversed loading begins must be included in the analytical methods.
5. The shape of hysteresis loops is affected by the reduction of frame stiffness under reversed loading due to
   a) Spread of yielding in the plastic hinge locations.
   b) The Bauschinger effect in the material.
6. Local flange buckling in the beam does not seem to affect the behavior or the hysteresis loops of the frame.

6. PREDICTIONS OF BEHAVIOR OF TEST FRAMES

6.1 Second-Order Elastic-Perfectly Plastic Reversed Load Behavior

The basic second-order elastic-perfectly plastic analysis as described in Article 3.2 was applied to the test frames subjected to the test conditions. The load versus deflection curves at various amplitudes are shown for Frame A in Fig. 6.1 and for Frame B in Fig. 6.2. These curves may be compared with the experimental curves presented in Figs. 5.2 and 5.6 respectively. For a typical case Fig. 6.3 shows the relative definition of the experimental curve by a second-order elastic-plastic analysis. Three conclusions can be made. The shapes of the respective load versus deflection curves do not compare closely. The maximum load obtained during the test has relatively good agreement with the maximum load obtained during the analysis at this amplitude. Thirdly, the areas enclosed by the respective hysteresis loops do not compare favorably, with the elastic-plastic loop unconservatively estimating the energy absorption capacity of the frame at this amplitude.

Figure 6.4 shows the elastic-plastic results for Frame B with the beam loads at the locations used during the tests and with the loads at the quarters points which are commonly used during analytical studies. Comparison of the dashed curve and the solid curve in Fig. 6.2 shows the effect of analytically moving the centerlines of the columns to the inside flange of the columns. The dashed curve shows an effective shortening of the beam for analysis to account partially for the finite

size of the panel zone effect on the strength and stiffness of the frame. In conclusion the figure indicates that this method shows small effects in either case.

For completeness, the elastic-plastic reversed load behavior of the alternate frame which saved 13 percent steel as described in Article 4.5 is shown in Fig. 6.5. The maximum lateral load is clearly in excess of the design loading and in fact is nearly equal to the monotonic load capacity of Frame B determined from elastic-perfectly plastic analysis.

6.2 Ramberg-Osgood Reversed Load Behavior

Considering the versatility of the moment versus curvature Ramberg-Osgood formulation given in Article 2.2, determination of the appropriate constants for each case must be based on facts existing prior to commencing the analysis. As recognized by Popov, a clear lack of experimental data exists on the behavior of the structural steels during load and strain cycling. Therefore, primary reliance must be placed on determining the characteristics of moment versus curvature curves resulting from beam or beam-to-column connection tests. Popov concluded that an r value of 8 and $\alpha = 0.5$ fit the load versus deflection hysteresis results of the cantilevered beam tests. The beams were connected to a short steel column in Popov's tests by fully welded beam-to-column connections which are similar to those used in the frames described in Chapters 4 and 5. The corresponding moment versus curvature relationship may be found for the cantilever as

$$\frac{\phi_x}{\phi_y} = \frac{M_x}{M_y}\left(1 + \beta \left(\frac{M_x}{M_y}\right)^{R-1}\right), \text{ for } M_x > 0, \tag{6.1}$$

where ϕ_y and M_y are the curvature and moment corresponding to the point of perfectly plastic behavior as used by Popov. Therefore

$$\Delta_p = \frac{\phi_y}{M_y}\left[\frac{PL^3}{3} + \beta P \left(\frac{P}{M_y}\right)^{R-1} \frac{L^{R+2}}{(R+2)}\right] \tag{6.2}$$

Since $M_y = M_p = P_{PLASTIC}\, L$ and $\Delta_{PLASTIC} = P_{PLASTIC}\, L^3/3EI$,

$$\Delta_P = \frac{\Delta_{PLASTIC}}{P_{PLASTIC}}\, P \left(1 + \beta \left(\frac{3}{R+2}\right)\left(\frac{P}{P_{PLASTIC}}\right)^{R-1}\right) \tag{6.3}$$

Following Masing's hypothesis, the monotonic or skeleton curve given by Eq. 6.3 is one half the scale of the hysteresis loop. Therefore, the hysteresis loop is given by

$$\frac{\Delta_p - \Delta_o}{2\Delta_{PLASTIC}} = \frac{P - P_o}{2P_{PLASTIC}}\left[1 + \beta \left(\frac{3}{R+2}\right)\left(\frac{P - P_o}{2P_{PLASTIC}}\right)^{R-1}\right] \tag{6.4}$$

Equation 6.4 may be compared to the following equation describing Popov's tests.

$$\frac{\Delta_p - \Delta_o}{2\Delta_{PLASTIC}} = \frac{P - P_o}{2P_{PLASTIC}}\left[1 + \alpha \left(\frac{P - P_o}{2P_{PLASTIC}}\right)^{r-1}\right] \tag{6.5}$$

Comparing Eqs. 6.4 and 6.5 indicates that

$$\beta \left(\frac{3}{R+2}\right)\left(\frac{P - P_o}{2P_{PLASTIC}}\right)^{R-1} = \alpha \left(\frac{P - P_o}{2P_{PLASTIC}}\right)^{r-1} \tag{6.6}$$

If the exponent of the skeleton loop is assumed to be equal to the exponent of the hysteresis loop, R equals r. As a result,

$$\beta = (R + 2)\,\alpha/3 \tag{6.7}$$

Therefore for r = 8 and α = 0.5, β = 1.67.

By way of comparison Wilson[55] suggests in a discussion of Ang's paper[56] that the moment versus curvature relationship used by Ang could be expressed with R = 8.0 and α = 3.0. However, Ang's curves were generated directly from the complete stress versus strain curve to fracture without consideration of any realistic effects which normally restrict the member behavior such that the ultimate stresses are not realized microscopically.

With reference to Fig. 2.1, the value of α basically locates the point where the nonlinear curve crosses the value of the yield moment whereas the exponent controls the sharpness of the rounding at the knee of the curve. Both values are a function of the length of the curve to be utilized. Kaldjian's analysis[38] indicates that the value of R increases slightly as a larger portion of the curve is utilized. Kaldjian indicates[38] that for sections typical of those used during this experimental program a value of R = 10.0 should be used with α = 1.0. However, if the monotonic moment versus curvature curve is constructed for the W10x29 with a standard pattern of residual stresses, R equals approximately 43.0 with α = 1.0 for the portion up to strain-hardening strain only.

Figure 6.6 compares the monotonic load versus deflection elastic-plastic curve with the curves generated with the Ramberg-Osgood formulation. The larger exponents agree more clearly with the monotonic elastic-plastic curve up to the maximum loads. However, as indicated by

Arnold, Adams and Lu[33], strain-hardening should be included at least beyond the point of maximum load for better agreement between experimental and elastic-plastic theoretical predictions. In addition, Sheninger and Lu[57] have shown experimental corroboration of the effects of strain hardening in the moment transmitted to a column by a beam is such that the moment at the face of the column normally exceeds the fully plastic moment by approximately 10 percent. The slope of the reversed loading curves after the maximum load as indicated in Article 5.4 also indicates the effects of strain hardening since the unloading slope beyond the maximum lateral load is approximately one third of the elastic-perfectly plastic unloading slope.

In addition, other comparisons[32] have shown that the second-order elastic-plastic analysis gives good estimates of the load versus deflection behavior of frames subjected to monotonic loading conditions without strain hardening considered and that with consideration of strain hardening close comparisons are possible.[33]

However, based primarily on fatigue considerations previous investigators have selected some form of skeleton or locus curve to form the basis of the computations during reversed loadings as described in Section 2.2.1. In addition these investigators have utilized the monotonic load versus deflection curve or moment versus curvature curve to define the skeleton curve. To date all investigators have assumed that the exponent of the skeleton curve and of the hysteresis loop are equal, with the exception of Tanabashi.[42] Tanabashi concluded that the strain hardening exponent for the skeleton curve is about one-

half of the exponent of the hysteresis curve. In his study the hysteresis loop exponent was selected as an average value of 9.0 which had a maximum deviation of about 3.0 and an average deviation of about 1.0. The same study indicated that the skeleton curve exponent varied between 4.3 and 5.5 for the same conditions. The scatter in their results was explained to be a consequence of a dependence on strain amplitude. The effect of the smaller exponent is shown in Fig. 6.7 for a given amplitude cycle used during the test of Frame A. In addition, Fig. 6.8 shows the relative insensitivity of the hysteresis curve to the value of the exponent R where the skeleton curve exponent is one-half of the hysteresis loop exponent for the same value of α in both cases.

The value of α, however, has an appreciable effect on the predicted magnitude of the maximum horizontal loading for the amplitude shown. The shape of the curve is also altered especially during the initial loading. For fixed values of yield moment and exponent, the value of α permits an allowance for the Bauschinger effect. AlMuti[4] merely multiplied the computed displacements by a factor of 1.2 to permit his theoretical work to more closely match his experiments. In general both the efforts of Tanabashi[42] and Al Muti[4] gave good predictions based on stress versus strain data, but in both cases the theoretical curves passed outside of the experimental hysteresis loops in the curved portions.

The above discussion indicates that the Ramberg-Osgood parameters which typify the monotonic loading response are values of

R about 8 to 10 and α near 1.0 with the yield moment in the Ramberg-Osgood formulation determined by a least squares fit of the monotonic moment versus curvature curve to strain hardening. This moment is equal to about 1190 kip-in for the beams of the test frames with the handbook value of M_p = 1235 kip-in. By way of comparison, the moment equals 1222 kip-in. for the fit with R = 43 and α = 1.0 for the same nominal beam characteristics with a standard pattern of residual stresses. In both instances, $\phi_y = M_y/EI$.

However, the experimental results for Frames A and C show that a slight adjustment of the parameters R, α and ϕ_y are necessary to give good predictions of the frame behavior. Figure 6.9 shows a good comparison between the predicted curve and Cycle 47 of the test of Frame A for the values of the parameters indicated.

Figures 6.10, 6.11, 6.12 and 6.13 compare the experimental results of Frame C with predictions based on similar values of the Ramberg-Osgood parameters. These comparisons show that the combination of values of R = 8 and α = 3/7 for both the skeleton and hysteretic moment versus curvature curves are appropriate. As in AlMuti's tests, the value of the basic elastic ϕ_y based on the experimental properties of the beam had to be multiplied by about 1.2 to give better correlation of the overall frame stiffness. In addition, Figure 6.13 shows the effect on load capacity of the frame when the diagonal stiffener welds were broken. The plates were attempting to be subjected to tensile forces for horizontal displacements to the west (-).

The following articles in the chapter discuss further the stiffness of the frames and the stability of the hysteresis loops.

6.3 Overall Stiffness of Test Frames Relative to Ramberg-Osgood Solutions

Due to strain hardening, the Ramberg-Osgood moment versus curvature relationship implies that loads significantly greater than M_p may exist at a cross section subjected to monotonic and/or reversed curvatures. The net result is an increase in end moment in the beam at the face of the column flange above the basic design value of M_p used in the elastic-perfectly plastic analysis.

There are two effects which result from the increased end moment in the beam. The first is the increased shear that must be resisted by the panel zone of the beam-to-column connection. The elastic shear capacity of the panel zone may be exceeded which causes a softening of the overall frame behavior. Figure 6.14 shows the yielding characteristics in both the diagonally stiffened and doubler plate stiffened connections for Frame A described in Chapter 5.

The second effect concerns the increased moment above and below the joint in the column member. In general both column moments will increase to place the joint in equilibrium with the increased forces applied by the beam. These increased moments may cause partial yielding in the column members which would violate the basic assumption of elastic columns used in the analyses. In elastic-plastic analyses, the columns remain elastic until M_{pc} is reached where M_{pc} is given by the following equations.[52]

For columns subjected to major axis bending,

$$M_{pc} = 1.18\ (1 - P/P_y)\ M_p \text{ for } P/P_y > 0.15 \qquad (6.8)$$

and for columns subjected to minor axis bending

$$M_{pc} = 1.19\ [1 - (P/P_y)^2]\ M_p \text{ for } P/P_y > 0.40 \qquad (6.9)$$

These equations imply an equilibrium of forces at a cross section of a member subjected to moment and axial compression. However, the stiffness of the member is undefined except that it is assumed to be elastic between adjacent cross sections at M_p. However the members have many cross sections at moments causing yielding but not at M_p. Figure 6.15 shows that yielding which reduces the stiffness of the frame occurred above and below the panel zone in the column of Frame A.

The partially plastic or simply inelastic analysis would be more appropriate for column members in a frame especially for bending of members about their minor axes where the shape factor is very significant.[60] For this case, the experimental behavior of the frame would indicate an overall softening of the load versus deflection characteristics.

Because of the softening effect, the frame must deflect more at a given horizontal load. At this increased deflection, the P-Δ effects on the frame are increased thereby producing an additional deflection, known as "secondary deflection".

The stress versus strain characteristics indicate a general softening when the stresses are reversed repeatedly in the inelastic

range. The softening is exhibited in two ways. First, the extent of the essentially linear behavior when the stress is reversed becomes less than two times the basic yield stress during the initial monotonic loading. A previous investigation shows the nonlinearity beginning immediately after reversal of stress with the rate of nonlinearity increasing more rapidly after a reversed stress of one times the basic yield stress is applied.[58] The nonlinearity is gradually rounded and is the indication observed by Bauschinger. The nonlinearity of measured stress versus strain characteristics of tension-compression and compression-tension specimens has been included in the investigation by Side-bottom and Chang[58] to determine the influence of Bauschinger's effect on the inelastic bending of beams. Younger[59] has also indicated the considerable nonlinearities in copper alloys subjected to reversed straining at several amplitudes.

Secondly, when the coupon is subjected to repeatedly reversed stresses at a given amplitude the essentially linear slope upon reversed stressing becomes flatter as a function of the number of cycles. The reasons for the general softening apparently lie in the micro-structural behavior of the metal and the micro-residual stresses and strains existing in the metal's structure throughout the loading history. In the absence of fracture, the effect may be considered to be small and negligible for steel structures in the realm of the severely reversed loading problem. Any softening of the basic macroscopic behavior of the material will correspondingly soften the moment versus curvature relationship for the members and the resulting load

versus deflection characteristics of the structure with successive cycles.

Several effects are likely to be present when the actual differential areas of a cross section are assumed to arrive at the member's properties at each location along its length. The yielding of the beam flange occurred initially near the column flanges. These yield lines were at 45^{o} to the axis of the beam flanges and in the plane of the flange plate on the tension flanges of the beam. On the compression flanges of the beam the initial yielding occurred at 90^{o} ro the axis of the flange and in the plane of the plate. However, both types of yield bands progressed at 45^{o} through the thickness of the flange plates.

As this situation is progressing near the ends of the beams the web elements are still elastic since they are located near the neutral axis of the beam. At higher moments and corresponding curvatures some of the web elements will yield while the elements nearest the neutral axis do not yield until severe curvatures are present. The flange elements are at various strains below and above strain hardening strain macroscopically. The residual strains in the beam due to cooling, straightening, welding and prior loading history also affect the initiation of the nonlinear straining.

At the microscopic level the whole process of yielding is discontinuous. The discontinuous nature of the yielding is exhibited macroscopically by the bands of yield lines wherein the material is at

strain hardening strains and between the bands the material is below yield strain.

Strains were measured on the web of the welded beam of Frame C as well as on the flanges. The locations of the strain gages permitted two sets of measurements to be taken independently during the test. These measurements were used to compute the average experimental moment for the one inch long beam segment defined by the one inch gage length of the strain gages. These same strain gages permit an examination of the average strain distribution for the one inch segment of the beam. The two strain gages at each level of the cross section were averaged and the four average strains plotted in Figs. 6.16 and 6.17. For the cases shown, the cycles 4, 15, 25 and 32, initially indicate an approximately linear strain distribution.

The latter of these first cycles indicates a nonlinear strain distribution for the compression side of the beam only. Cycles 41 an 48, however do not indicate a discernable behavior. The lack of apparent uniformity in the strain readings for cycles 41 and 48 is due in part to the extremely yielded situation in the member including the web and the behavioral changes occurring throughout the frame. The nonlinearity is also affected by the local buckling of the beam flanges and the reliability of the strain gages when used at large strains. The principal cause for the apparent lack of uniformity at large amplitude cycles is believed to be the local buckling of the beam flanges in each of the strain gage locations on the flanges. The evidence presented and other experimental observations lead to a conclusion that the strain distribution

remains linear at least up to initial yielding and after initial yielding in the absence of local buckling.

An additional source of nonlinearity is removed in the analysis by the assumption that there is no axial load effect on the strains in the beam although a small axial load exists at all times (up to values of $\pm$ 10 kips due to horizontal loading). Initial axial load existed in the test frames due to welding since the tops and bottoms of the columns were restrained to a greater degree than the center portion of the columns.

In conclusion, the experimental results should be expected to indicate an overall softening relative to the Ramberg-Osgood solution as presented herein.

6.4 Stability of Load Versus Deflection Hysteresis Loops

Two effects are apparent analytically and experimentally during the stabilization of the load versus deflection hysteresis loops at various amplitudes of deflection.

The first effect is exhibited by a "shaking down" to "elastic" conditions for a frame which previously had a plastic hinge or a pronounced rounding of the hysteresis loop. Figure 6.18 indicates the effect analytically by a first-order elastic-plastic analysis on a single-story frame. The figure shows a rapid stabilization to an elastic condition of the frame. Figure 6.19 gives experimental corroboration of this type of stabilization although some nonlinear characteristics remain after stabilization.

The second effect concerns the stabilization of the hysteresis loops of the larger amplitude nonlinear cycles. Figure 6.2 showing the cycles for the elastic-plastic analyses of the three-story Frame B indicates the stabilization of the shape and size of the hysteresis loops after approximately two half cycles. Observation of Fig. 6.20 for Frame A and Fig. 6.21 for Frame B indicates the stability of the shape and size of the hysteresis loops. The analytical and experimental results presented above indicate that the hysteresis loops do stabilize for all of the large amplitude cycles even for deflections larger than the deflection at the maximum horizontal load.

Table 1 gives the comparison of the respective experimental and analytical areas within hysteresis loops for Frame B. The results for the alternate Frame B are also indicated to continue with the comparison of the lighter weight alternate to the three-story frame. The general observation is that the elastic-plastic hysteresis loop areas are somewhat greater than the experimental curves. Secondly the areas included in the hysteresis loops for the alternate Frame B are not greatly reduced from the areas given for Frame B itself.

Figure 6.21 shows that the hysteresis loops become very stable even for the large deflection amplitudes for Frame B. However, Frame C which had the non-compact beam did indicate slight variations with successive cycles which is indicated in Fig. 6.22. Refinements of the current code provisions should provide for a wide range of b/t values and lateral bracing spacings including values above the currently

fixed limits which when combined give consistent designs for the beams during reversed loadings.

In conclusion, both analytical and experimental results presented herein indicate that the load versus deflection hysteresis loops are stable in size and shape within relatively small variations even for a large b/t of a beam and for large amplitude cycles.

7. DESIGN IMPLICATIONS

The weak-beam strong-column design has adequate validity in earthquake zones when adequately proportioned and braced members are fully welded together as the frame. As shown the present designs on a monotonic basis for ultimate capacity have a large reserve during reversed loading. Alternate Frame B has been shown analytically to possess adequate ability to perform the function for which Frame B was designed and for 13% less steel.

The effects of ductility can be dealt with directly once the section and steel have been defined by calculating the Ramberg-Osgood moment-curvature relationship (or just assuming one) and then inserting the hysteretic behavior directly into the dynamic frame response calculations. A percentage of critical damping can still be considered in the dynamic analysis since a significant portion of the frame's response is elastic or nearly so. The response characteristics of fixed partitions, floor slabs, curtain walls, etc. should be evaluated so their effects can be more rationally included in the dynamic analysis-perhaps as a combination of hysteretic behavior, coulomb and viscous damping.

As has been discovered during many inspections after major earthquakes, the structural details must be carefully attended to during the design process. The details used in the frames described herein were found to be adequate. Some savings may be realized by

only bolting the web of the beam to the erection angle. The hysteretic behavior is stable during both conditions of fastening. Joint stiffening against shear deformations was found to be necessary to realize the largest load response of the frame during large amplitude cycles. However, frames could still be designed allowing for the unstiffened joint once the inelastic behaviors of unstiffened joints can be properly evaluated for their complete behavior during reversed loading. In either case, the hysteretic behavior of the frame is stable.

The problem of proper lateral bracing of the beam members is reduced since the frames of a typical building are considered to be attached to the floor deck and slab.

Comparison of the experimental results of Frames A and C shows that local buckling does not constitute "failure." However, since the effective bracing spacing used during the test of Frame C was more favorable (since r_y for the Frame C beam was about 40 percent greater), some care should be taken when comparing the respective behavior of these frames.

In addition, Frame C showed that under severe strain conditions, the possibility of low cycle fatigue of the base metal near the welds should be investigated.

The local buckling of the beam flanges during equal amplitude cycling of the frame does not occur and disappear alternately. The alternating buckling and complete straightening does not occur since

gravity loads are also on the beam. Therefore, the completely reversed conditions which have been used previously in cantilever beam tests should be applied carefully to the behavior of frames with gravity loads on the beams.

The problem of alternating plasticity does not occur for the strong-column weak-beam design with significant gravity loads on the beam. However, incremental collapse or deflection instability of the beam is a possibility. The results of vertical beam deflection show a gradual drop in the level of the beam for each amplitude of displacement applied to the frames. But the maximum displacement remains constant during the repetition of cycles at a given amplitude. The amount of the total permanent vertical deflection movement would be of concern when the design is based on a given damage estimate and when architectural details of suspended ceilings and mechanical distribution systems are positioned and supported by the beam and slab.

The analytical comparison shows the effects of the spread of yielding and Bauschinger effect on the shape of the hysteresis loops especially in the elastic-plastic case. The analytical comparison also indicated the need to take into account the second order effect of the gravity loads acting through the sway displacement on the behavior of the frame.

Design of shear stiffening for the panel zones at the beam-to-column intersections for all frames was based on the maximum shearing resistance provided by the web and the shear stiffening. Each frame required additional stiffening since the web capacity was equal

to approximately one-half of the total requirement. The design method used is based on the maximum beam moment which can be applied to the connection as being equal to the fully plastic moment of the cross-section. Previous frame testing programs usually placed heavy stiffening in the panel zones to ensure that inelastic behavior would occur only in the clear span of the members. Secondly, previous frame testing programs usually were concerned with monotonically increasing lateral loadings. Generally the effects of strain hardening in these situations is small until the frame instability load has been reached or a mechanism has formed. The behavior of panel zones with various methods of stiffening and strengthening against the effects of tension distortion, web crippling and shear have not been thoroughly researched from the behavioral point of view. The effects of the coexisting axial load from the stories above on a given panel zone are still a subject of concern. The behavior of the panel zone during load reversals and adequate ductility or rotation capacity are of primary concern here.

The test results presented herein show the beam moment applied to the column to be larger in magnitude than the fully plastic moment. This increased moment can be anticipated by observing the basic moment versus curvature diagram during reversed and repeated curvatures. The test results also indicate the magnitude of the moment which was actually present in the members. Further the general yielding of the shear stiffening and the web of the column in the panel zone indicate that the applied moment exceeded the fully plastic moment. In addition, the welds at the ends of the diagonal stiffening fractured at advanced stages of the tests. The weld cracks may be

precipitated by the quality of fabrication, but more likely the severely constrained weld attempted to absorb strains greater than the fracture strain during the reversed and repeated loading on the weld. In addition, the rigidity of the pair of diagonal stiffeners is greater than the rigidity of the web of the column in shear which leads to a higher proportion of load on the stiffener.

Two primary effects on the behavior of the panel zones subjected to reversed and repeated loads can be anticipated from the previous comments. Primarily, the anticipated moments for design of the shear stiffening, tension distortion and web crippling should be based on an increased moment of approximately 1.2 times the fully plastic moment for situations which are similar to those tested herein. Secondly, the shearing deformation of the panel zone should be anticipated in the analysis of the overall frame. The load versus deformation behavior is required since it is clearly nonlinear and especially so in the case of the diagonally stiffened panel zone. The diagonally stiffened case could be represented by an overall behavior of the trilinear type.

By comparison the panel zone which was shear stiffened by means of doubler plates on both sides of the web yielded extensively during the tests as with the diagonally stiffened panel zone but had no visual evidence of weld failures.

8. GENERIC AREAS FOR CONTINUING RESEARCH

Several areas of research which relate directly to the problems discussed previously are delineated in the following paragraphs.

1. The low cycle tension-compression data now available for copper alloys should be duplicated for the structural steels. In particular, the properties should be observed from a behavioral point of view with the fatigue properties being of secondary importance.
2. Additional research should concentrate on the behavior of single members with steep moment gradient and uniform moment cases for beam members. Also, continuing research should be conducted on the effects of coexisting axial load on the behavior of bending members, i.e. beam-columns.
3. The behavior of stiffened and unstiffened connections requires continuing research to develop appropriate models to describe correlative experimental results. These models should also be capable of placement within a multi-story frame analysis computational program which uses member centerlines to describe the frame.
4. The inelastic behavior of the flanges of the beam at and near their attachment to the column flanges should be further investigated due to the biaxial state which exists at this location. The effects on moving the

center of rotation of the "plastic hinge" on the behavior of the elastic-perfectly plastic frame should be studied, since the elastic-plastic characteristics are the simplest to implant in a large frame analysis program.

5. Analytical evaluations of the many parameters which are involved in making theoretical evaluations more meaningful should be researched considerably beyond the current level. Emphasis should be placed on derivation of more complete analytical models from which simplified methods of design of frames subjected to reversed and repeated loads can be proposed.
6. Extend analytical technique to include effects of inelastic behavior in columns.
7. Continuing studies should be carried out on "full-scale" structures in a "shake-table" environment with earthquake excitations to indicate more fully the behavior of structures. Analytical studies should be concerned with a dynamic environment, utilizing the theoretical evaluation techniques described in Item 5 above.
8. Design techniques and code provisions should be developed based on the analytical and experimental research to date as well as the continuing research program indicated in Items 1 through 6.

9. SUMMARY AND CONCLUSIONS

An analytical method to define the behavior of steel frames subjected to gravity loads and repeated and reversed lateral loads or displacements has been described. The method is based on a second-order analysis of the frame so herein the beams are represented by a series of interconnected segments. Each beam segment is characterized by its moment versus curvature relationship in a Ramberg-Osgood type formulation. Generality permits different coefficients and exponents for the exponential term for the skeleton curve and the hysteresis curve. The technique is similar to that employed by Berg and Goel in their studies.

The effects of size of segments, incremental force, and deformation parameters were evaluated for their sensitivity on the analysis. Variations of the characteristics of the end segments of the beam indicated that a small increase in load would result when the effects of the finite size of the beam-to-column intersection were included in the analysis. The effects of variation in the Ramberg-Osgood coefficient and exponent as well as the effects of different values of the parameters are used for the skeleton curve and the hysteresis curves were examined.

Nonlinear effects which are not included or only partially accounted for in the analysis but which are exhibited in the tested frames have been discussed.

The stability of size and shape of the analytically determined load versus deflection hysteresis loops has been shown. The analytical results indicate that the stabilization occurs within two half cycles.

A series of tests on three full-scale steel frames was described. The plastic design method used for the frames initially assumes a likely-to-occur mechanism. Then a check is made that the plastic moment capacities (or reduced capacities for axially loaded members) are not exceeded. The test frames were analyzed for their second-order elastic-plastic behavior and checks were made at the working loads against the allowable stresses. The connections were typical of those used in earthquake active regions and the panel zones were reinforced according to plastic design methods.

The experiments have centered on the characteristics of the frames which had coexisting constant gravity loads during reversed amplitude cycling. Each of the frames was subjected to constant gravity loads at the working load value and a program of cycled displacements of the top of each frame. The experimental behavior indicated a considerable increase in lateral load capacity during reversed loading of up to 40% greater than an elastic plastic prediction of the frames indicated for a monotonic lateral loading. The experiments also indicated a gradual unloading slope after the deflection at the maximum horizontal loading had been exceeded. This effect was due primarily to strain hardening.

Comparisons of the experimental results with a second-order

elastic perfectly plastic reversed loading analytical solution show clearly the importance of the Bauschinger effect in the material and the spread of yielded zones near plastic hinges. The additional moments due to the gravity loads acting at the relative story sways is also obvious especially for the larger amplitudes of deflection. In addition, the stability of the lateral load versus deflection hysteresis loops for consecutively repeated displacement amplitudes was evident for all three frames. However, the maximum loads did decrease slightly for consecutive cycles at the same amplitude for Frame C which had a beam with $b/t = 21$. For Frames A and B which had extensive yielding of both beam flanges between each load point and the column, the maximum loads were consistent even though a progressive lateral (out-of-plane) movement of the yielded top flanges occurred.

The behavior of both types of shear stiffened panel zones was good even though the web and the stiffening were completely yielded during later portions of each test. However, the weld at the end of the diagonal stiffeners in all tests did break midway through the tests. The results also indicated that the reversed load behavior of Frame C was not altered by having the beam web bolted to the column flange rather than welded. The results of Frame C also indicated that the lateral load capacity of the frame was reduced with the shear stiffening removed from the panel zones.

Based on a comparison of the test results with the monotonic capacity of the frames, designs using the strong (elastic) column-weak beam approach should be satisfactory and conservative. However, attention to the details of the connections and the design moments for the shear stiffening is necessary.

The experimental results were also compared with the results obtained from the second-order, elastic-plastic predictions which utilized a Ramberg-Osgood function to define the moment versus curvature characteristics of each cross section of the beam. The correlation between the tests and reversed load estimates given by the Ramberg-Osgood formulation is good. However, the appropriate values of the parameters in the Ramberg-Osgood moment versus curvature relationship are not completely defined, in general. Various comparisons show that the combination of the parameters gleaned from other investigations does give a good estimate for the frames tested.

Based on the current investigation and other available experimental and analytical results, the estimate of frame response should be made with the following tentative values for the Ramberg-Osgood moment versus curvature parameters.

1) the value of M_y can be selected as the moment at first yielding including residual stresses but the most appropriate values tend to be nearer to 0.9 M_p. Therefore, select M_y as the value of first yield but without residual stresses included.
2) the value of ϕ_y should be selected to be approximately 1.15 to 1.20 times the basic elastic ϕ_y based on the M_y given in (1) above.
3) the Ramberg-Osgood exponent, R, should have two values and the value of R for the skeleton or locus curve can be taken as one-half the value used for the hysteresis curves. The value of R for the hysteresis curve is about 8 to 10.

4) the coefficient of the exponential term, α, should also have two values since the effects of a different value of α are necessary at this time and should be selected at 3/7 to 1/2 for both curves.

Areas for continuing and future research efforts generic to the reversed loading problem center around a better definition of the basic stress versus strain characteristics and member behavior. In addition, the analytical area should be more properly emphasized so that a more complete analytical model can be formulated to include beams, columns, and connection or panel zone characteristics. From the results of these and the continuing research more definitive design methods and code provisions can be formulated.

10. TABLES AND FIGURES

TABLE 1 COMPARISON OF AREAS WITHIN HYSTERESIS LOOPS

FRAME B EXP. CYCLE NO.	FRAME B MAX. Δ EAST (in.)	FRAME B MAX. Δ WEST (in.)	FRAME B LOOP AREA (kip-in.)	FRAME B ELASTIC-PLASTIC (kip-in.)	ALTERNATE FRAME B ELASTIC-PLASTIC (kip-in.)
16	+ 4.105	- 4.740	35.26	± 4.00"	
17	4.045	- 4.405	26.89		
18	4.110	- 4.410	22.47		
19	4.065	- 4.420	19.07		
20	4.045	- 4.425	18.81	32.4	42.4
21	5.045	- 5.470	60.17	± 5.00"	
22	5.070	- 5.425	48.32		
23	5.120	- 5.425	59.06		
25	5.105	- 5.605	59.27	109.0	102.6
26	6.055	- 6.510	106.95	± 6.00"	
31	6.385	- 6.535	106.41	185.6	162.6
32	6.980	- 7.455	159.41	± 7.00"	
33	7.010	- 7.420	185.94		
34	6.940	- 7.420	159.36		
35	6.960	- 7.425	166.75		
36	6.975	- 7.430	158.71	262.0	222.0
37	7.975	- 8.475	230.29	± 8.00"	
39	7.970	- 8.390	239.22		
40	7.965	- 8.395	234.69		
41	7.965	- 8.410	232.32	338.0	282.0
42	9.960	- 9.605	316.40	± 9.00"	
43	8.935	- 9.460	319.68		
44	8.980	- 9.475	311.70		
45	8.990	- 9.405	308.44		
46	8.970	- 9.410	309.12	415.8	342.0
47	10.030	-10.525	383.70	±10.00"	
49	9.960	-10.465	404.76		
50	10.035	-10.425	388.07	591.4	401.8

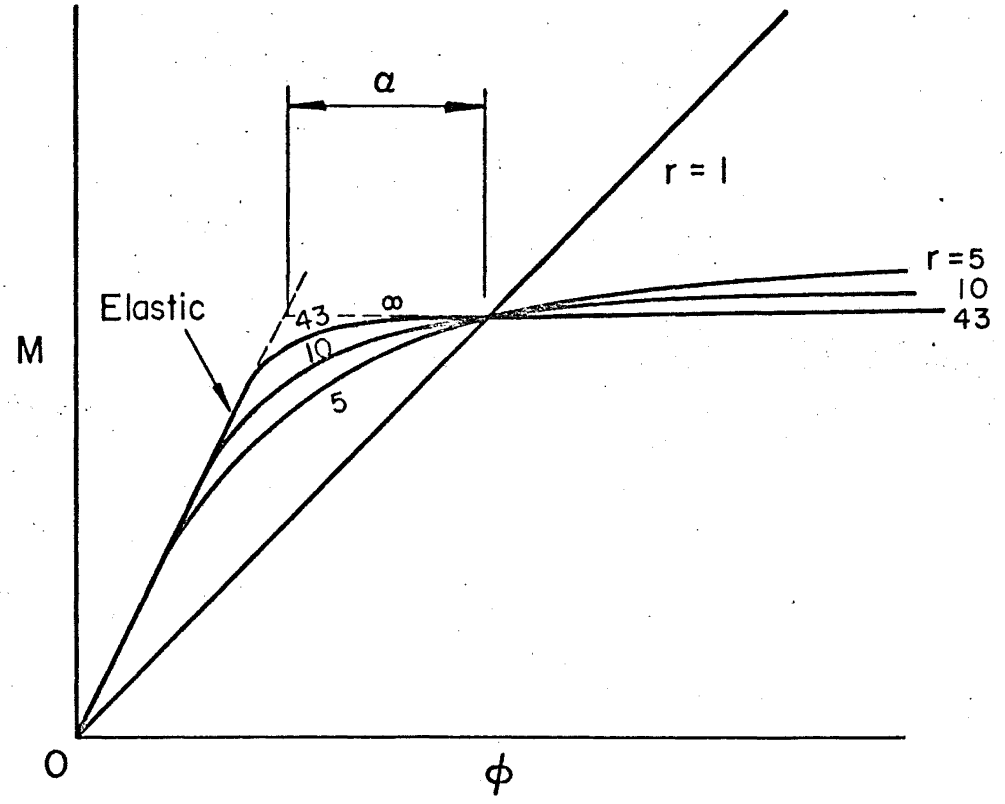

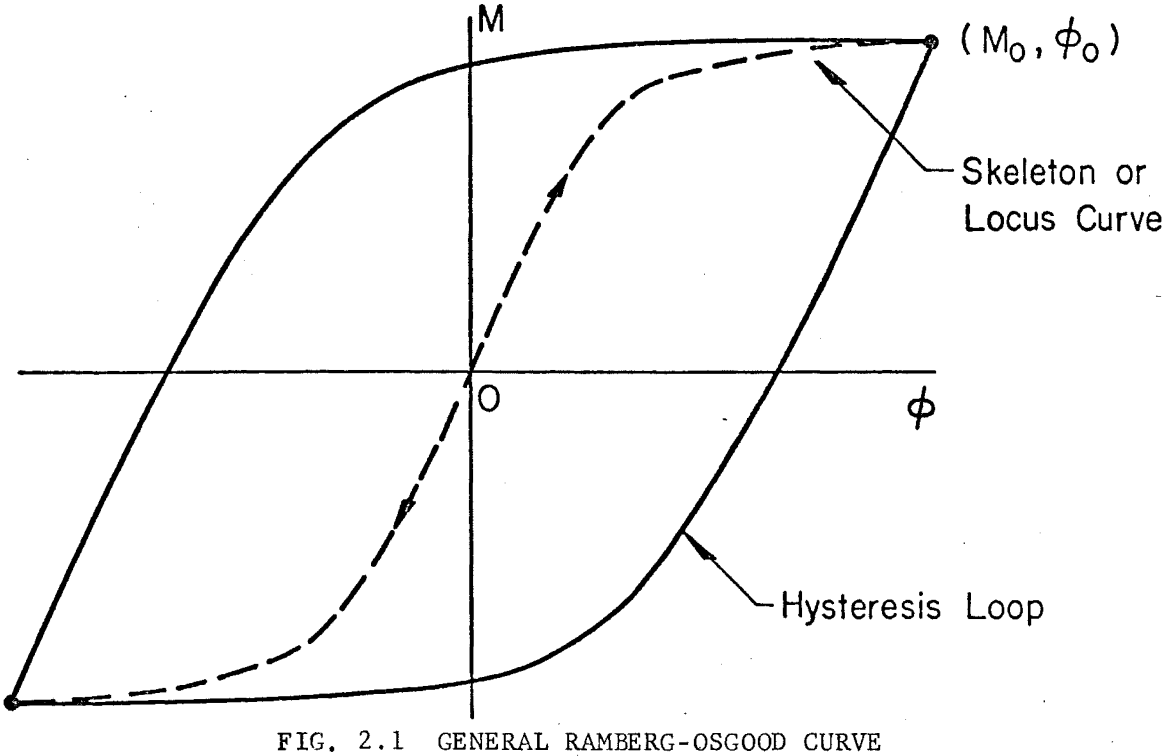

FIG. 2.1 GENERAL RAMBERG-OSGOOD CURVE

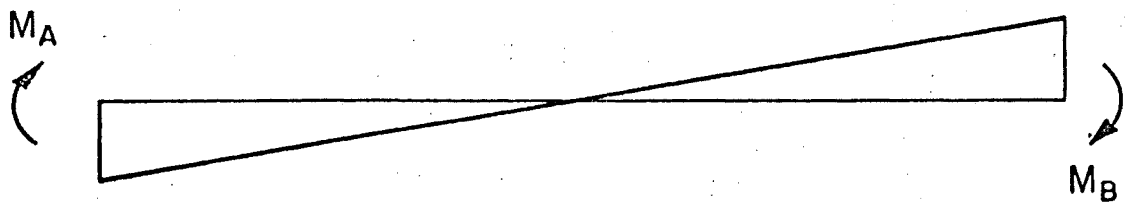

(a) INCREMENTAL HORIZONTAL LOAD MOMENT DIAGRAM

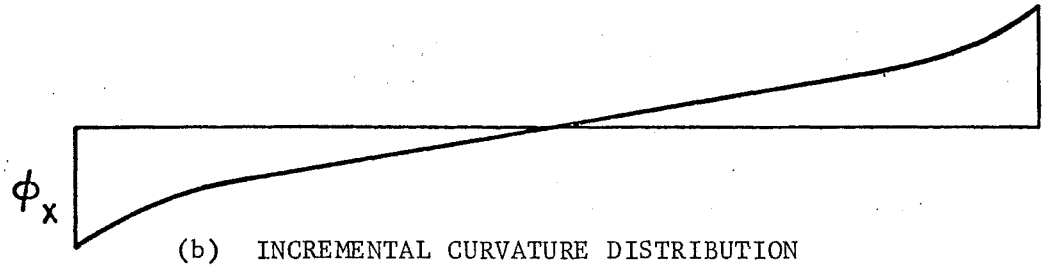

(b) INCREMENTAL CURVATURE DISTRIBUTION

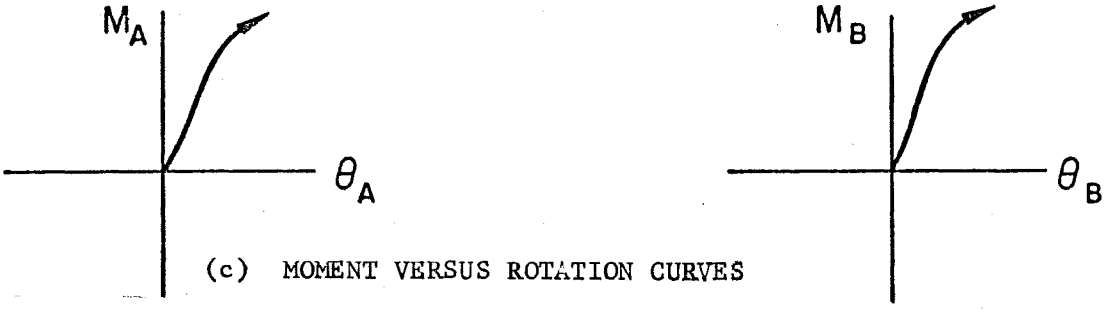

(c) MOMENT VERSUS ROTATION CURVES

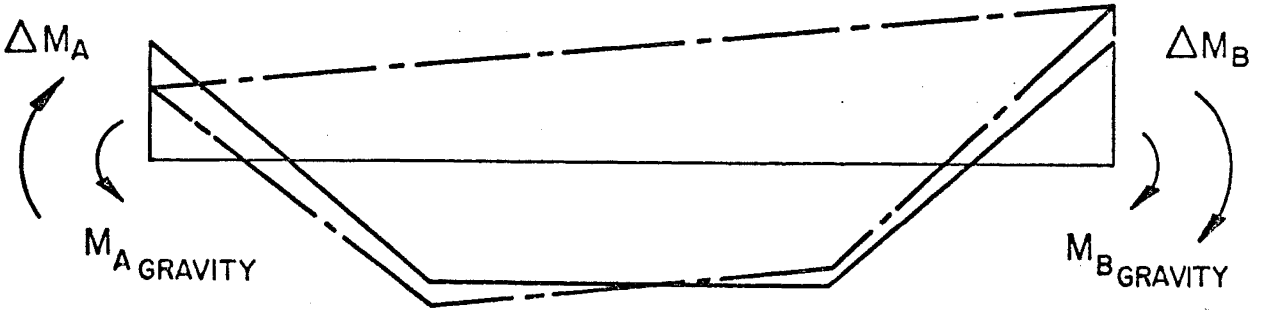

(d) INITIAL MOMENT DIAGRAM DUE TO GRAVITY LOADS

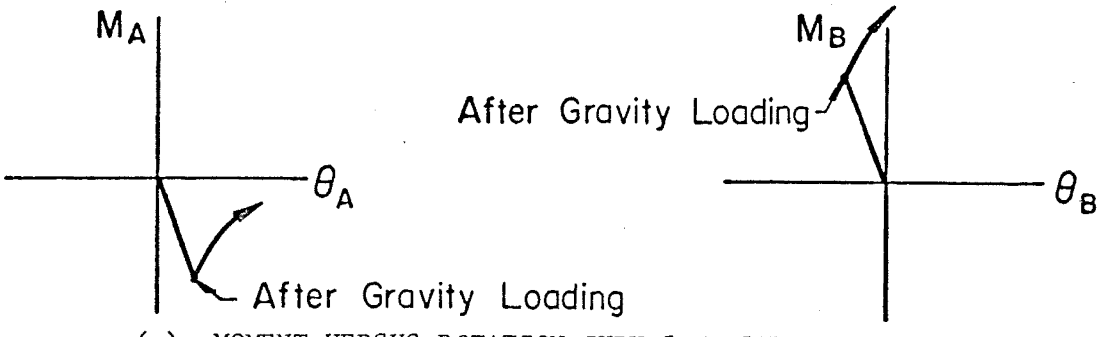

(e) MOMENT VERSUS ROTATION CURVES INCLUDING GRAVITY LOADS

FIG. 2.2 RAMBERG-OSGOOD BEAM

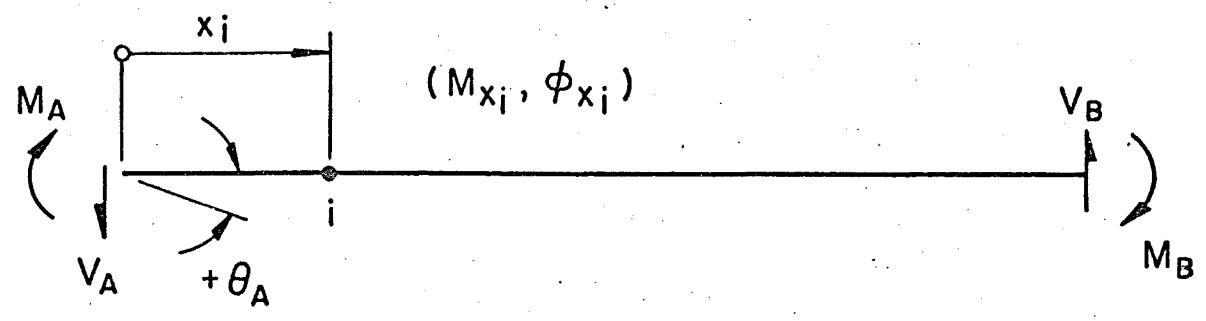

FIG. 2.3 RAMBERG-OSGOOD BEAM WITHOUT INTERMEDIATE LATERAL LOADS

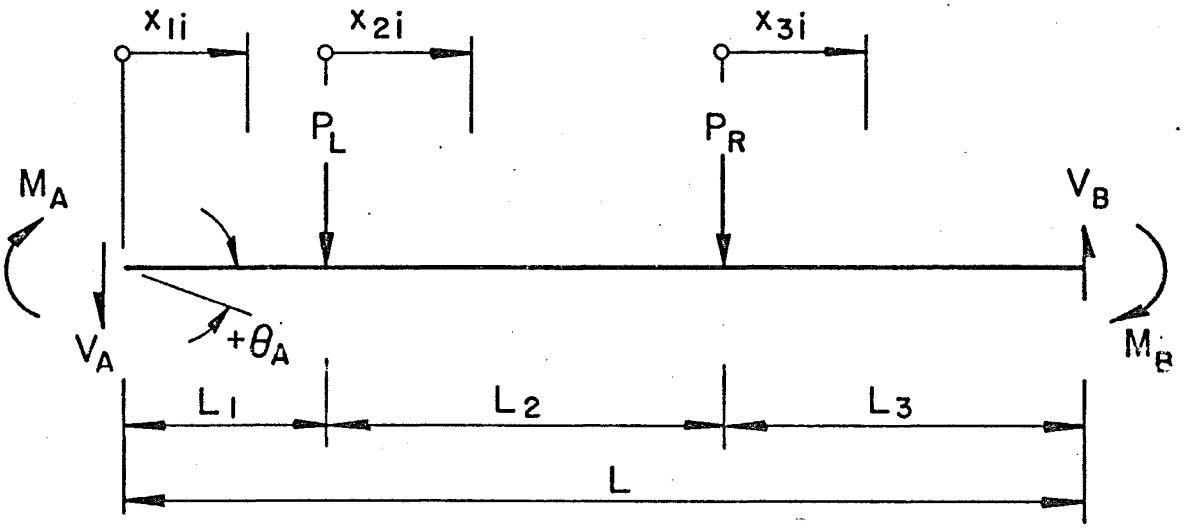

FIG. 2.4 RAMBERG-OSGOOD BEAM WITH TWO INTERMEDIATE LATERAL LOADS

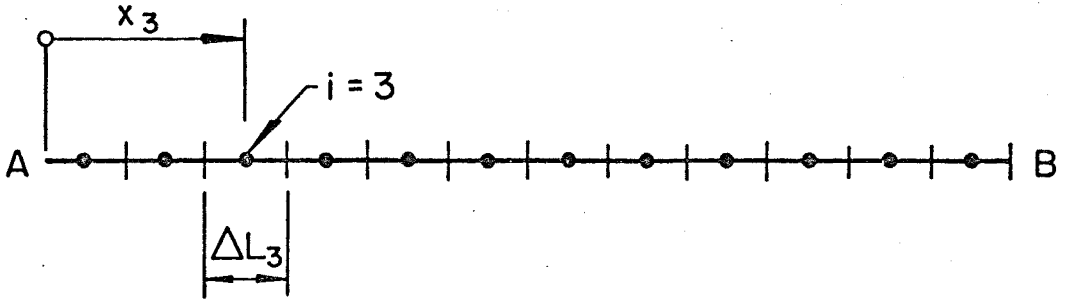

FIG. 2.5 LUMPED FLEXIBILITY BEAM MODEL

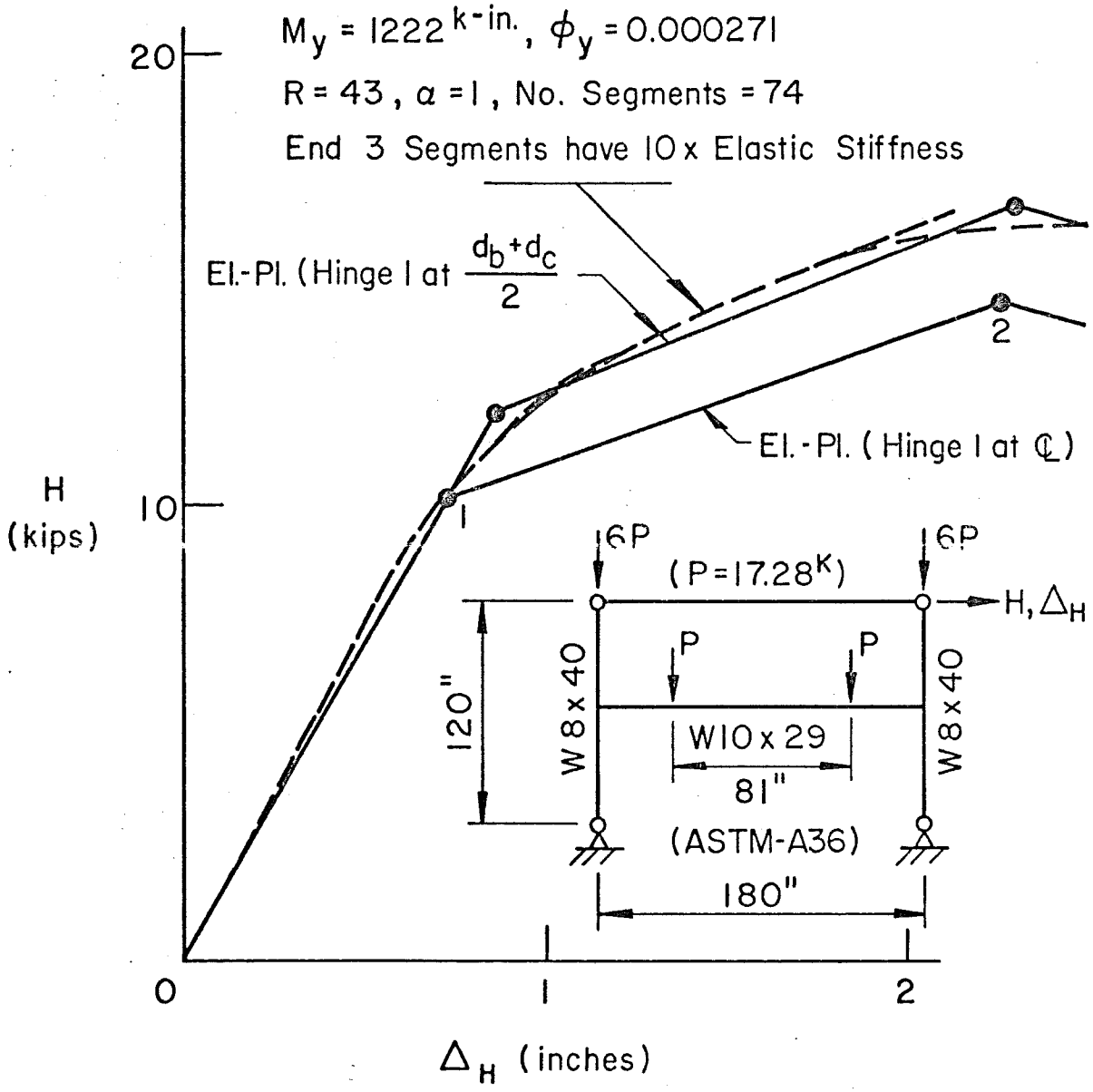

FIG. 3.1 EFFECT OF FINITE PANEL ZONE ON FRAME BEHAVIOR

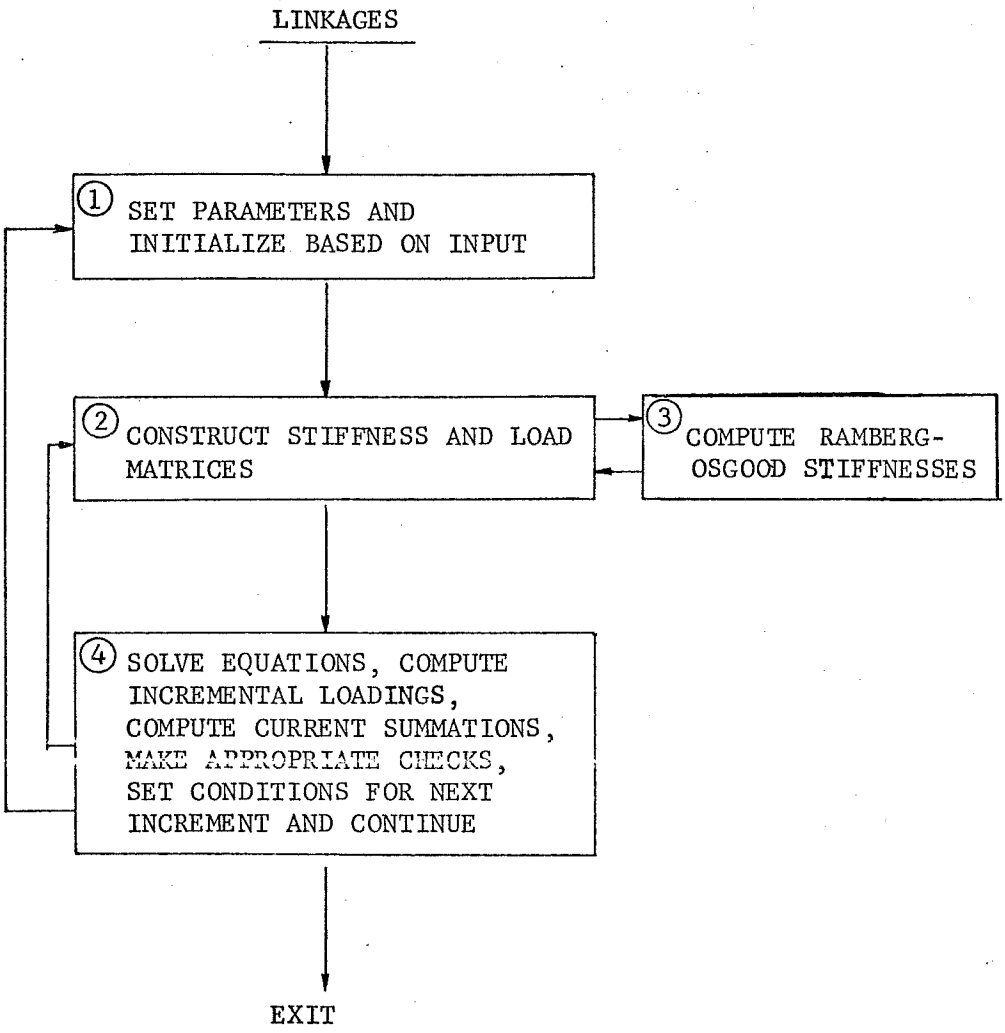

FIG. 3.2 GENERAL COMPUTATIONAL LOGIC

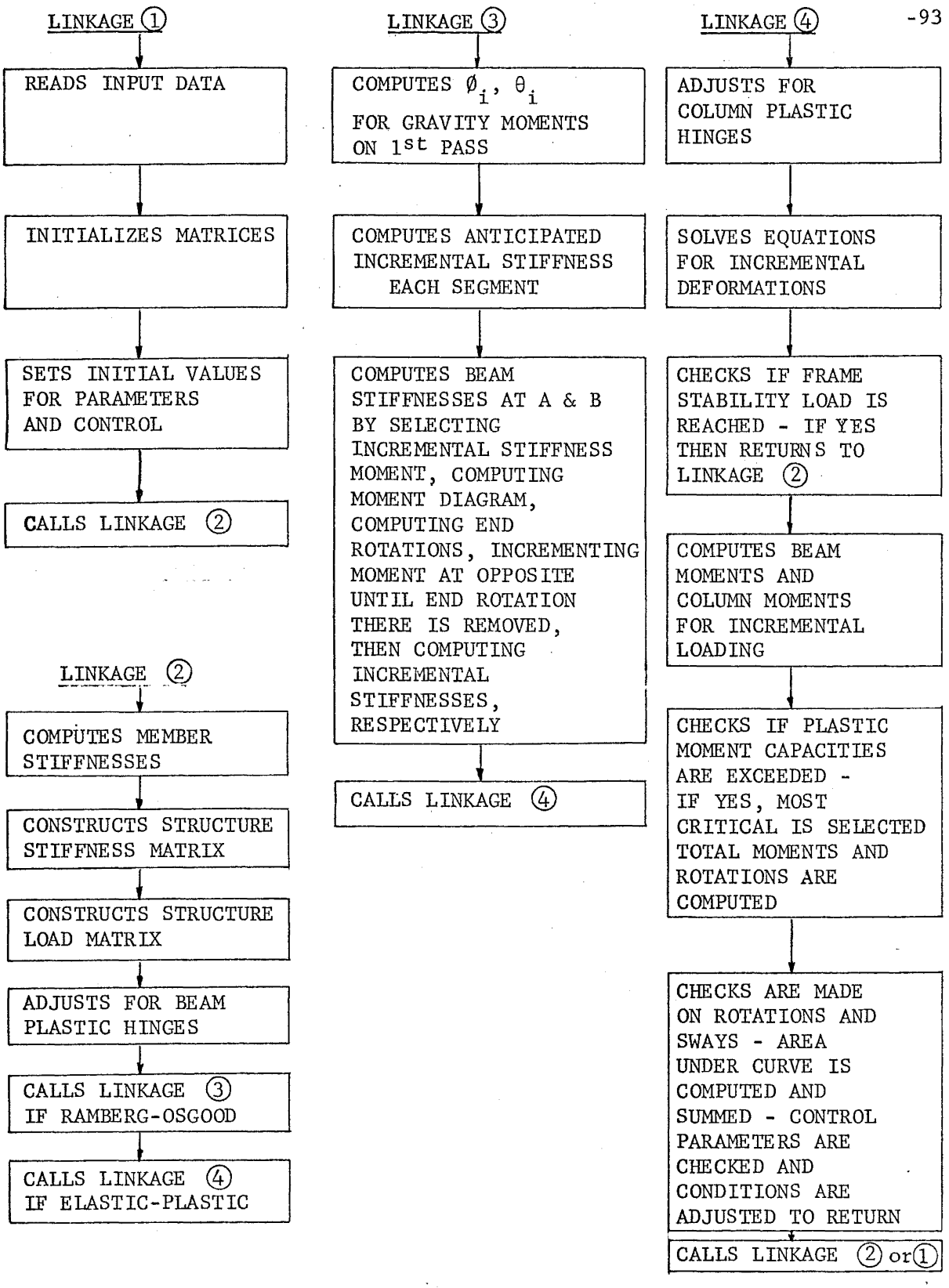

FIG. 3.3 LINKAGES FOR COMPUTATIONAL SCHEME

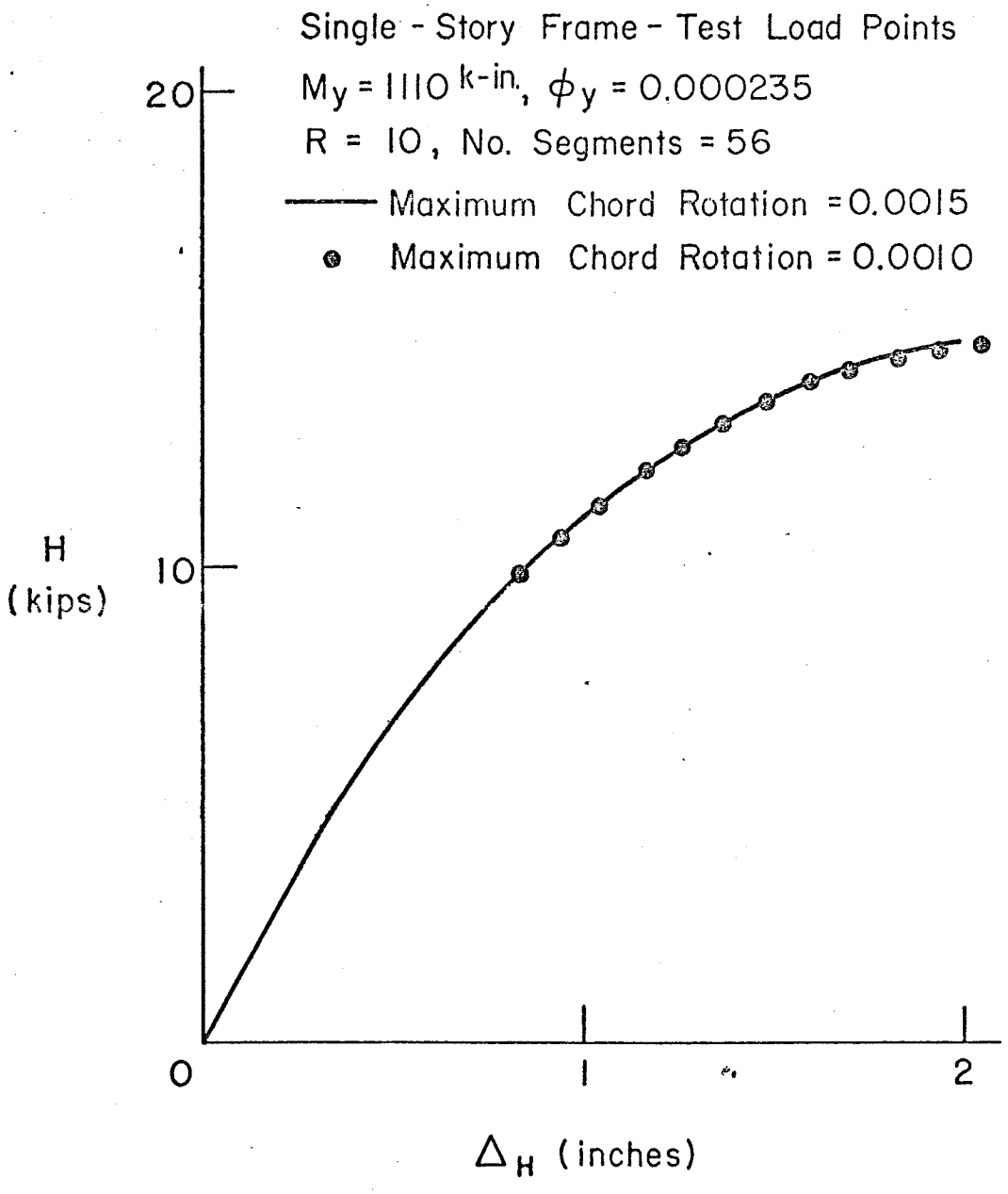

FIG. 3.4 EFFECT OF STORY CHORD ROTATION CONTROL

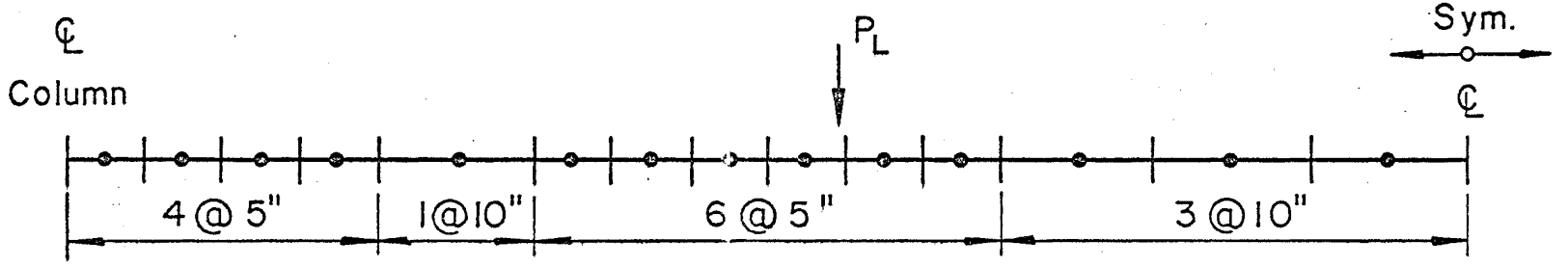

(a) TWENTY-EIGHT SEGMENTS

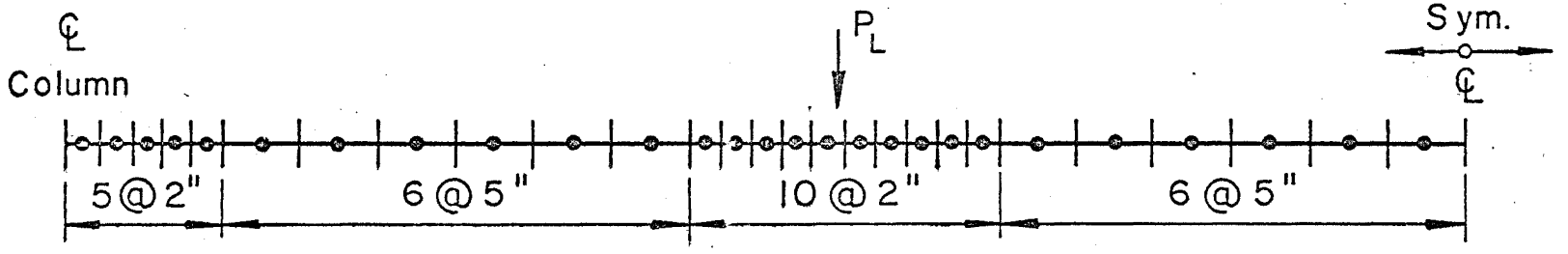

(b) FIFTY FOUR SEGMENTS

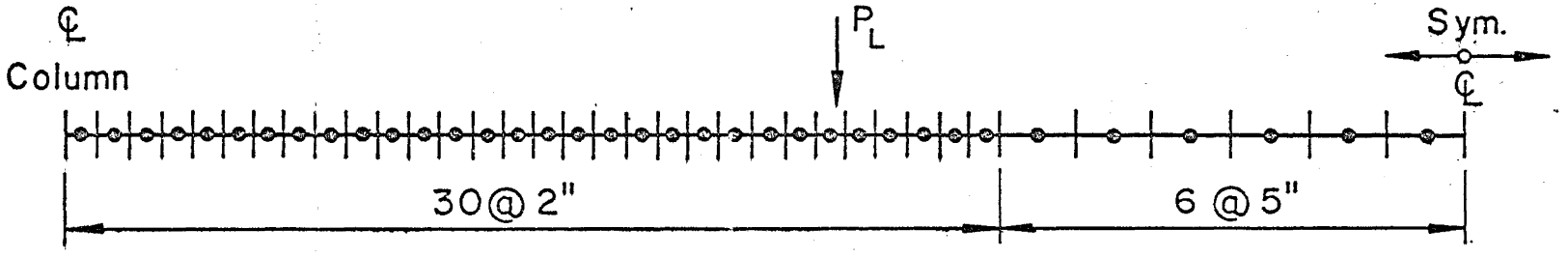

(c) SEVENTY TWO SEGMENTS

FIG. 3.5 TRIAL BEAM SEGMENTATIONS

Single Story Frame

Test Load Points

$M_y = 190^{k\text{-}in.}$, $\phi_y = 0.000252$

R = 10, End 3 Segments

I x Elastic

No. Seg. 74	No. Seg. 56
0.0" 0.0k	0.0" 0.0k
+1.90 +17.04	+1.90,+17.05
-1.80,-18.33	-1.80,-18.34
+1.90,+18.42	+1.90,+18.45
-1.80,-18.56	-1.80,-18.58
+1.90,+18.46	+1.90,+18.47
-1.80,-18.52	-1.80,-18.53

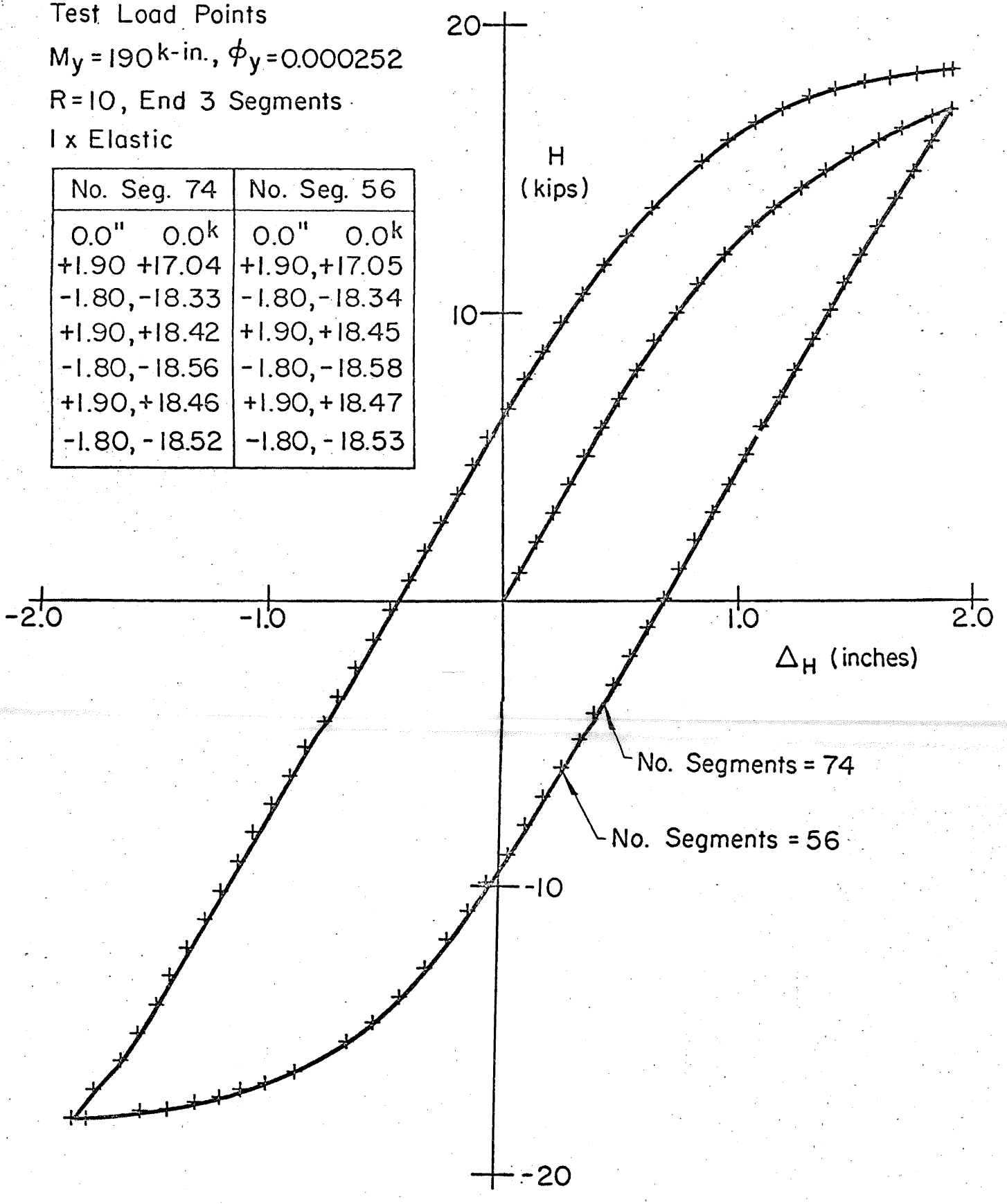

FIG. 3.6 EFFECTS OF SEGMENTATION ON PREDICTIONS OF FRAME BEHAVIOR

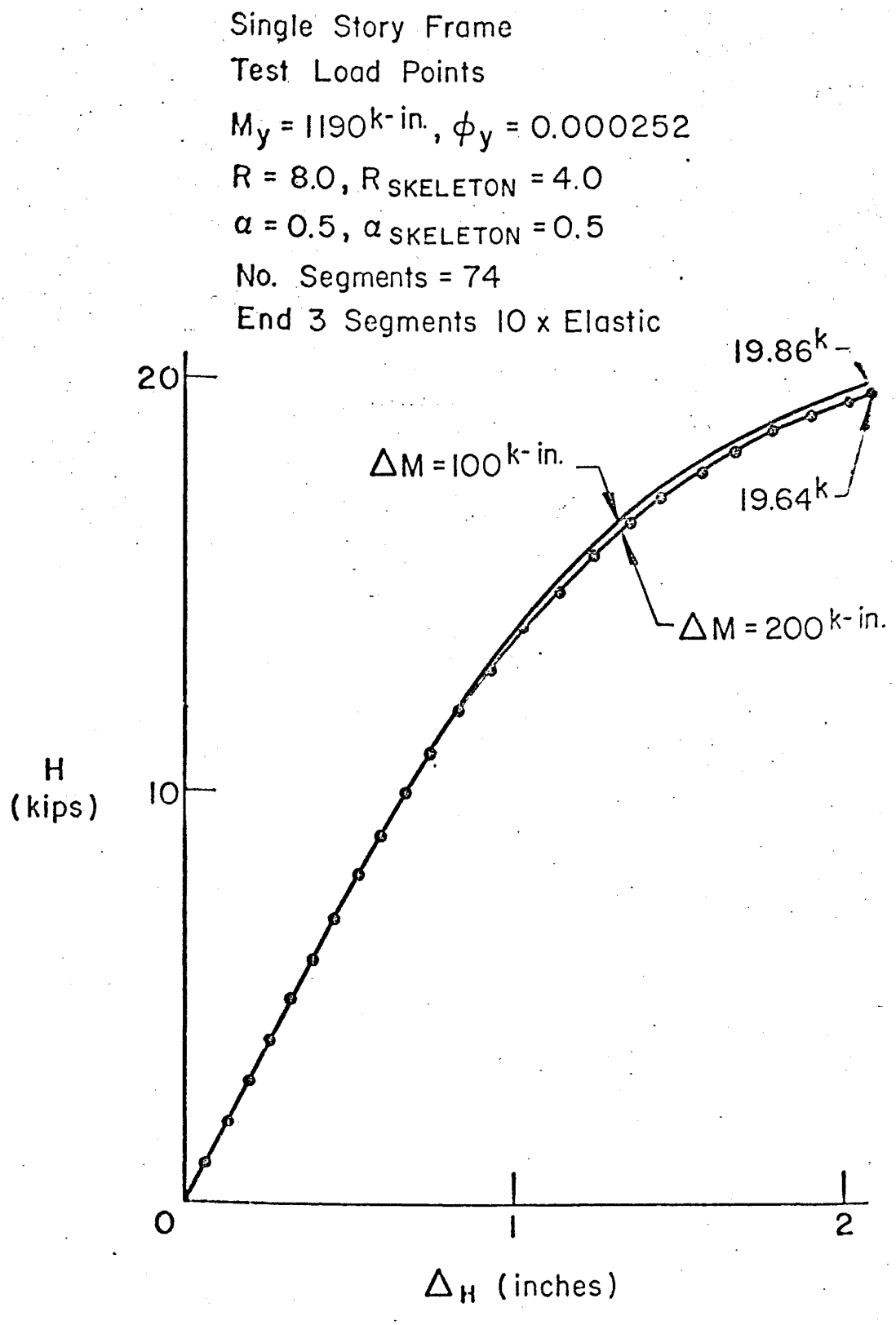

FIG. 3.7 EFFECT OF MAGNITUDE OF INCREMENTAL STIFFNESS MOMENT ON PREDICTIONS OF FRAME BEHAVIOR

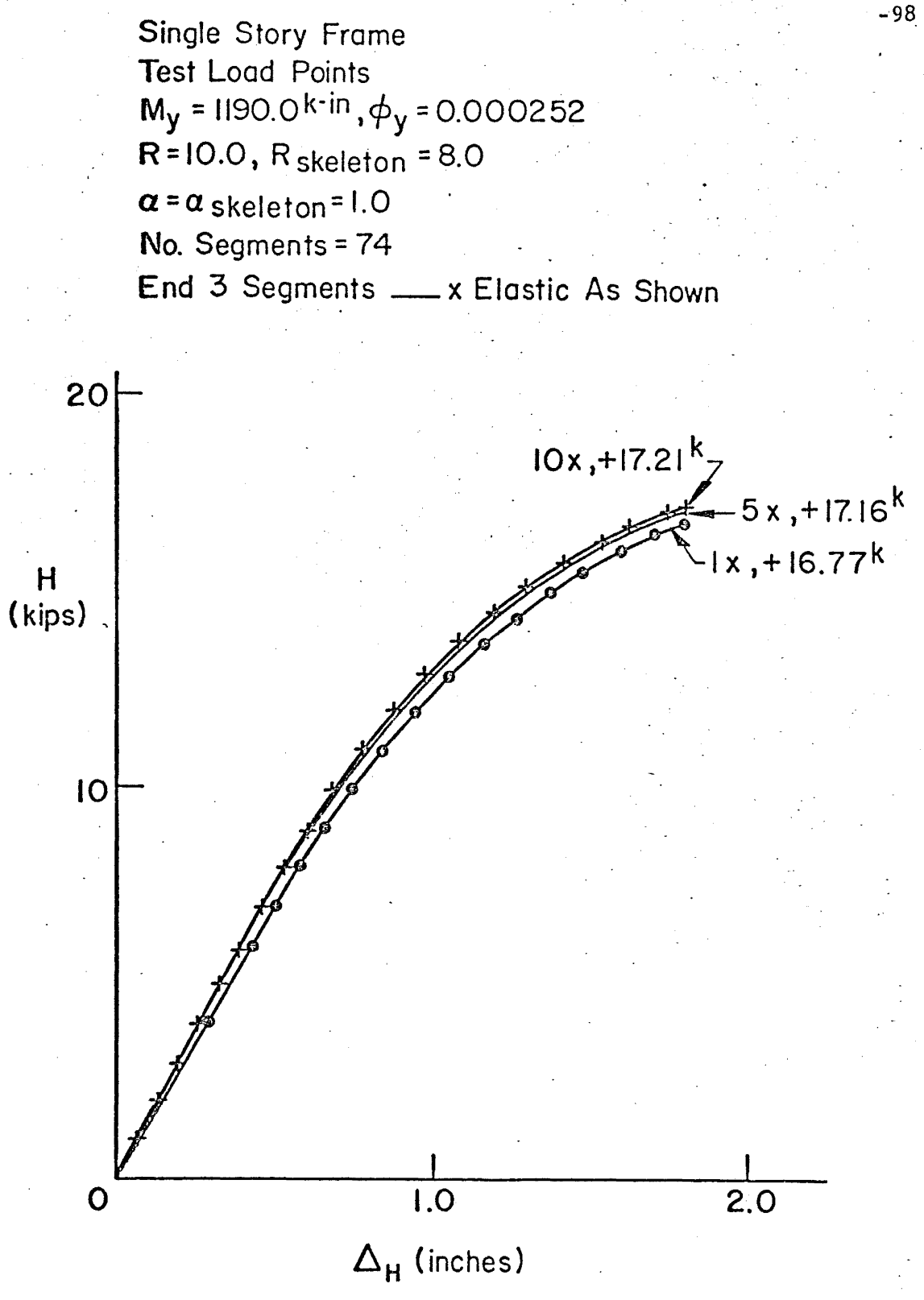

FIG. 3.8 EFFECTS OF STIFFNESS VARIATION OF END SEGMENTS ON PREDICTED LOAD-DEFLECTION CURVE

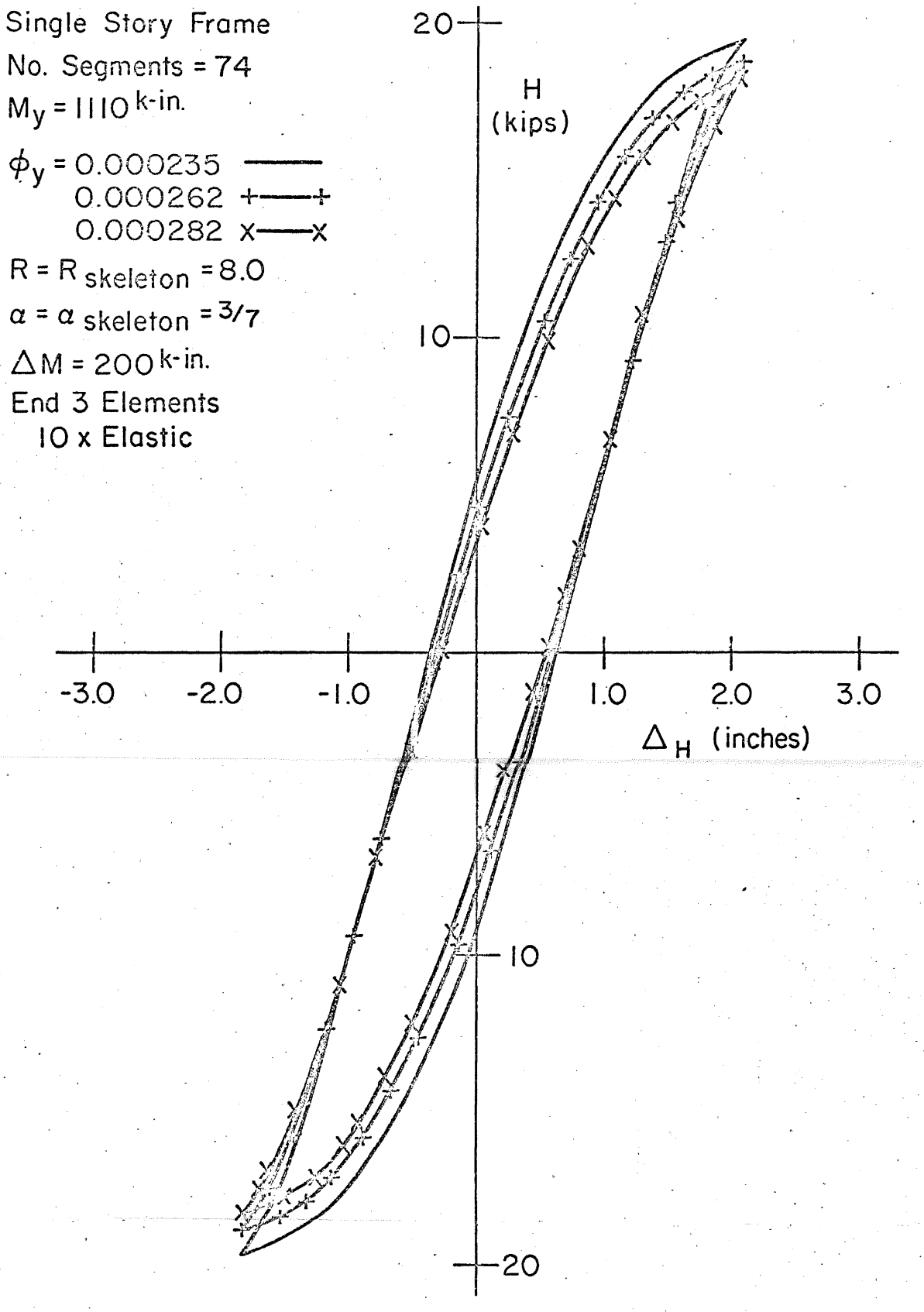

FIG. 3.9 EFFECT OF VARIATION OF ϕ_y ON PREDICTED FRAME BEHAVIOR

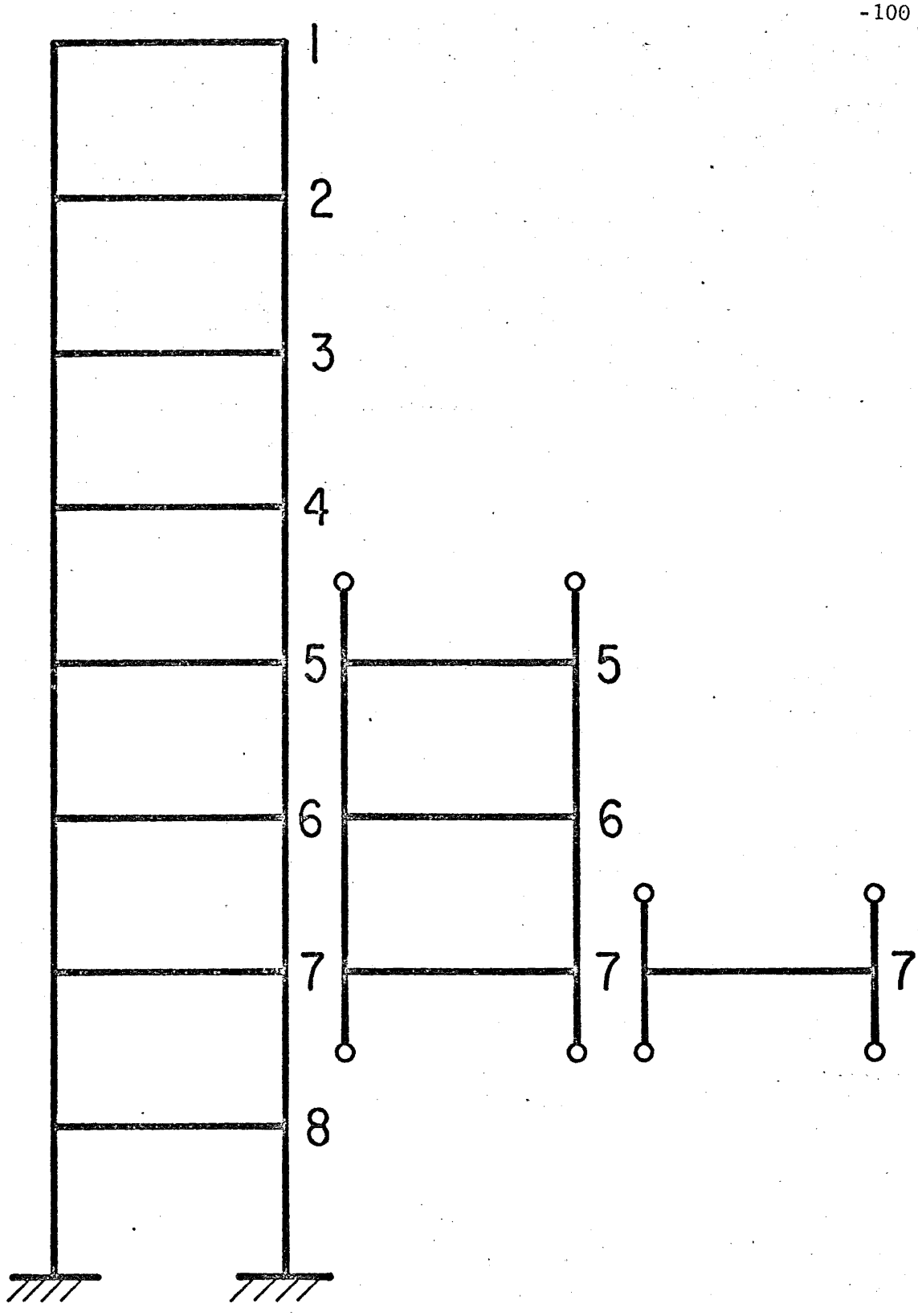

FIG. 4.1 PROTOTYPE STRUCTURE AND TEST FRAMES

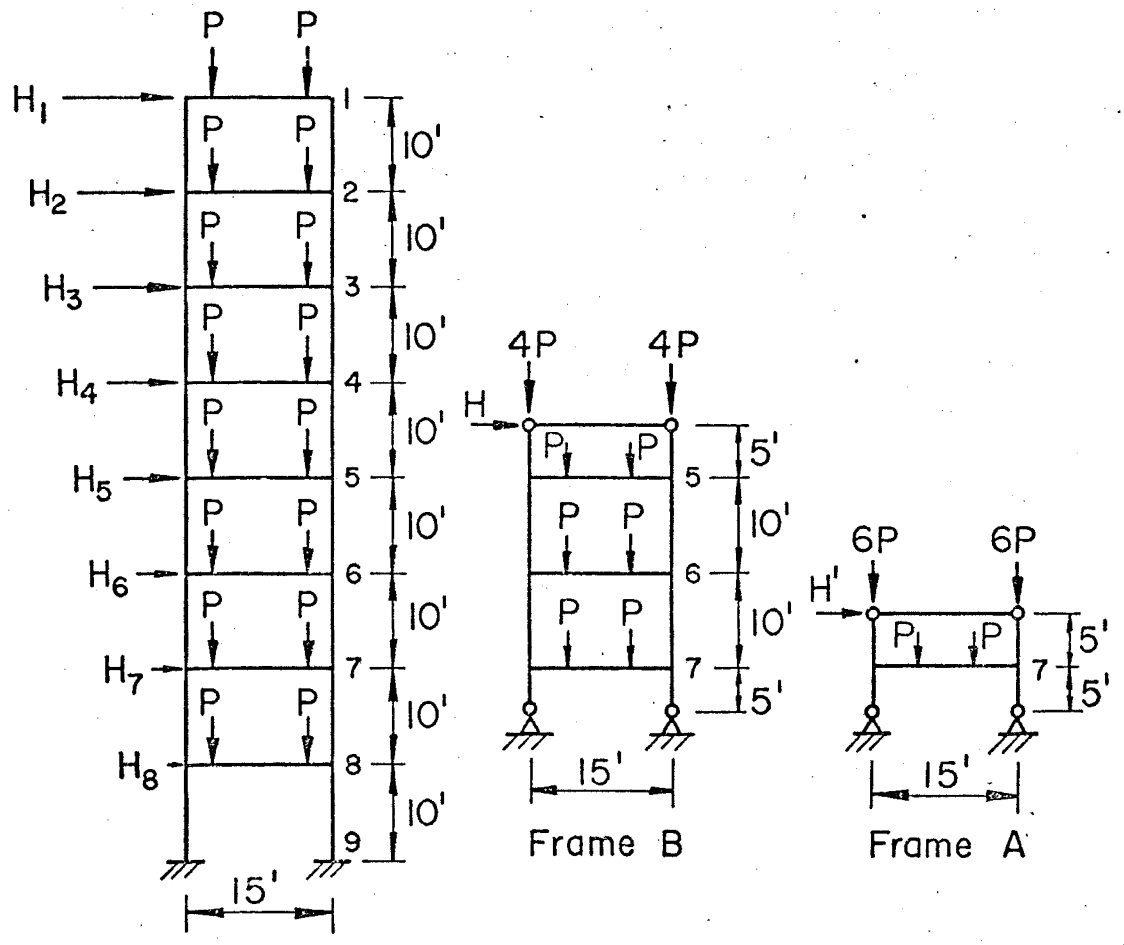

Working Loads Used in the Design of Test Frames

Gravity

Dead Load 80 psf = 1440 lbs/ft
Full Design Live Load 80 psf = 1440 lbs/ft
} 18 ft Bent Spacing

$$P_{DL} = \frac{W_{DL}(L)}{2} = \frac{1440(15)}{2} = 10.8^{k}$$

$P_{LL} = 10.8^{k}$; P_{LL} (design) = 60% $P_{LL} = 6.48^{k}$

P_{TOTAL} (design) = 17.28^{k}

Earthquake

$H = H_1 + H_2 + H_3 + H_4 + H_5 = 5.19^{k}$

FIG. 4.2 DESIGN LOADING OF THE TEST FRAMES

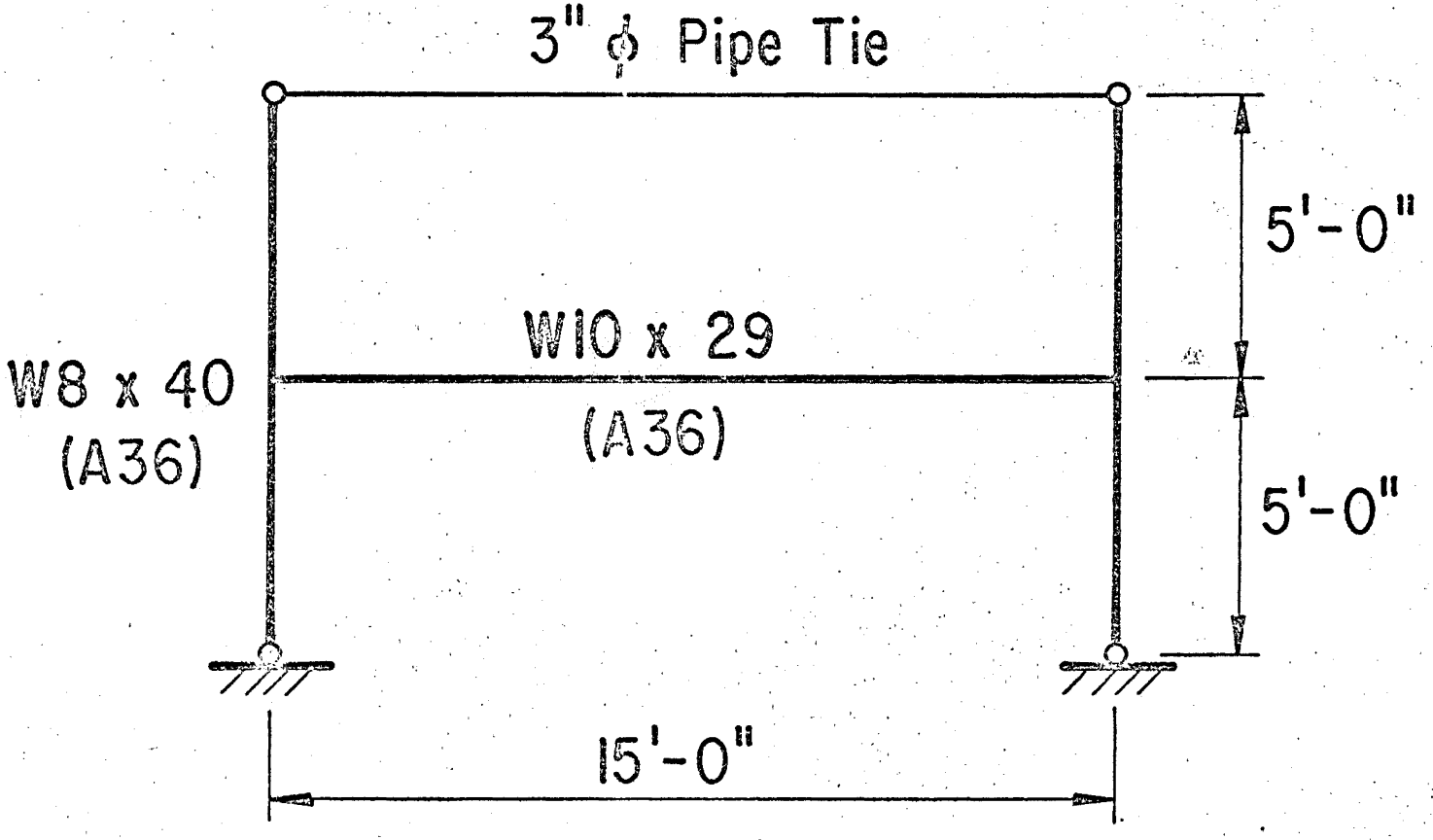

FRAME A

FIG. 4.3a GEOMETRY AND MEMBER SIZES FOR TEST FRAMES

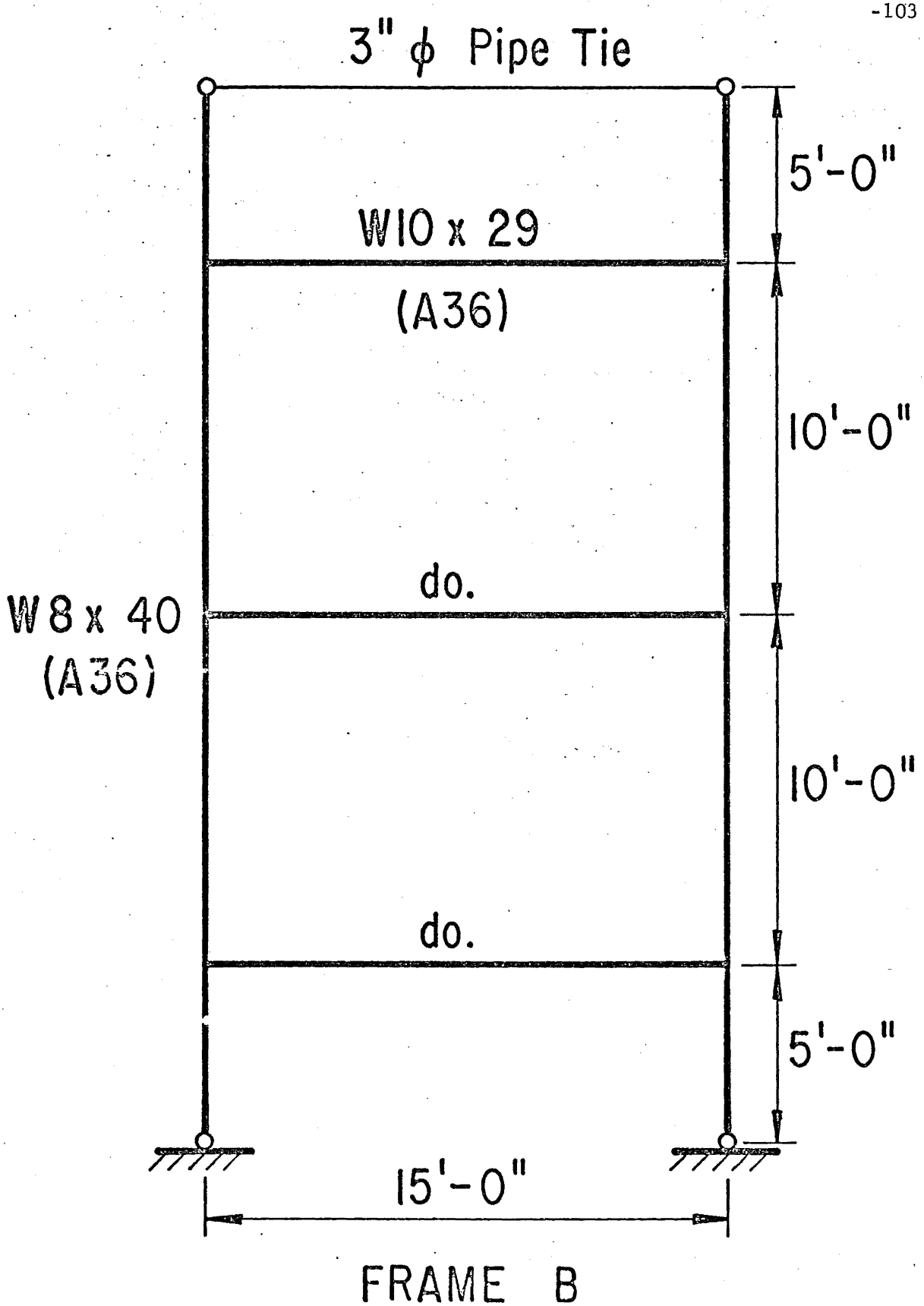

FIG. 4.3b GEOMETRY AND MEMBER SIZES FOR TEST FRAMES

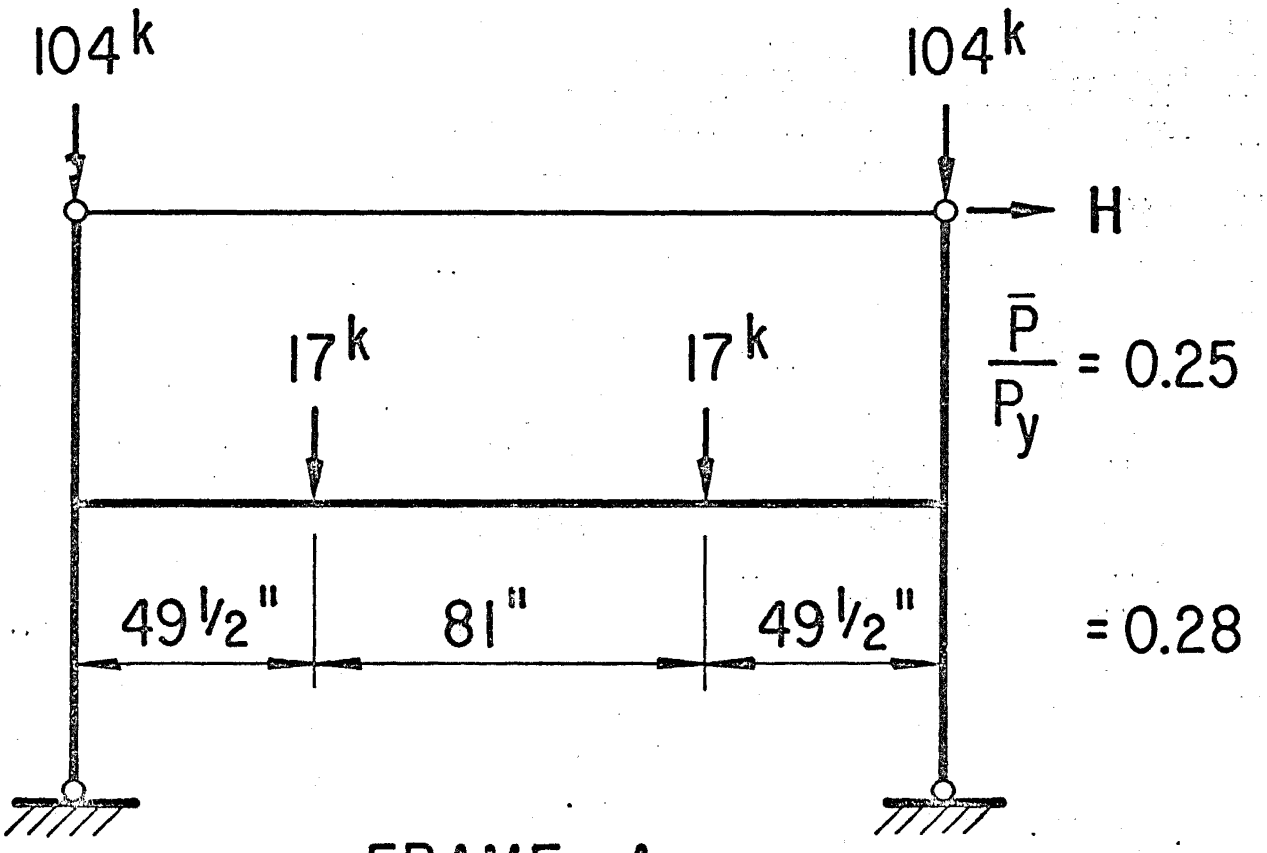

$\bar{P}$ = Axial Load in Column, P_y = Axial Yield Load of Column

FIG. 4.4a LOADS AND AXIAL THRUST RATIOS FOR TEST FRAMES

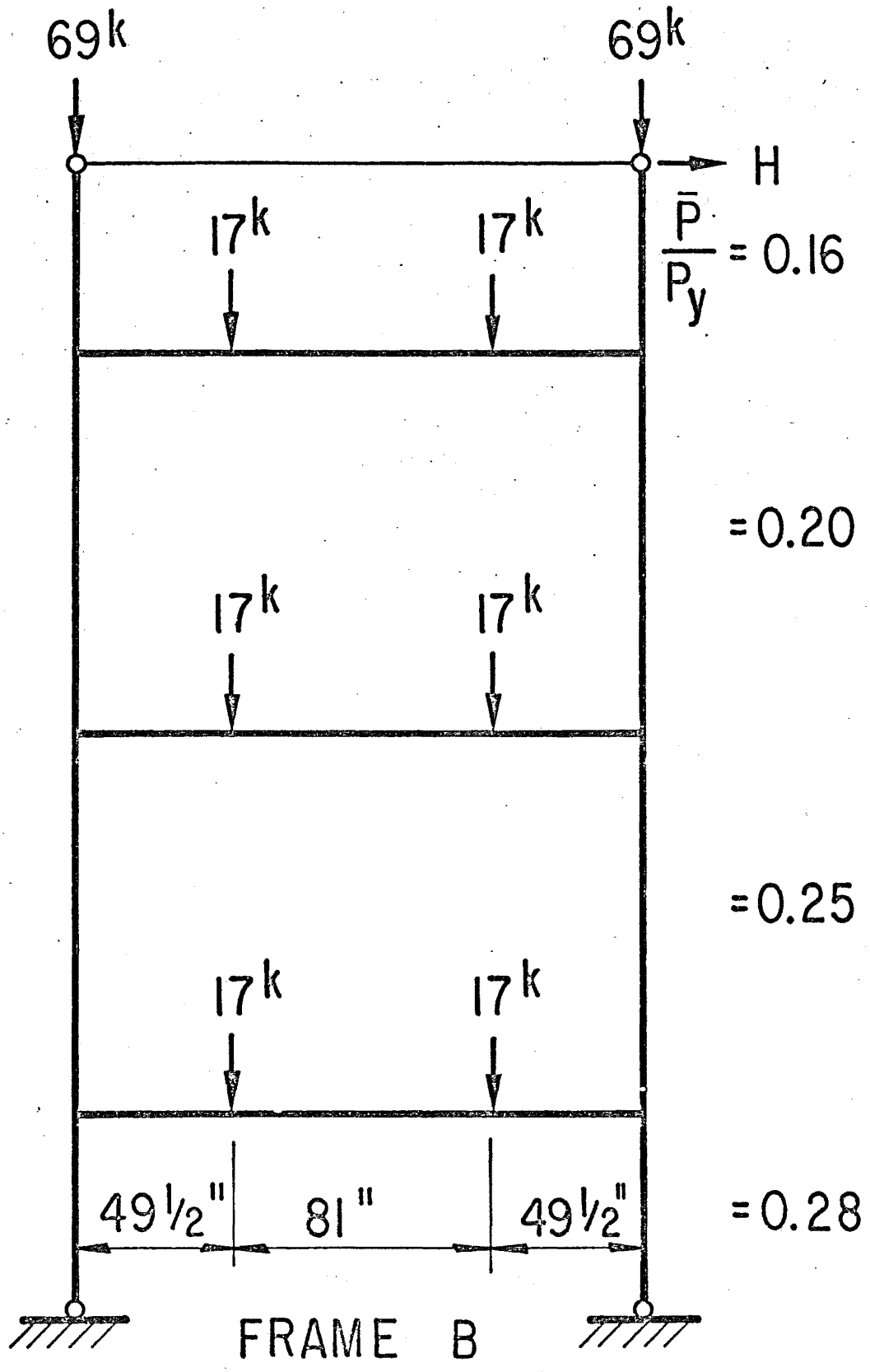

FIG. 4.4b LOADS AND AXIAL THRUST RATIOS FOR TEST FRAMES

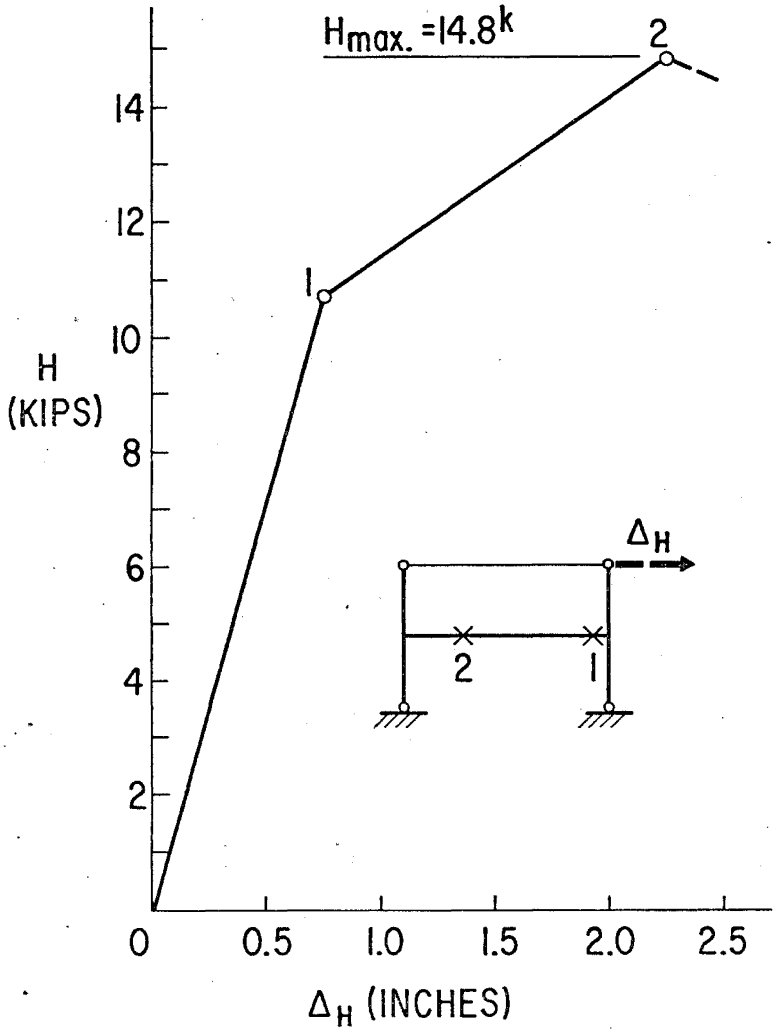

FIG. 4.5 LOAD-DEFLECTION CURVE FOR FRAME A

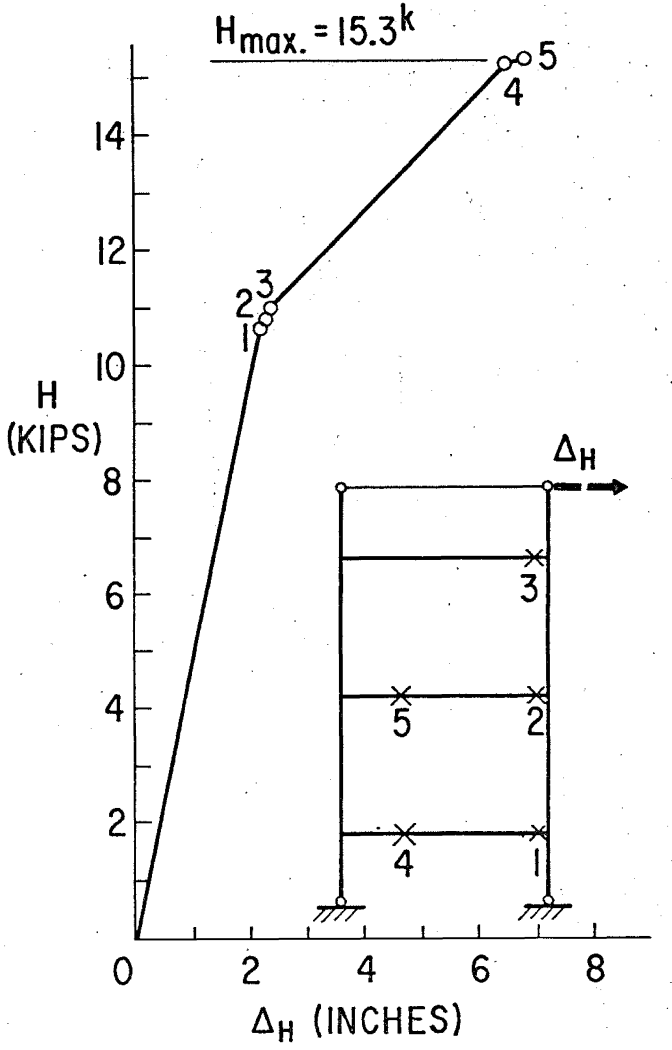

FIG. 4.6 LOAD-DEFLECTION CURVE FOR FRAME B

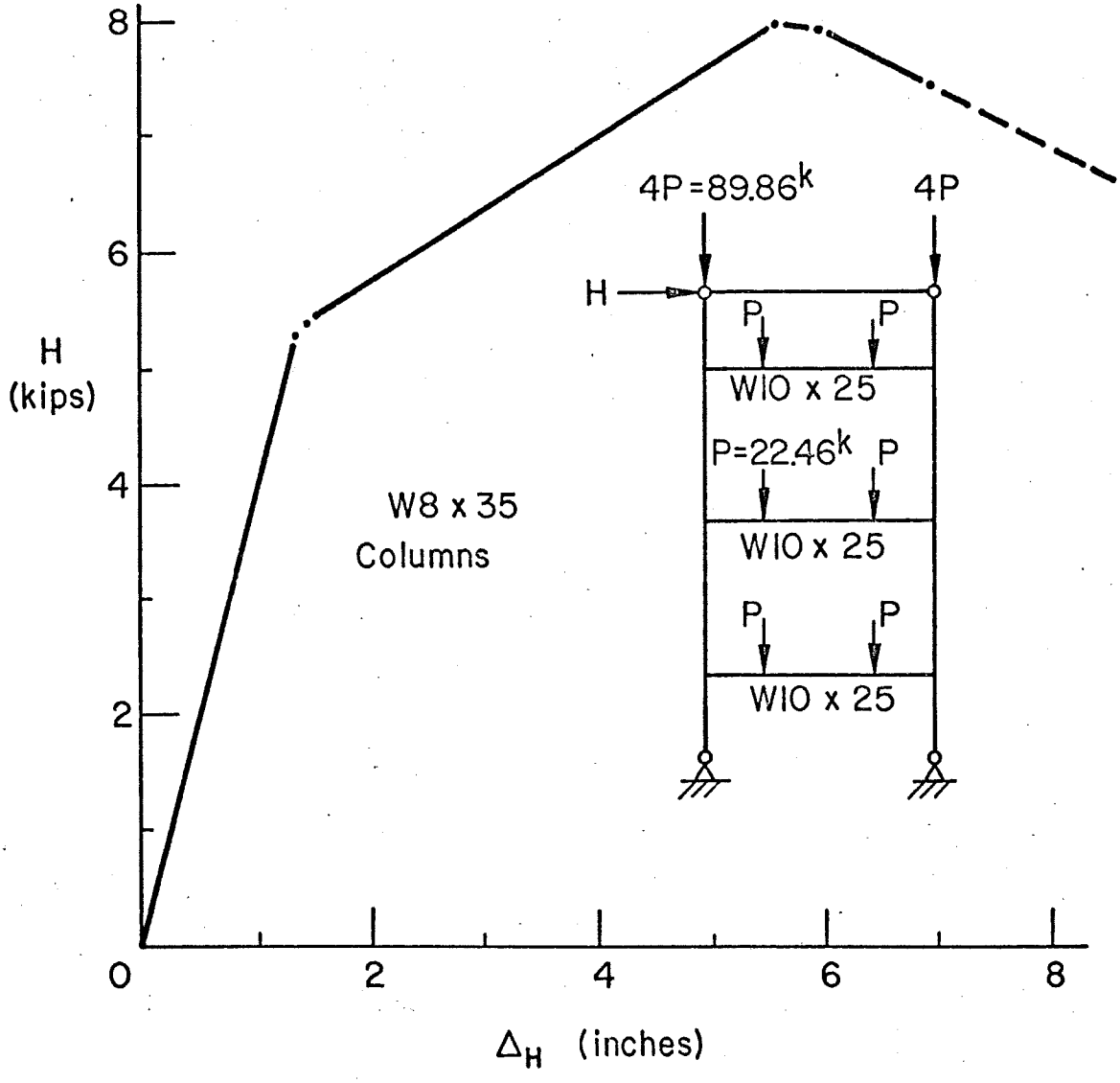

FIG. 4.7 PREDICTED LOAD VERSUS DEFLECTION CURVE FOR ALTERNATE FRAME B

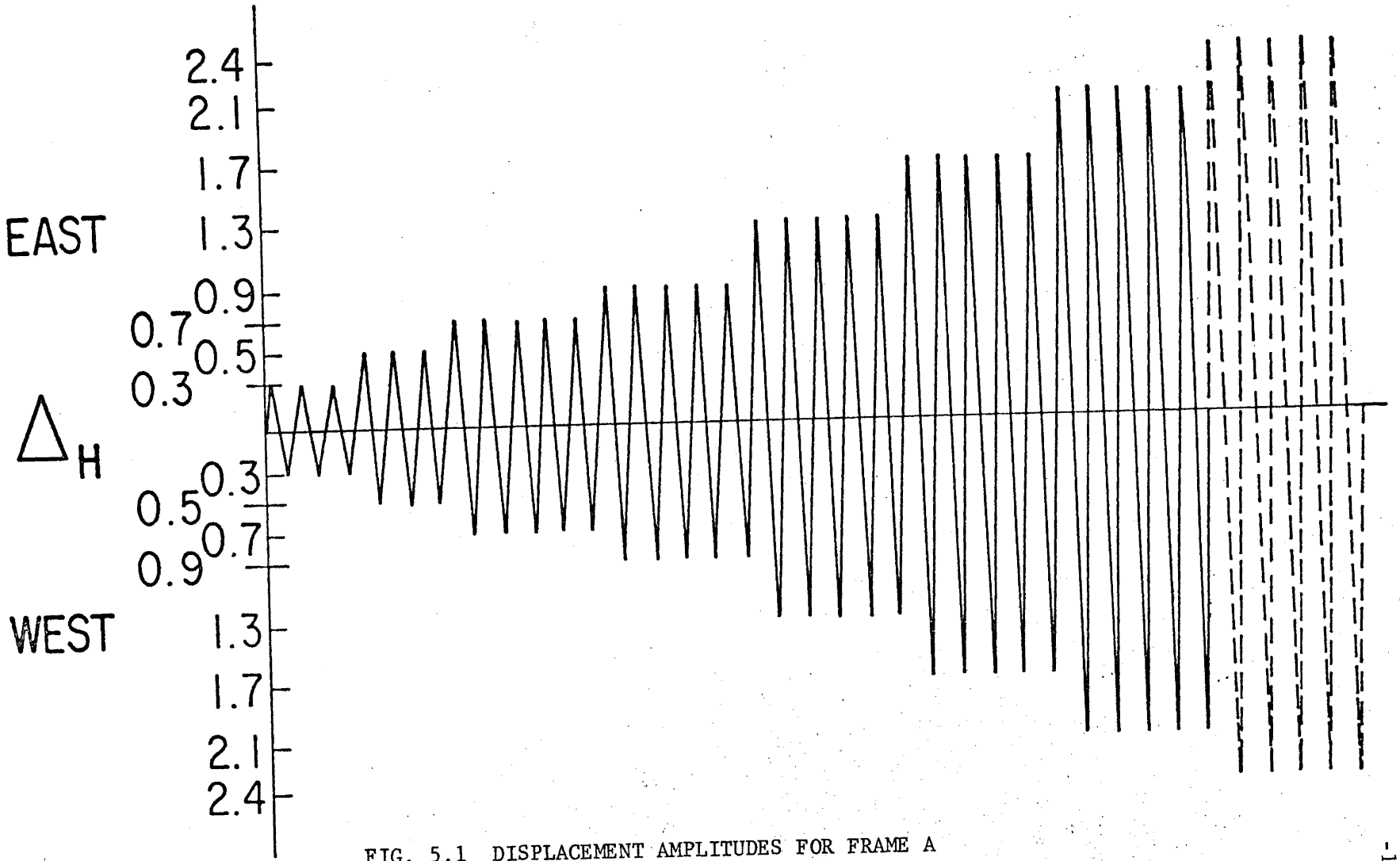

FIG. 5.1 DISPLACEMENT AMPLITUDES FOR FRAME A

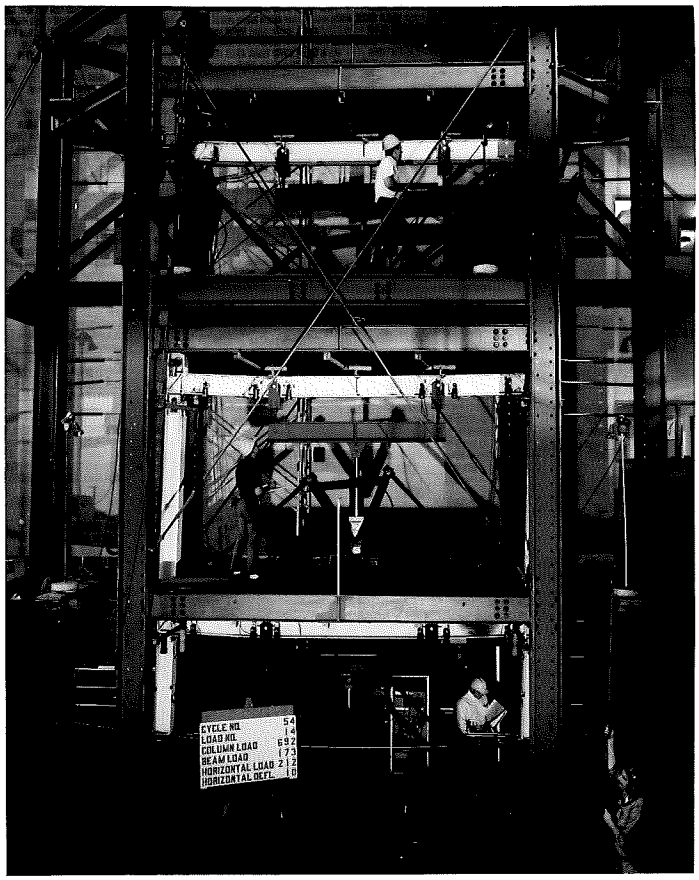

FIG. 5.2 TEST OF FRAME B

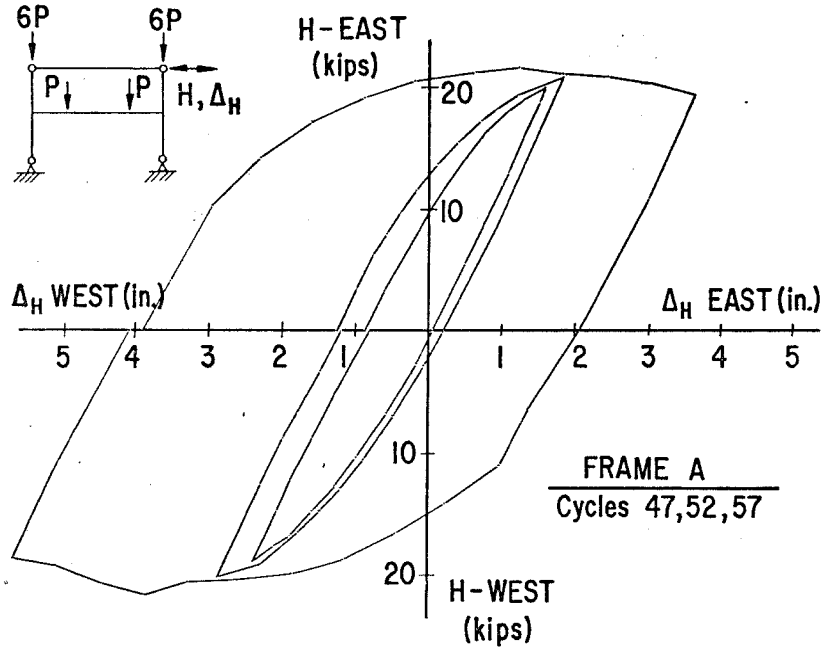

FIG. 5.3 LOAD VERSUS DEFLECTION CURVES AT SELECTED DISPLACEMENT AMPLITUDES FOR FRAME A

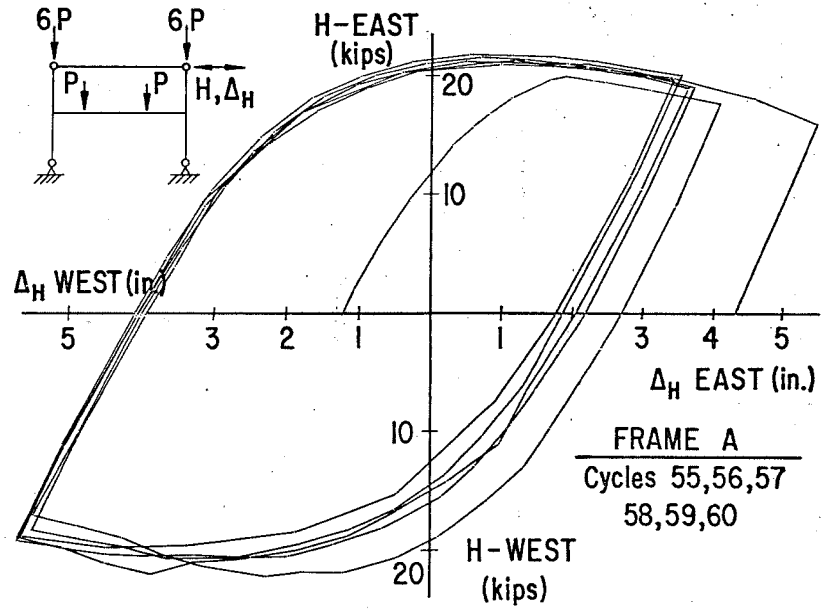

FIG. 5.4 STABILITY OF LOAD VERSUS DEFLECTION CURVES FOR FRAME A

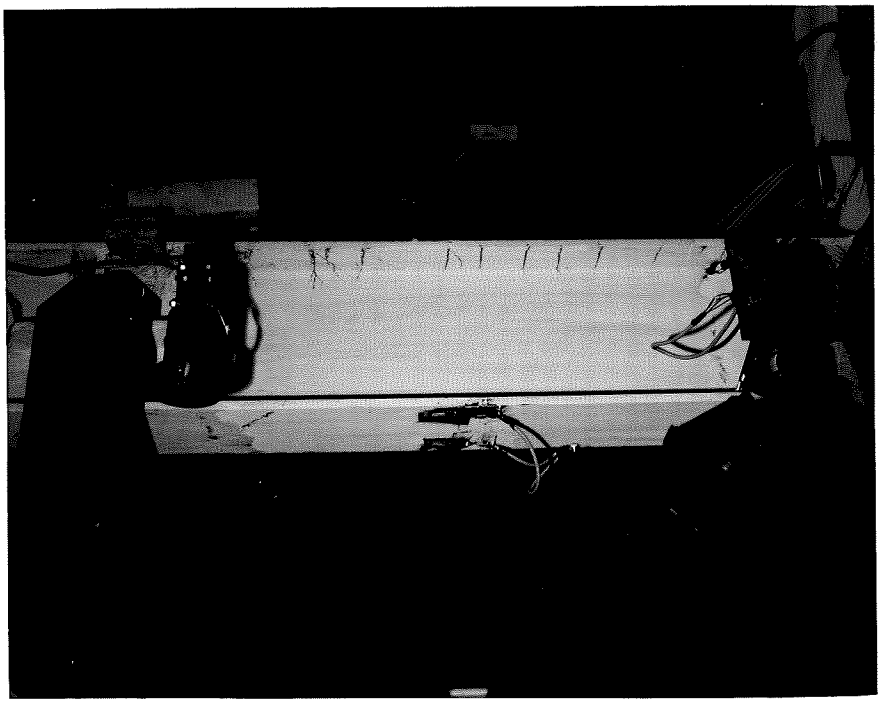

FIG. 5.5 SPREAD OF YIELDING IN BEAM OF FRAME A

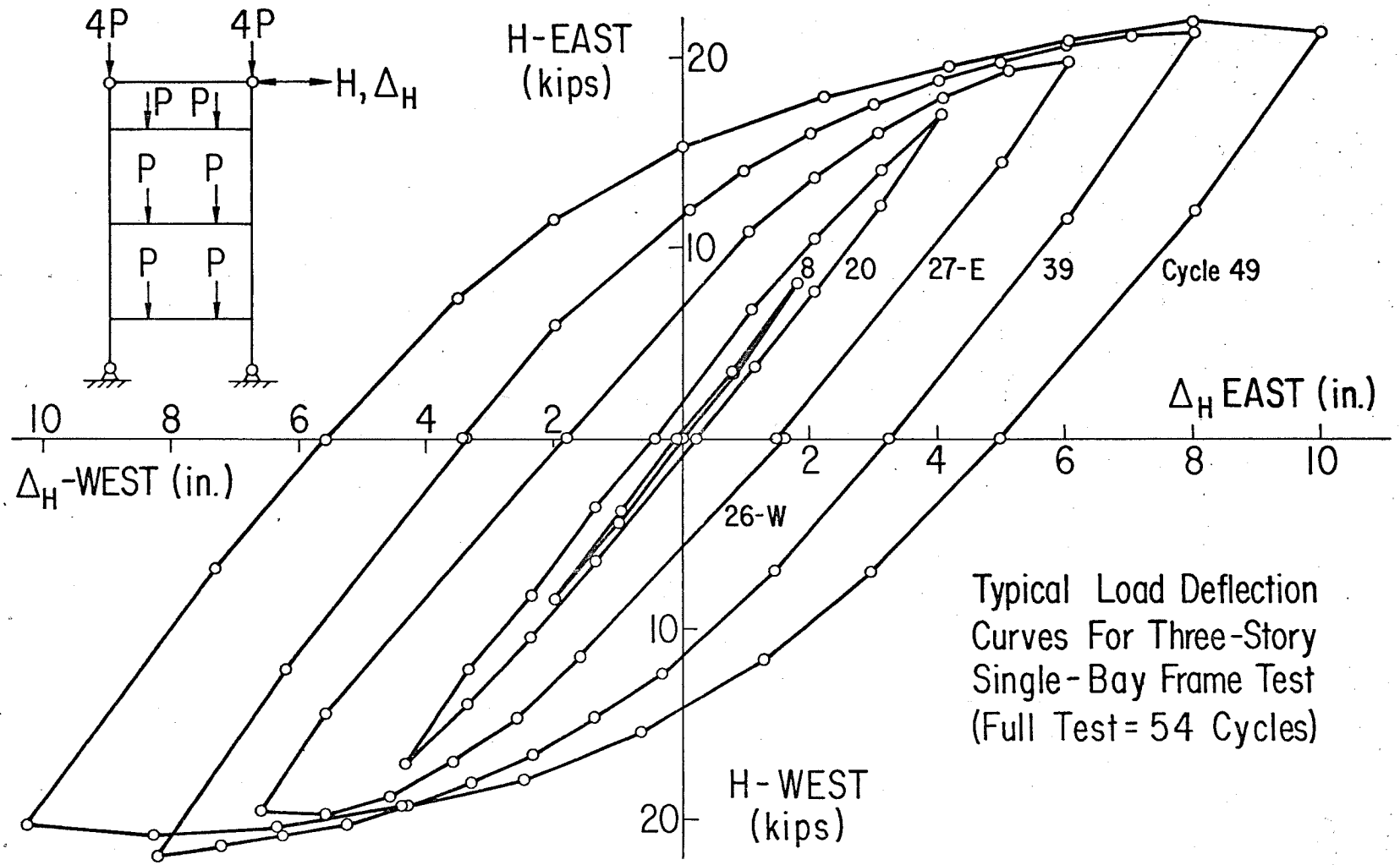

FIG. 5.6 SELECTED LOAD VERSUS DEFLECTION CURVES FOR FRAME B

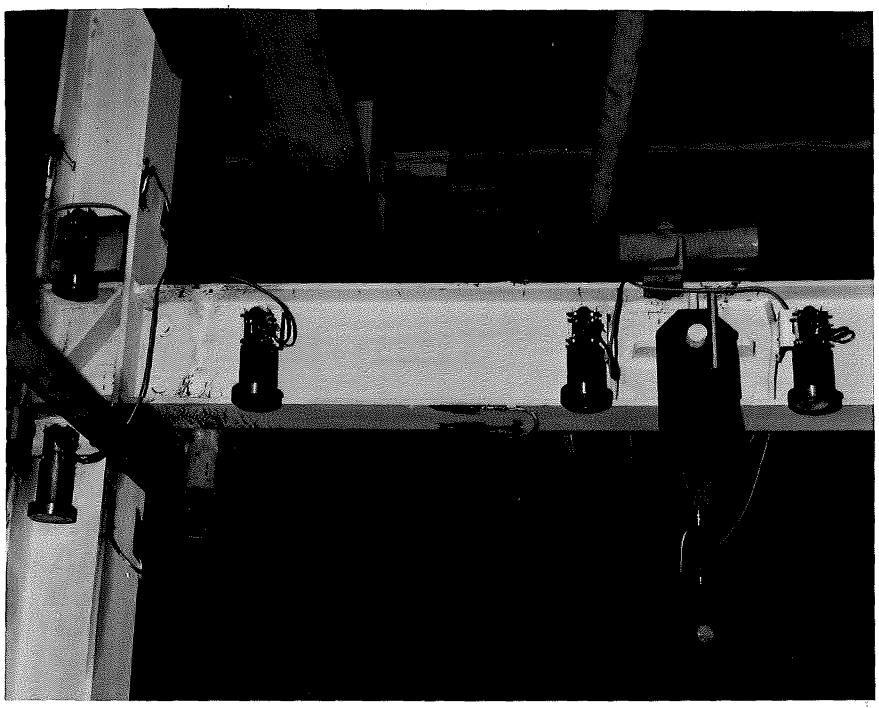

FIG. 5.7 SPREAD OF YIELDING IN BEAM OF FRAME B

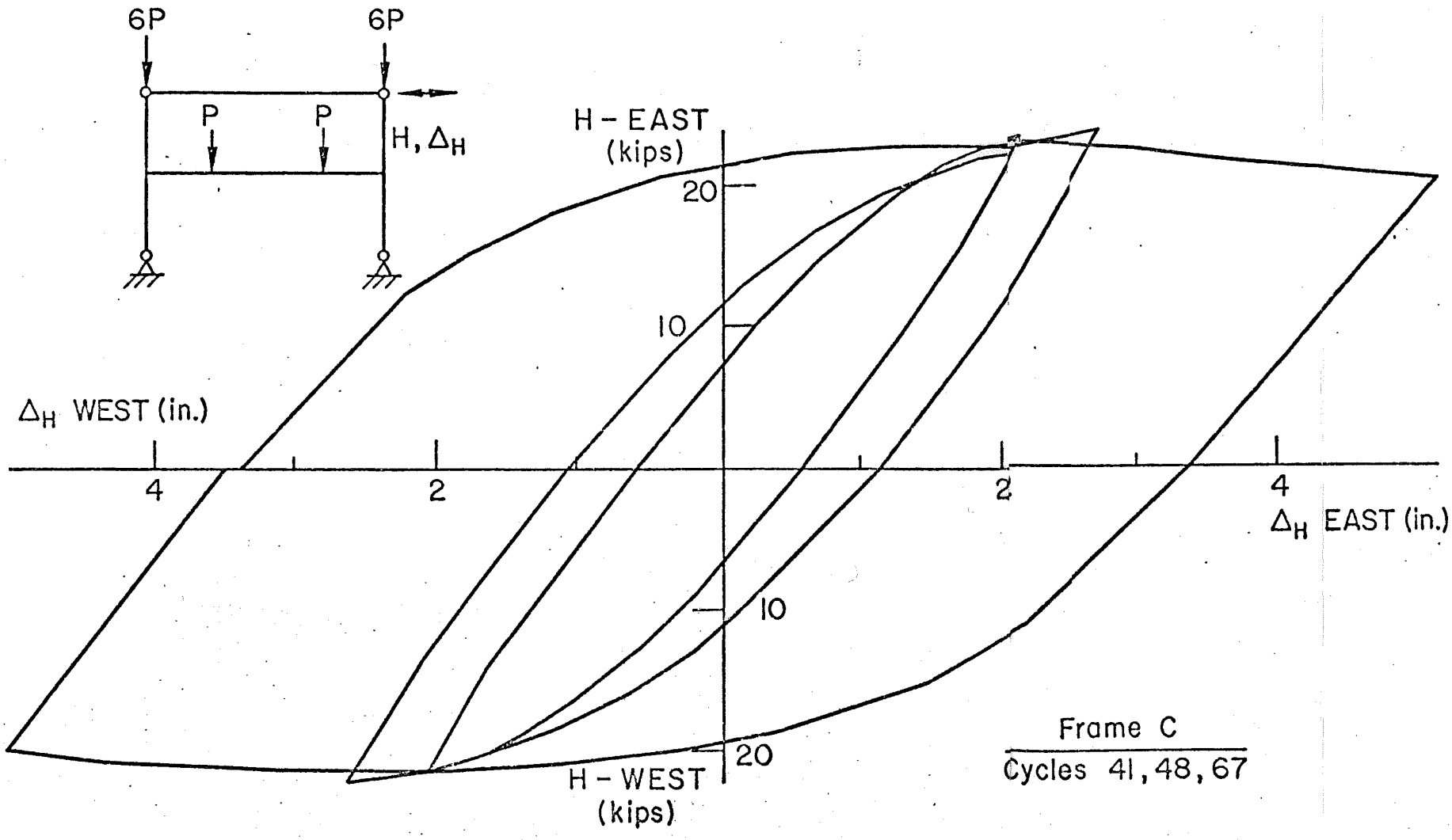

FIG. 5.8 SELECTED LOAD VERSUS DEFLECTION CURVES FOR FRAME C

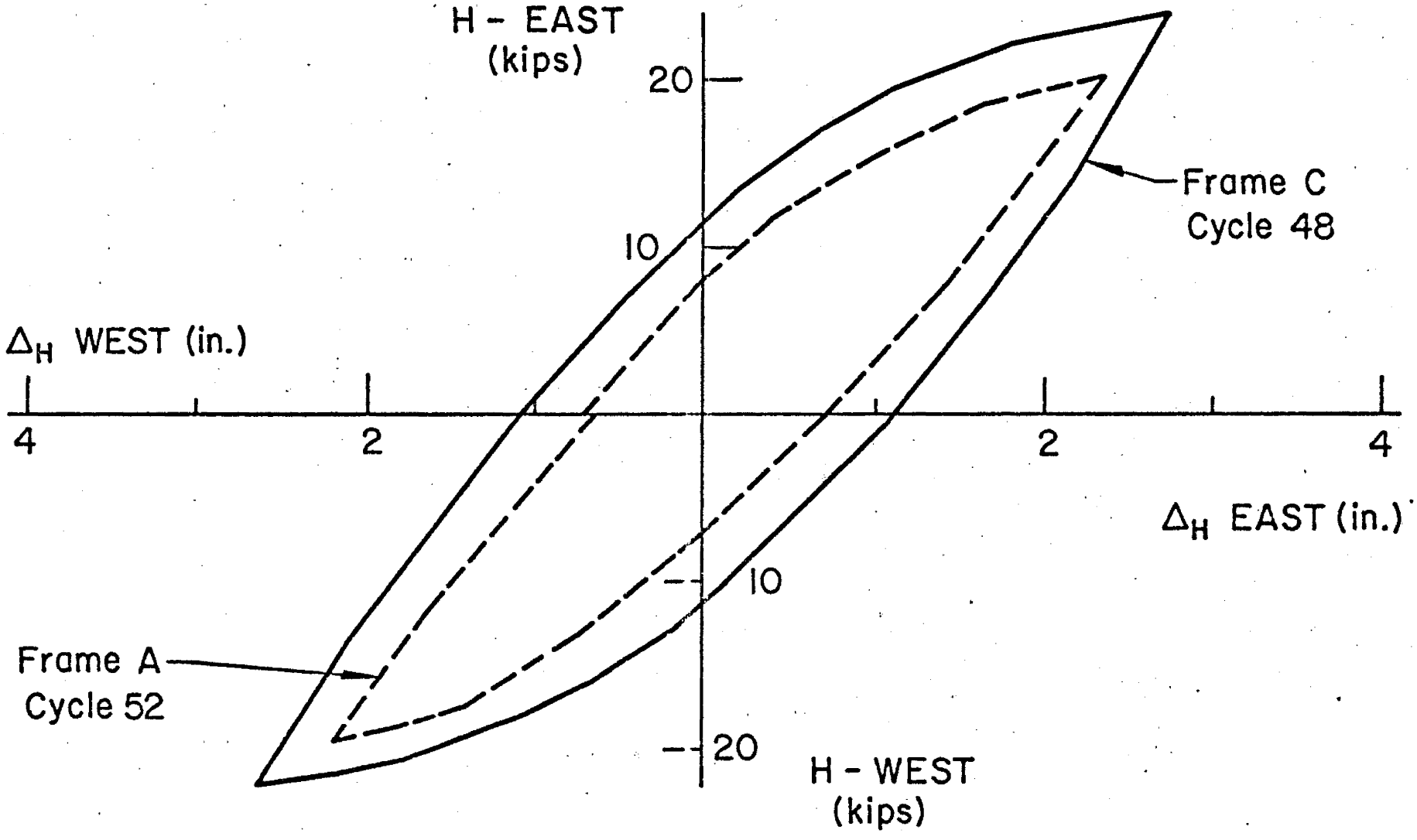

FIG. 5.9 COMPARISON OF LOAD VERSUS DEFLECTION CURVES FOR FRAME A AND FRAME C

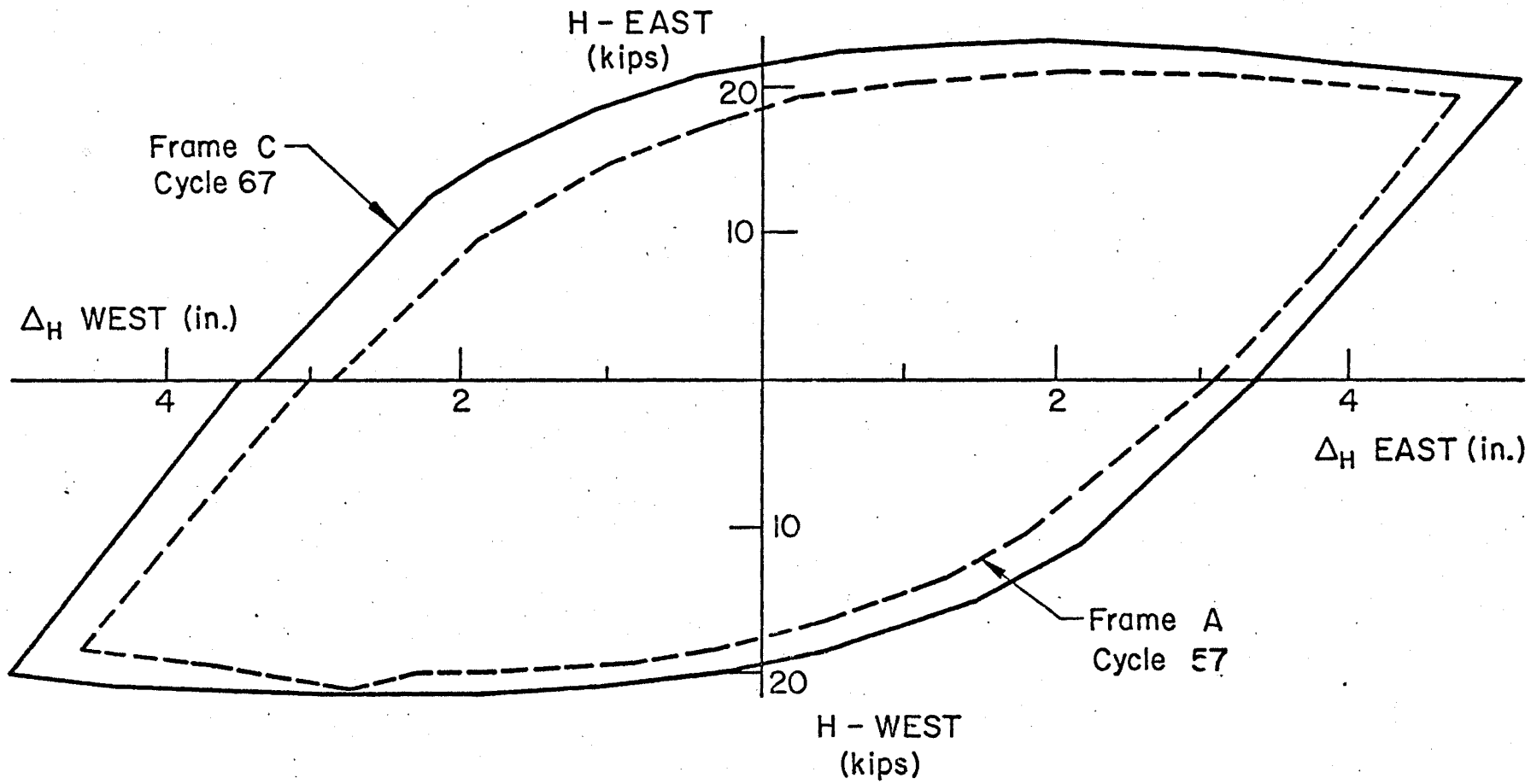

FIG. 5.10 COMPARISON OF LOAD VERSUS DEFLECTION CURVES FOR FRAME A AND FRAME C

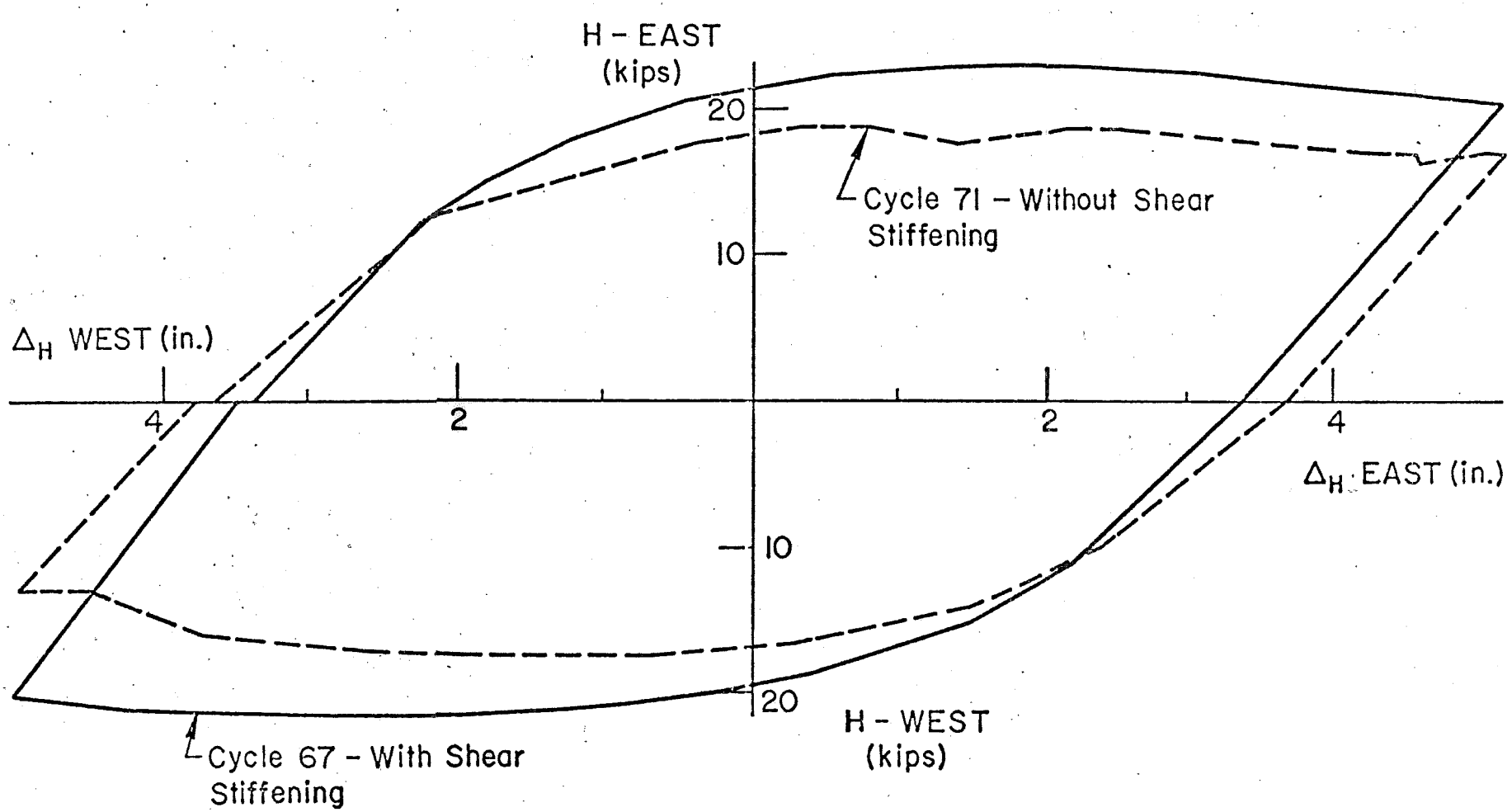

FIG. 5.11 EFFECT OF REMOVING SHEAR STIFFENING IN FRAME C

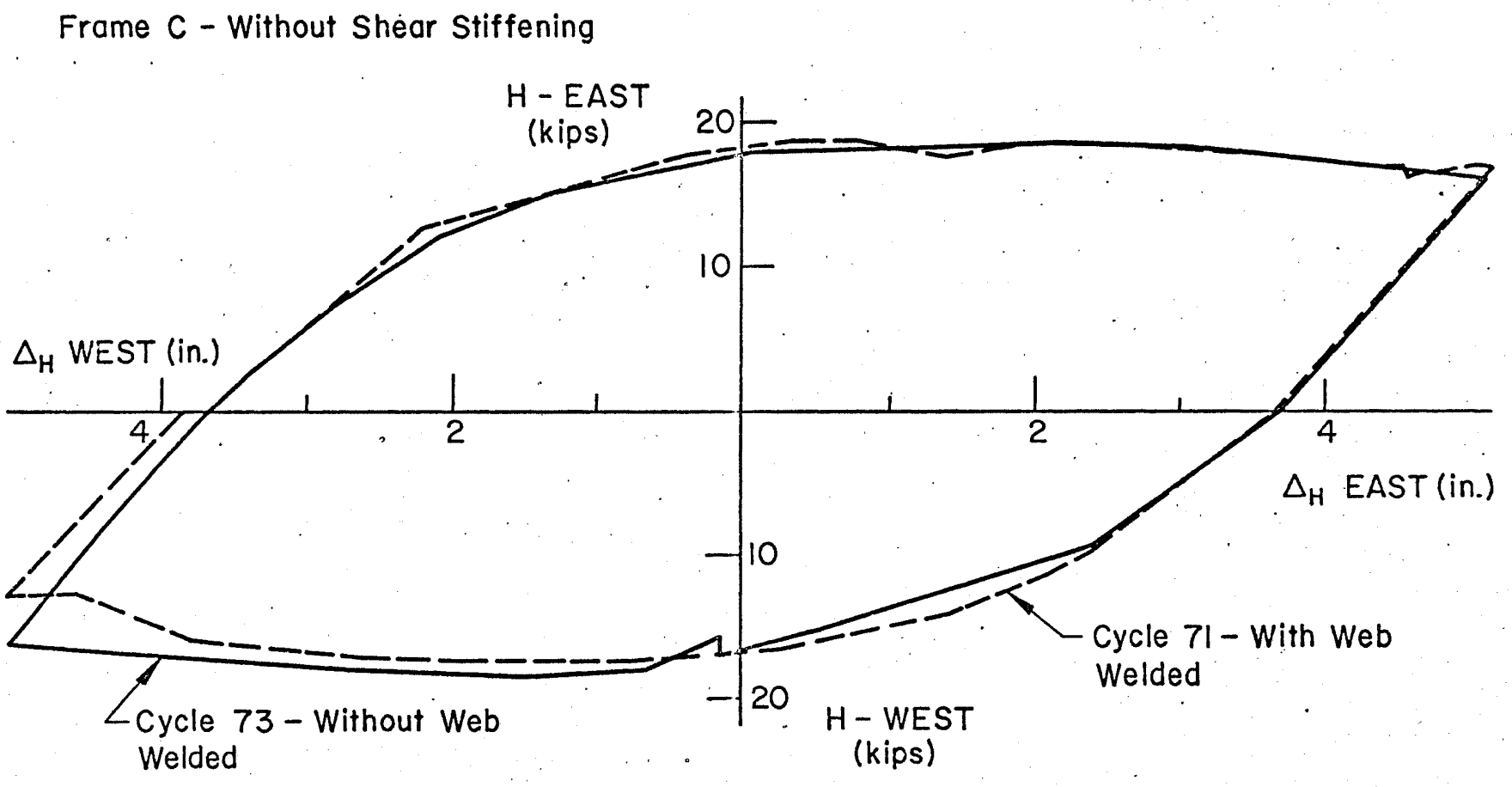

FIG. 5.12 EFFECT OF A BOLTED WEB AND SHEAR STIFFENING REMOVAL IN FRAME C

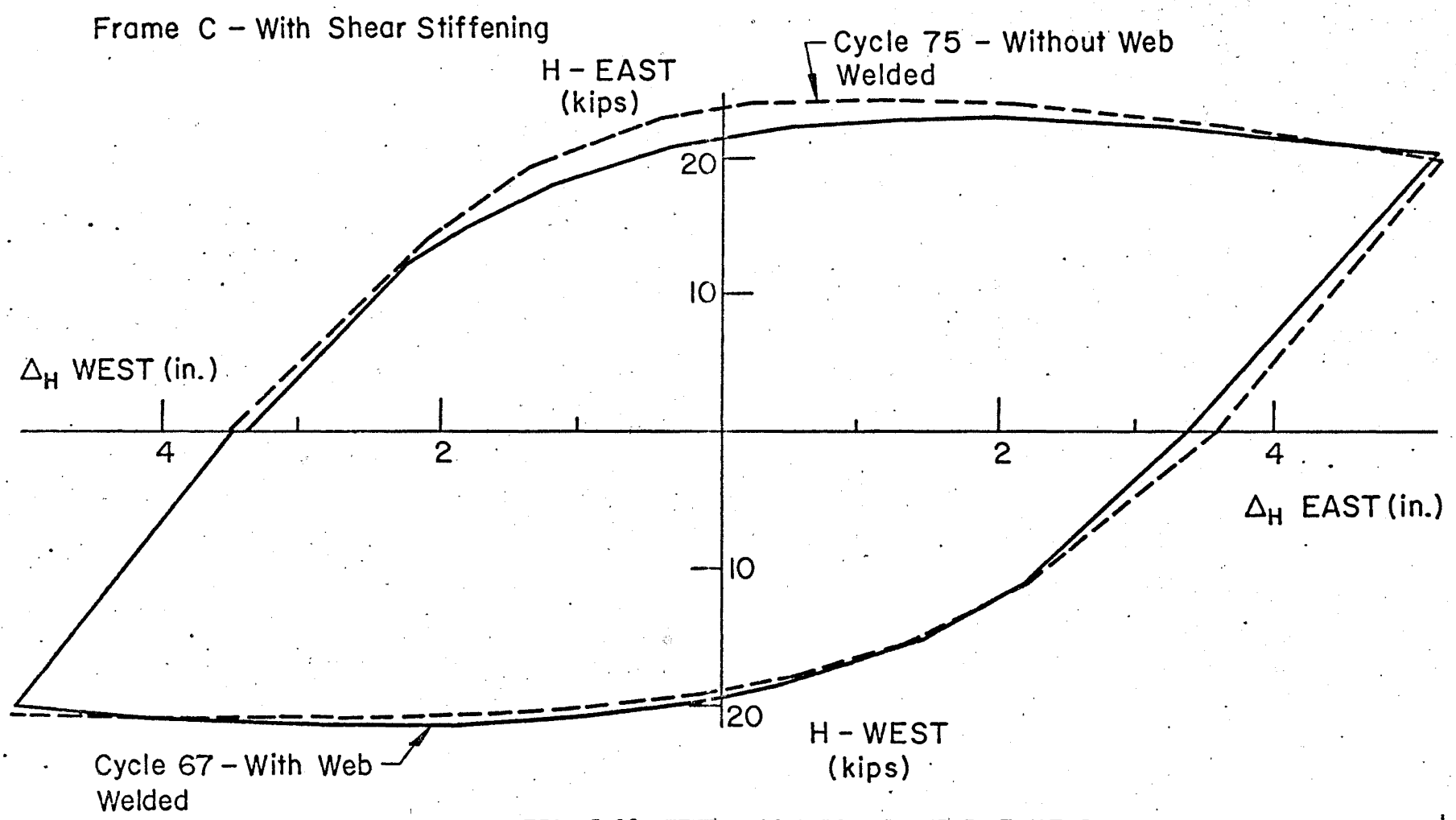

FIG. 5.13. EFFECT OF A BOLTED WEB IN FRAME C

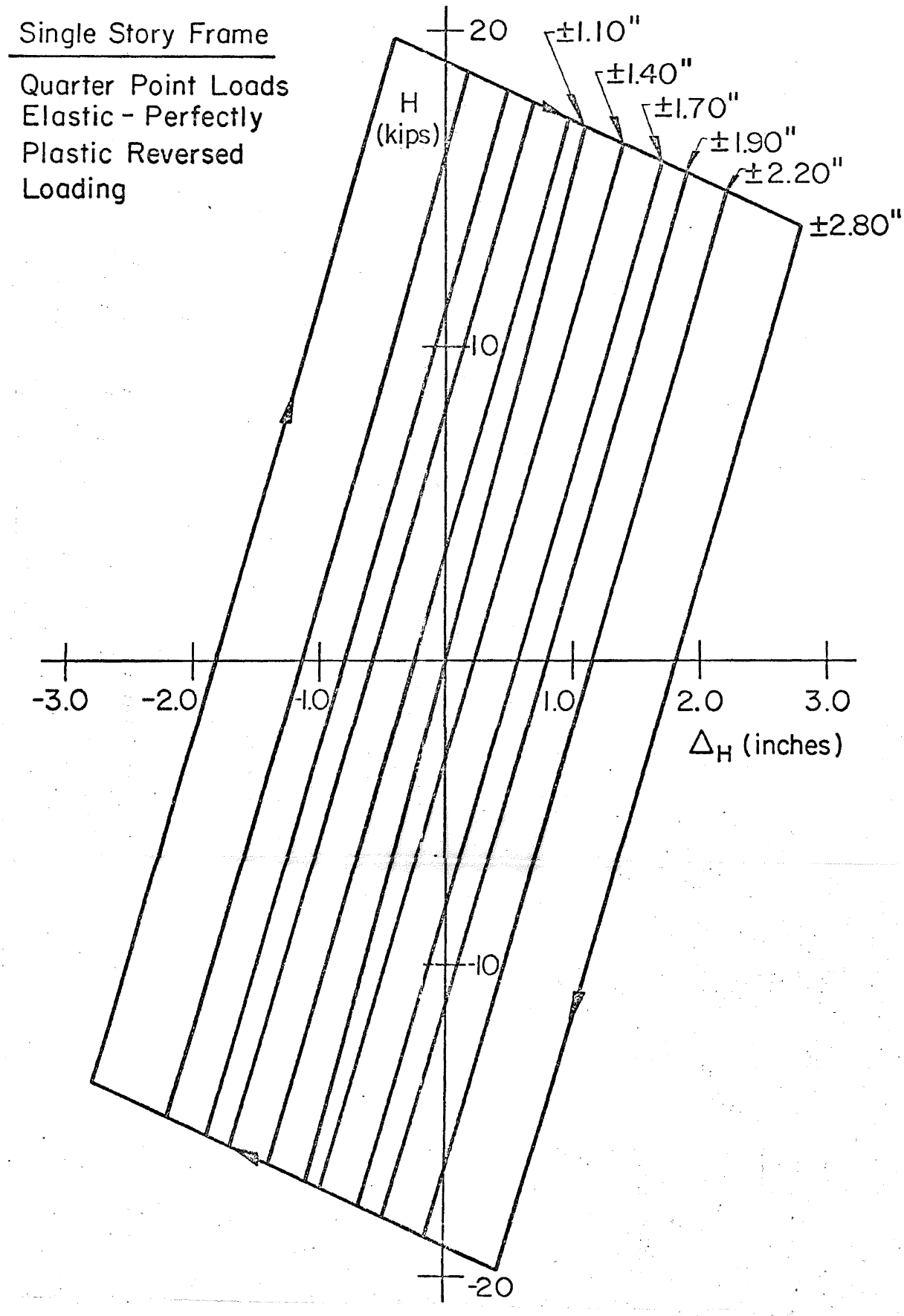

FIG. 6.1 PREDICTED ELASTIC-PLASTIC HYSTERESIS LOOPS FOR FRAME A

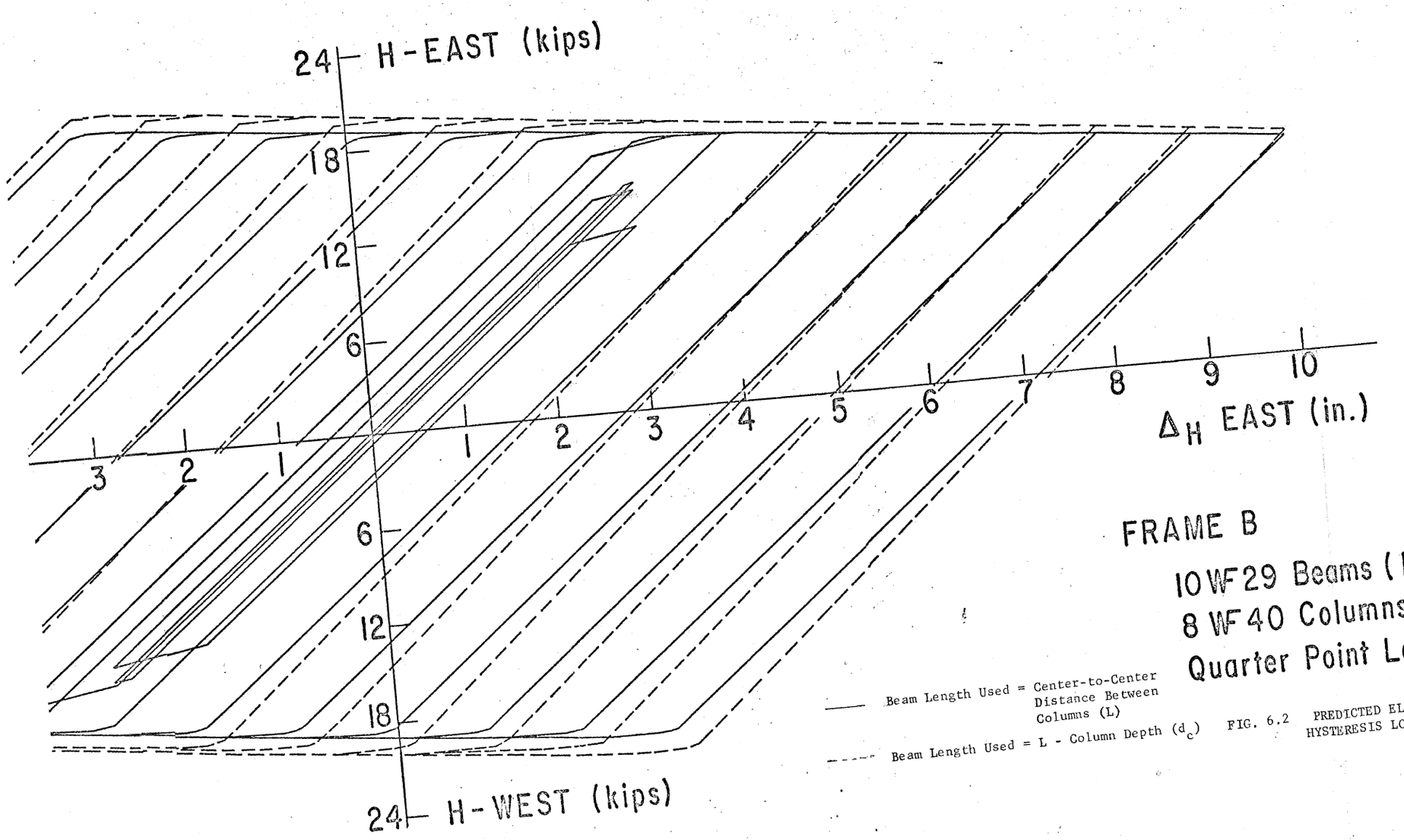

FIG. 6.2 PREDICTED ELASTIC-PLASTIC HYSTERESIS LOOPS FOR FRAME B

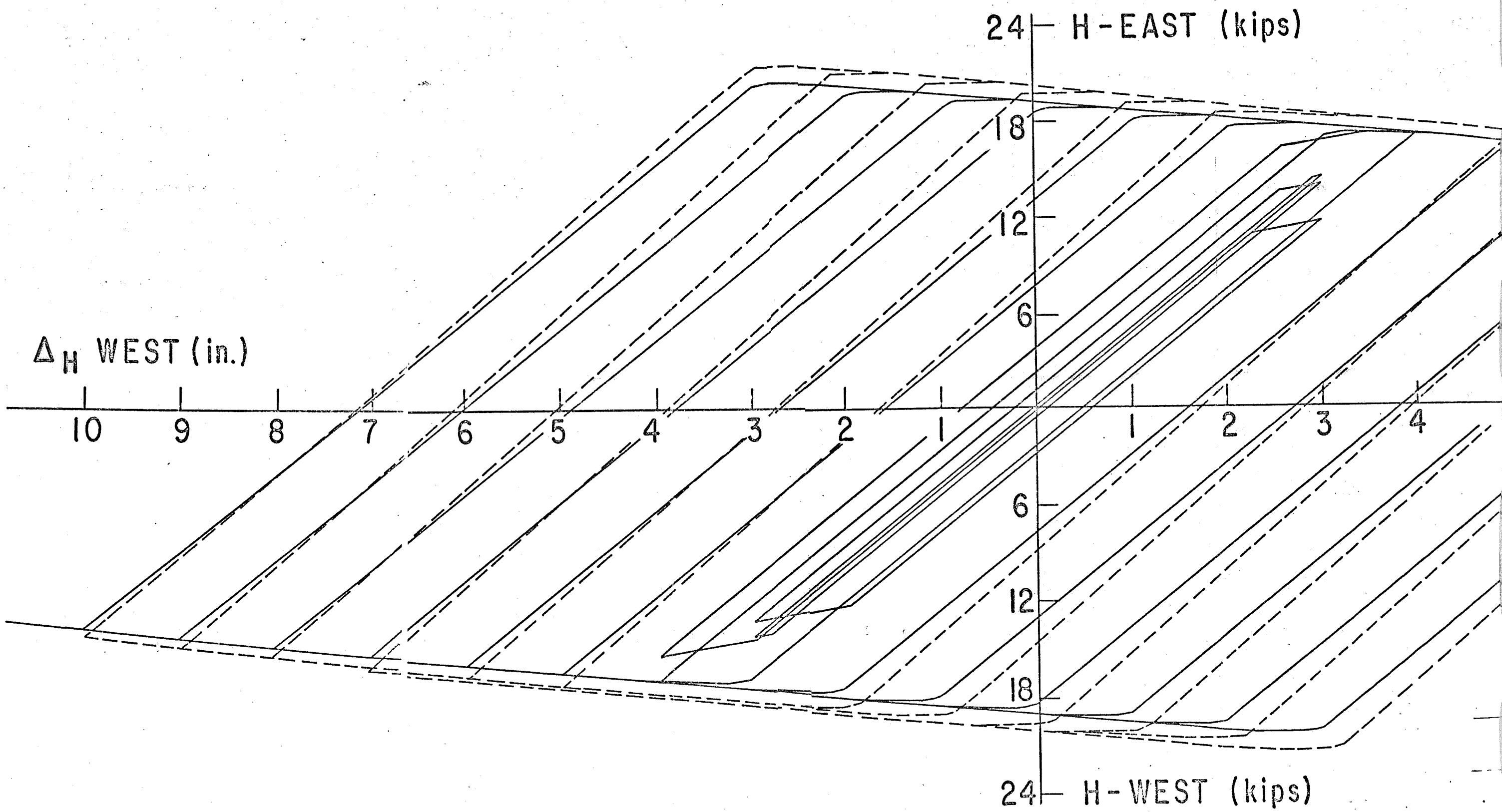
24
H - EAST (kips)
18
12
6
Δ_H WEST (in.)
10
9
8
7
6
5
4
3
2
1
1
2
3
4
6
12
18
24
H - WEST (kips)

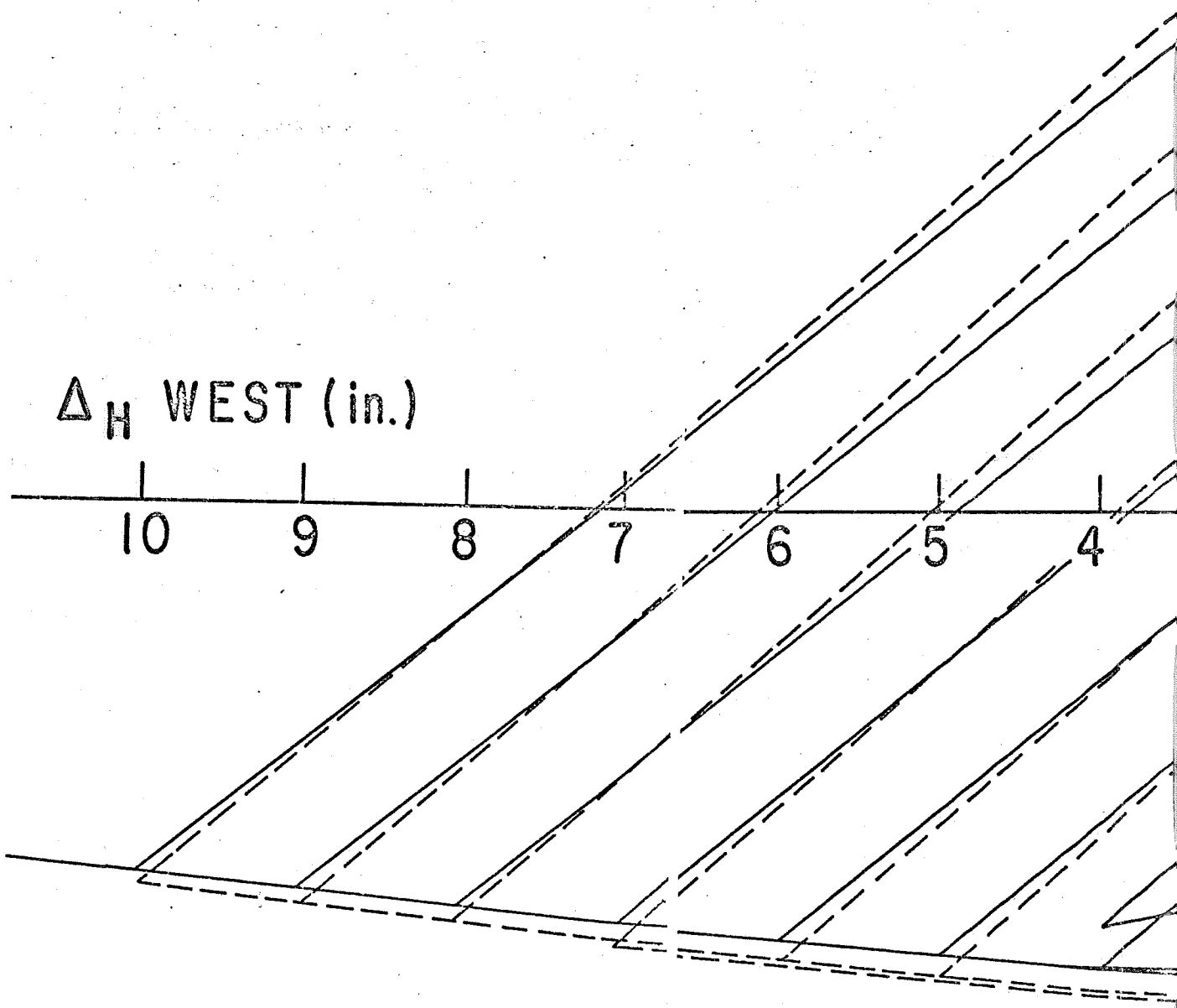
Δ_H WEST (in.)
10
9
8
7
6
5
4

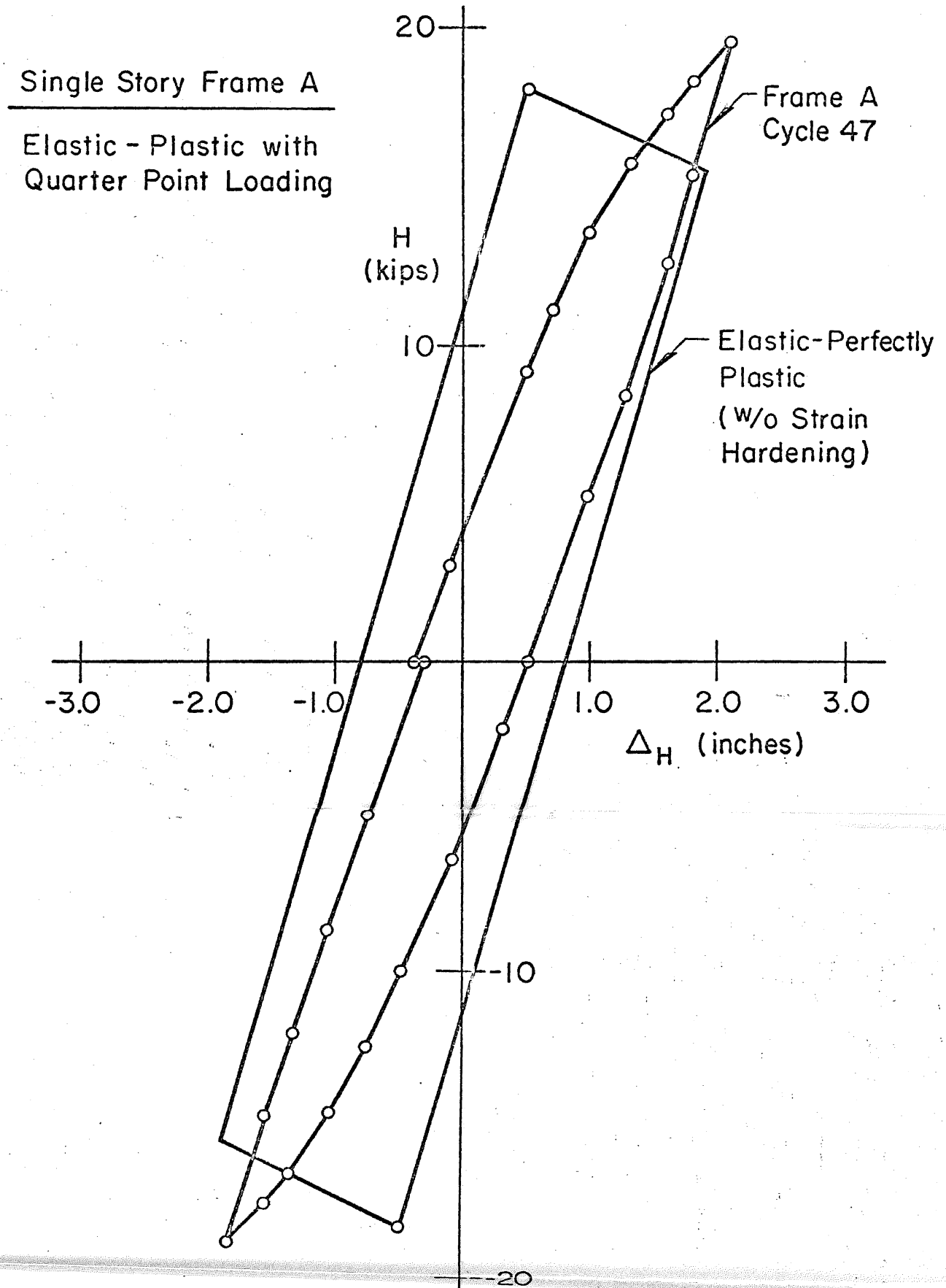

FIG. 6.3 ELASTIC-PLASTIC CURVE FOR FRAME A WITH EXPERIMENTAL CYCLE 47

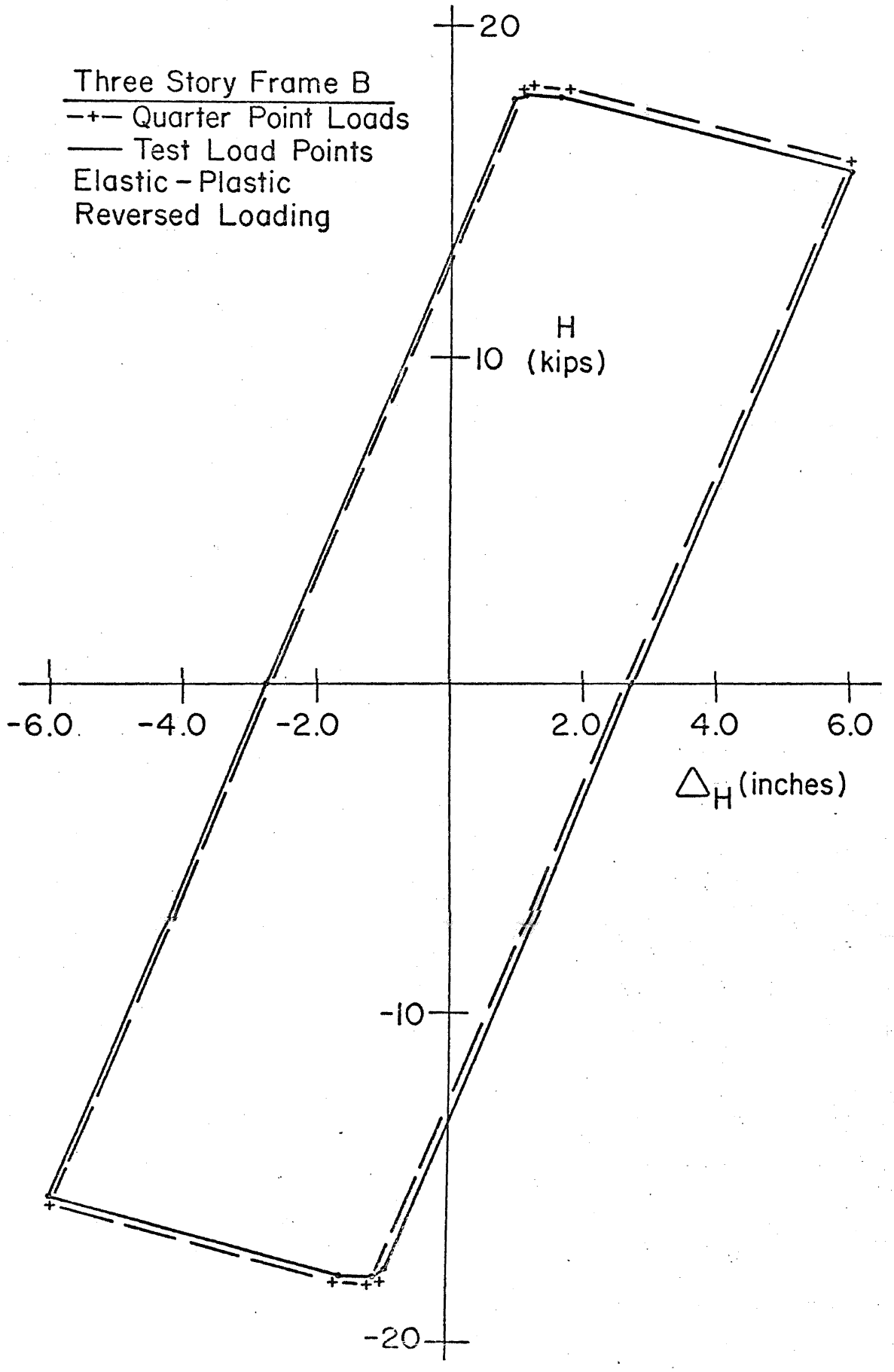

FIG. 6.4 TWO ELASTIC-PLASTIC CURVES FOR FRAME B SHOWING EFFECT OF BEAM LOAD POSITION

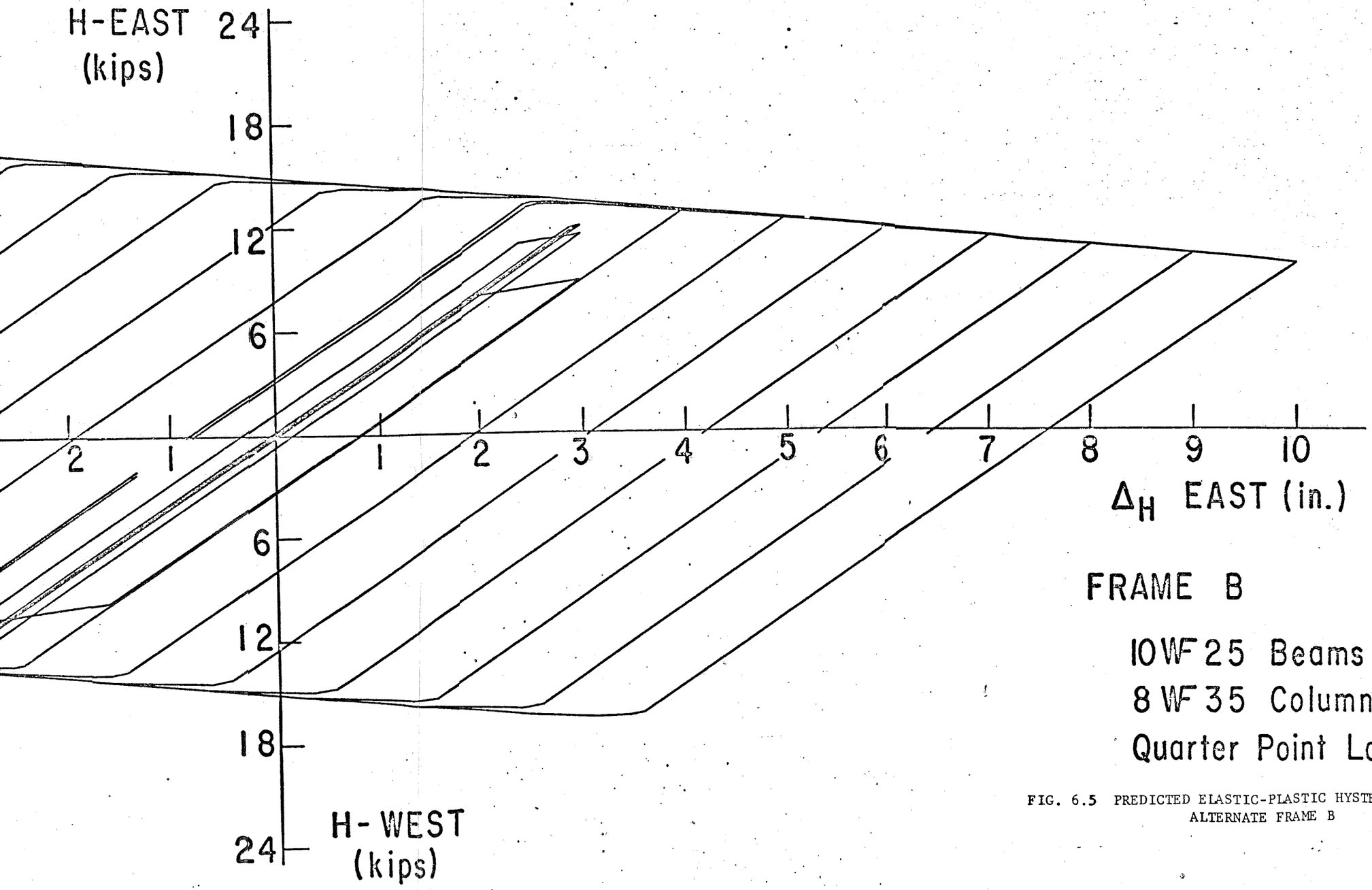

FRAME B

10WF25 Beams (Hdbk)
8WF35 Columns (Hdbk)
Quarter Point Loadings

FIG. 6.5 PREDICTED ELASTIC-PLASTIC HYSTERESIS LOOPS FOR ALTERNATE FRAME B

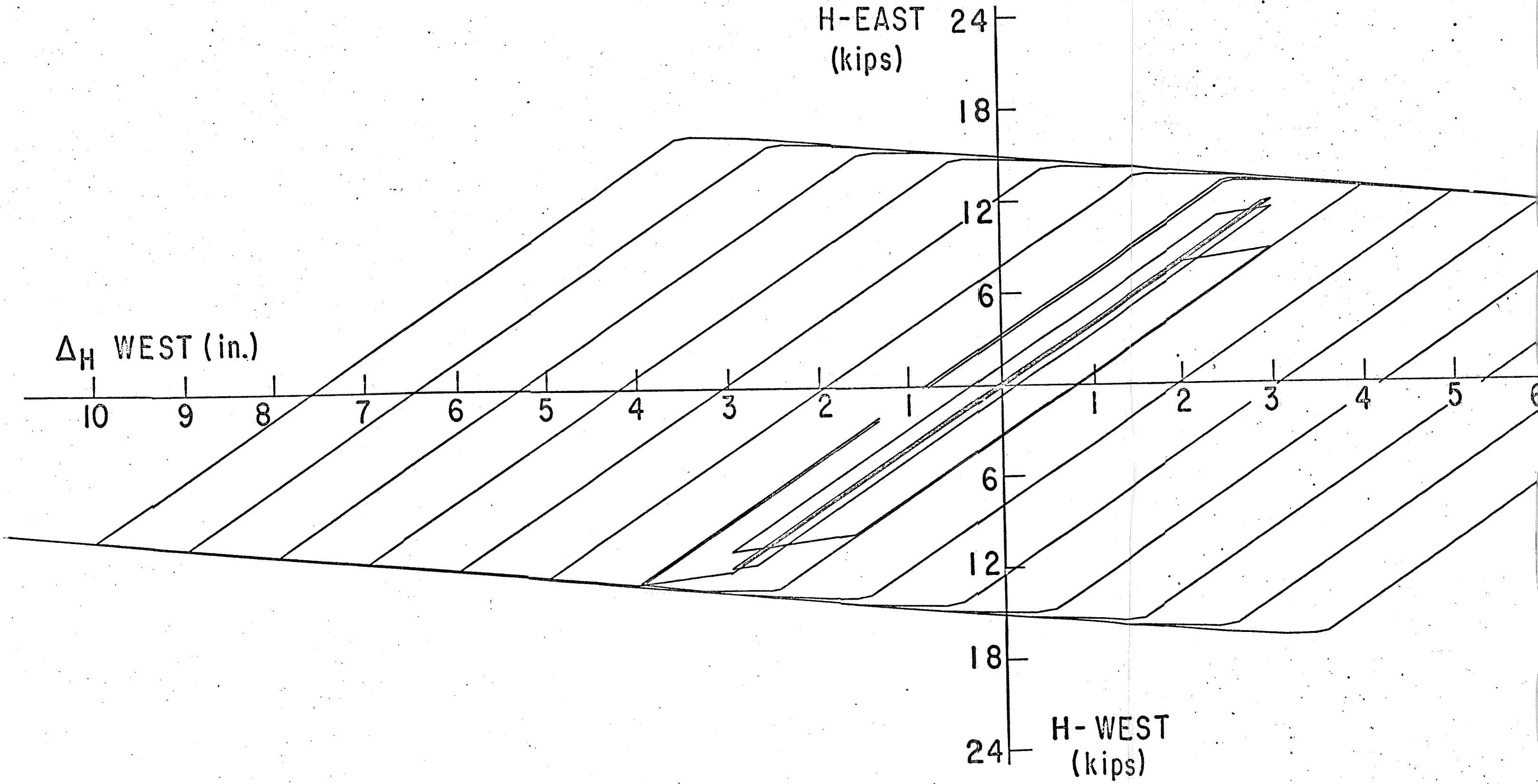
H-EAST 24
(kips)
18
12
6
Δ_H WEST (in.)
10 9 8 7 6 5 4 3 2 1
1 2 3 4 5
6
12
18
24
H-WEST
(kips)

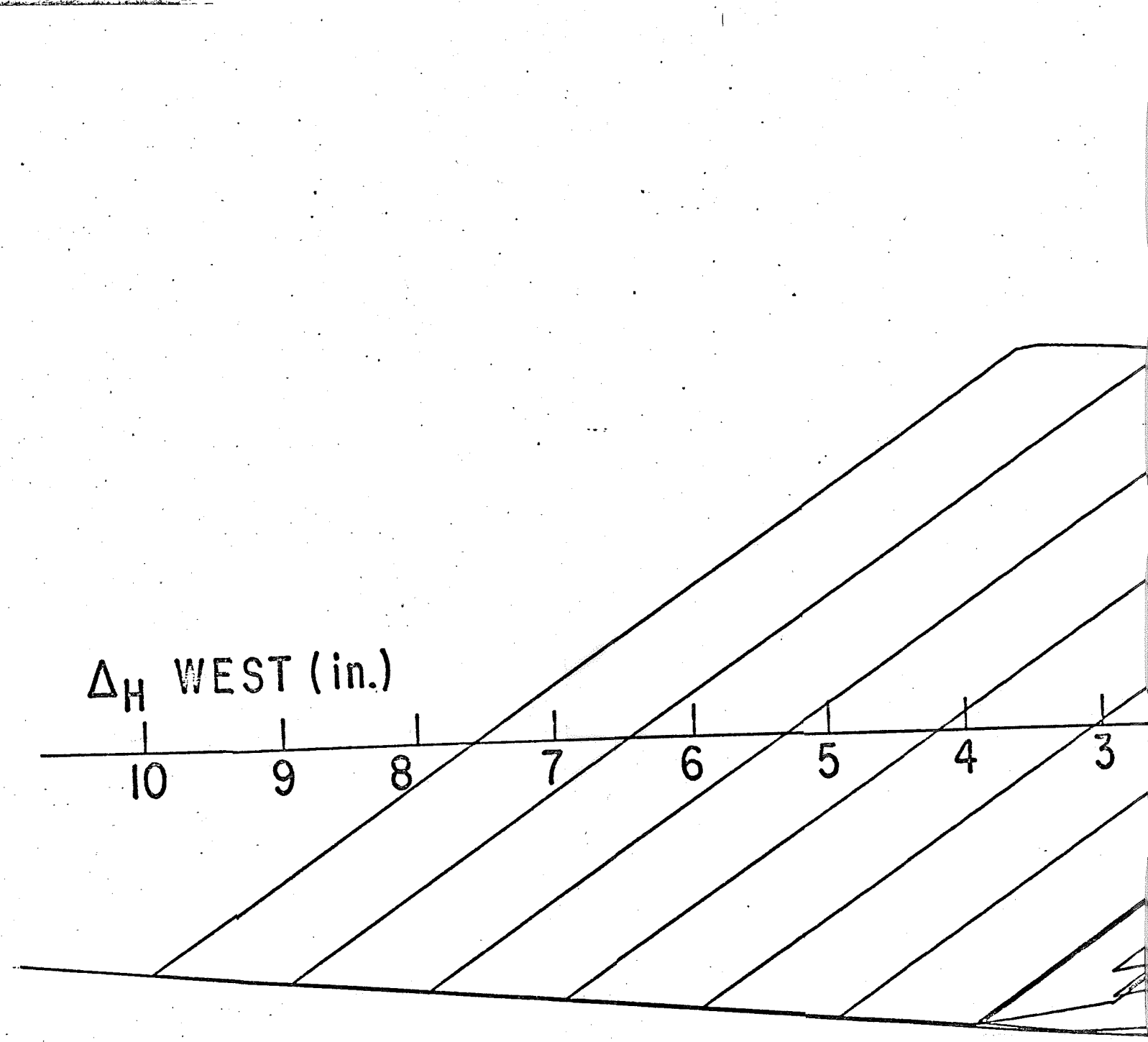
Δ_H WEST (in.)
10
9
8
7
6
5
4
3

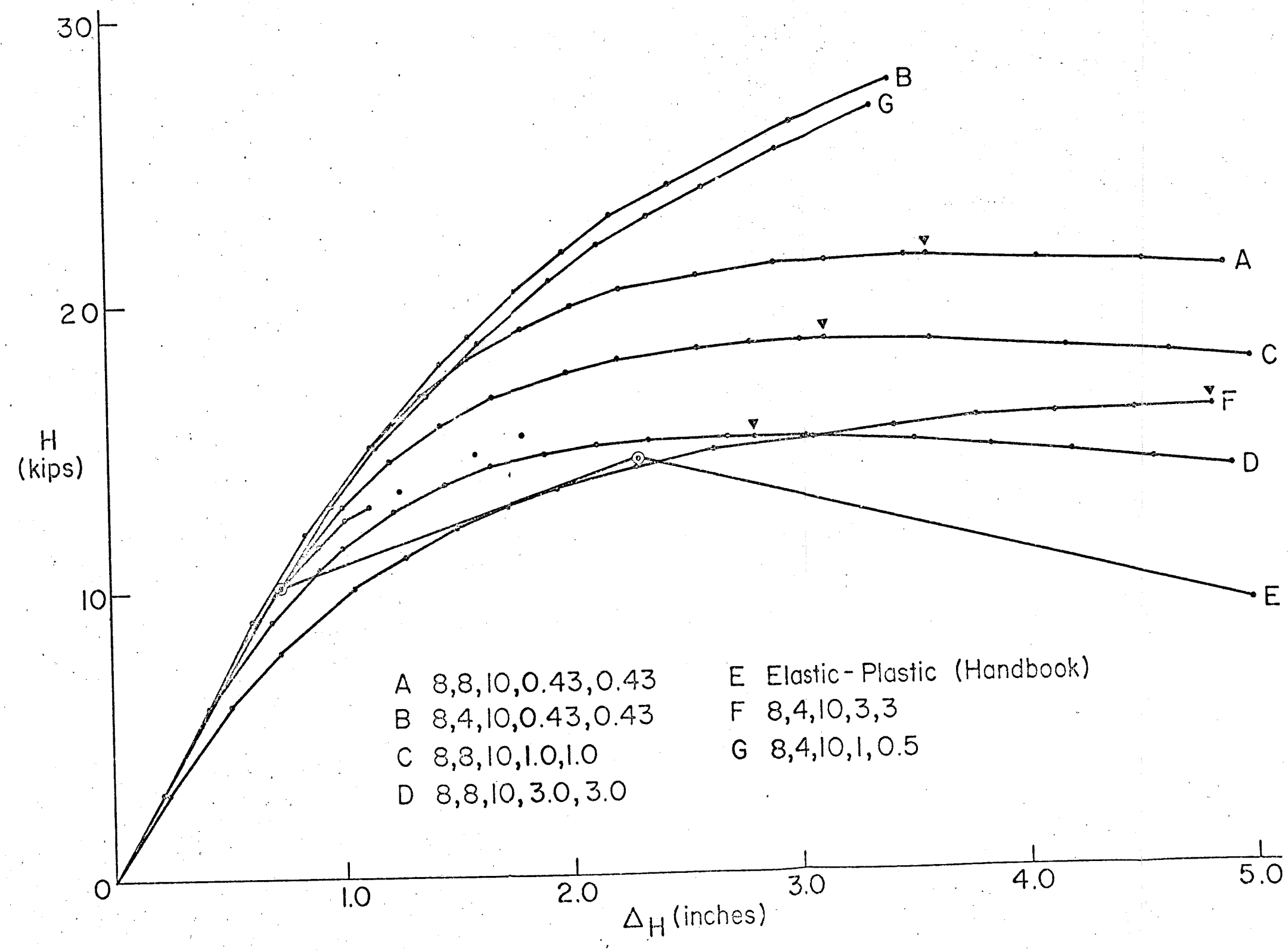

FIG. 6.6 VARIOUS MONOTONIC RAMBERG-OSGOOD CURVES AND ELASTIC-PLASTIC CURVE

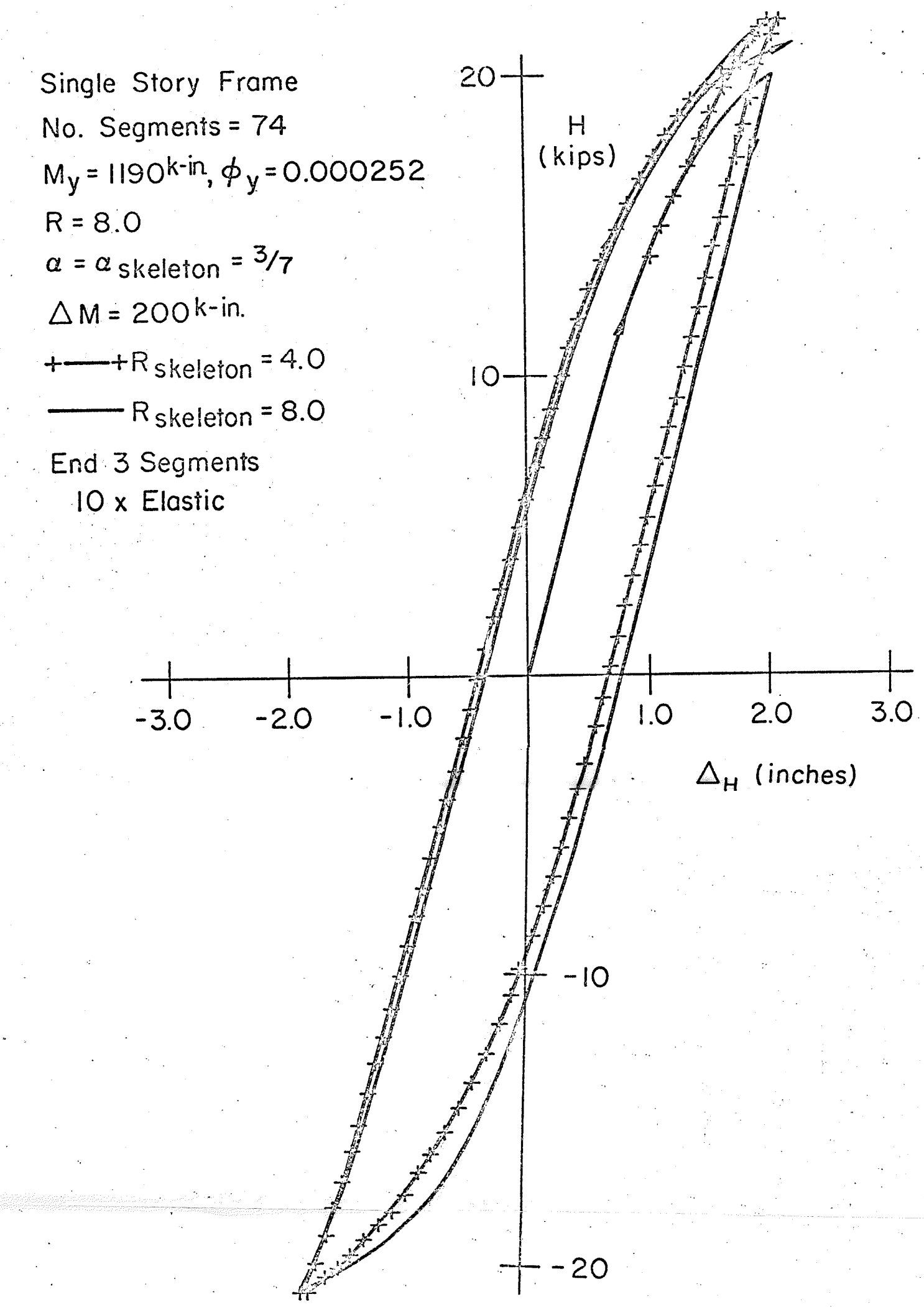

FIG. 6.7 EFFECT OF REDUCED SKELETON EXPONENT OF PREDICTED HYSTERESIS LOOP

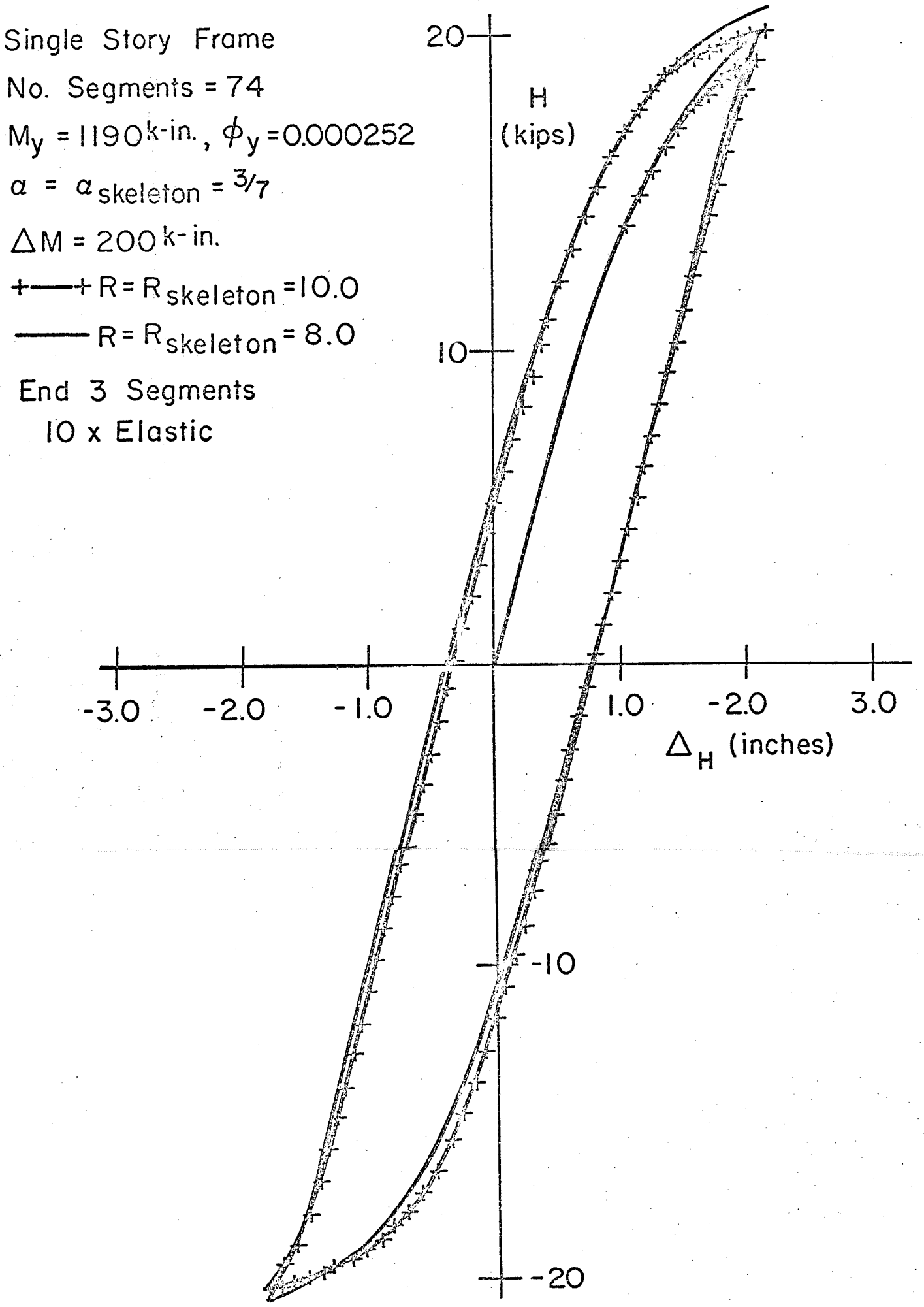

FIG. 6.8 INSENSITIVITY OF HYSTERESIS LOOP TO VARIATION IN THE RAMBERG-OSGOOD EXPONENT

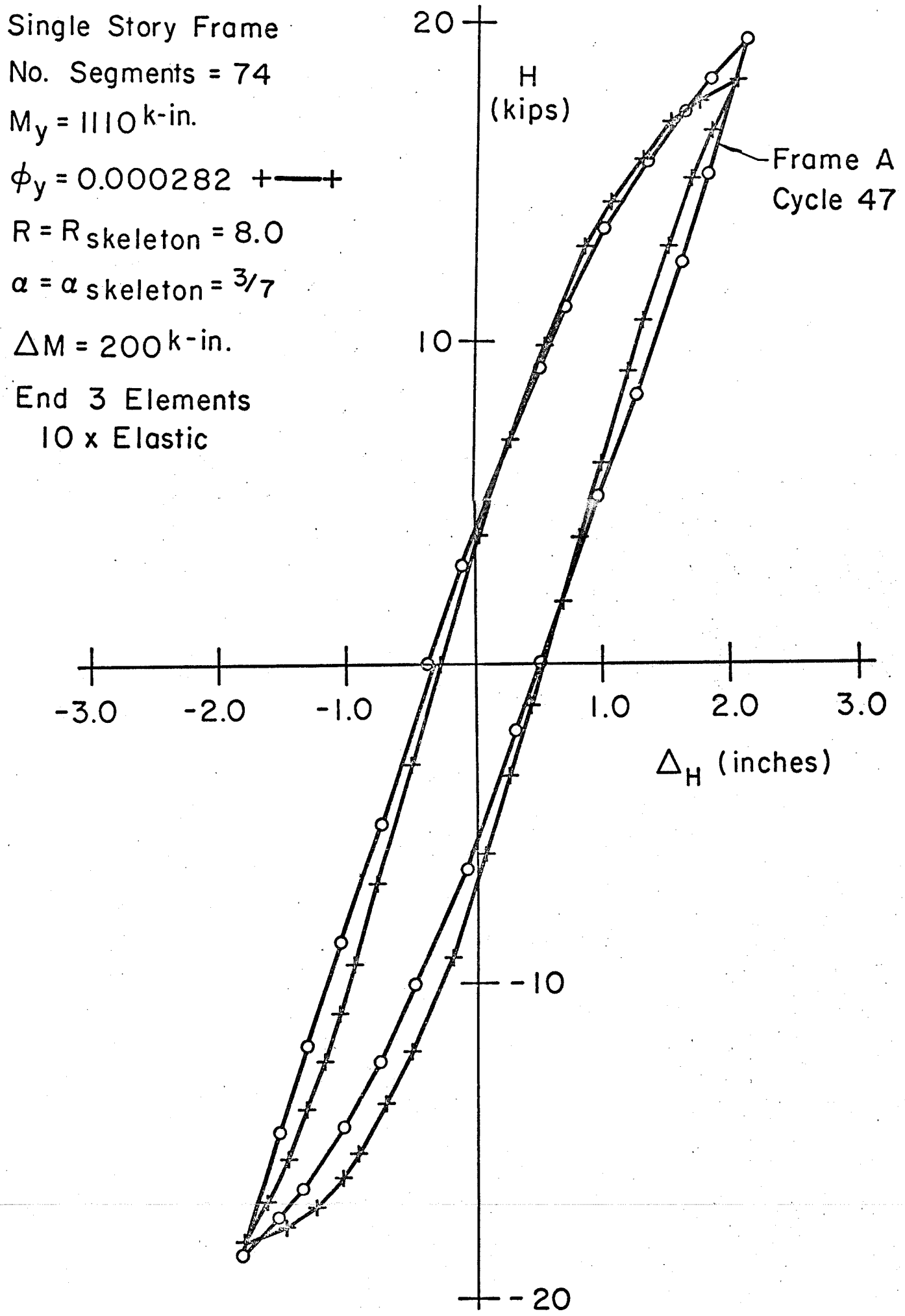

FIG. 6.9 COMPARISON OF EXPERIMENTAL AND PREDICTED HYSTERESIS LOOPS FOR FRAME A

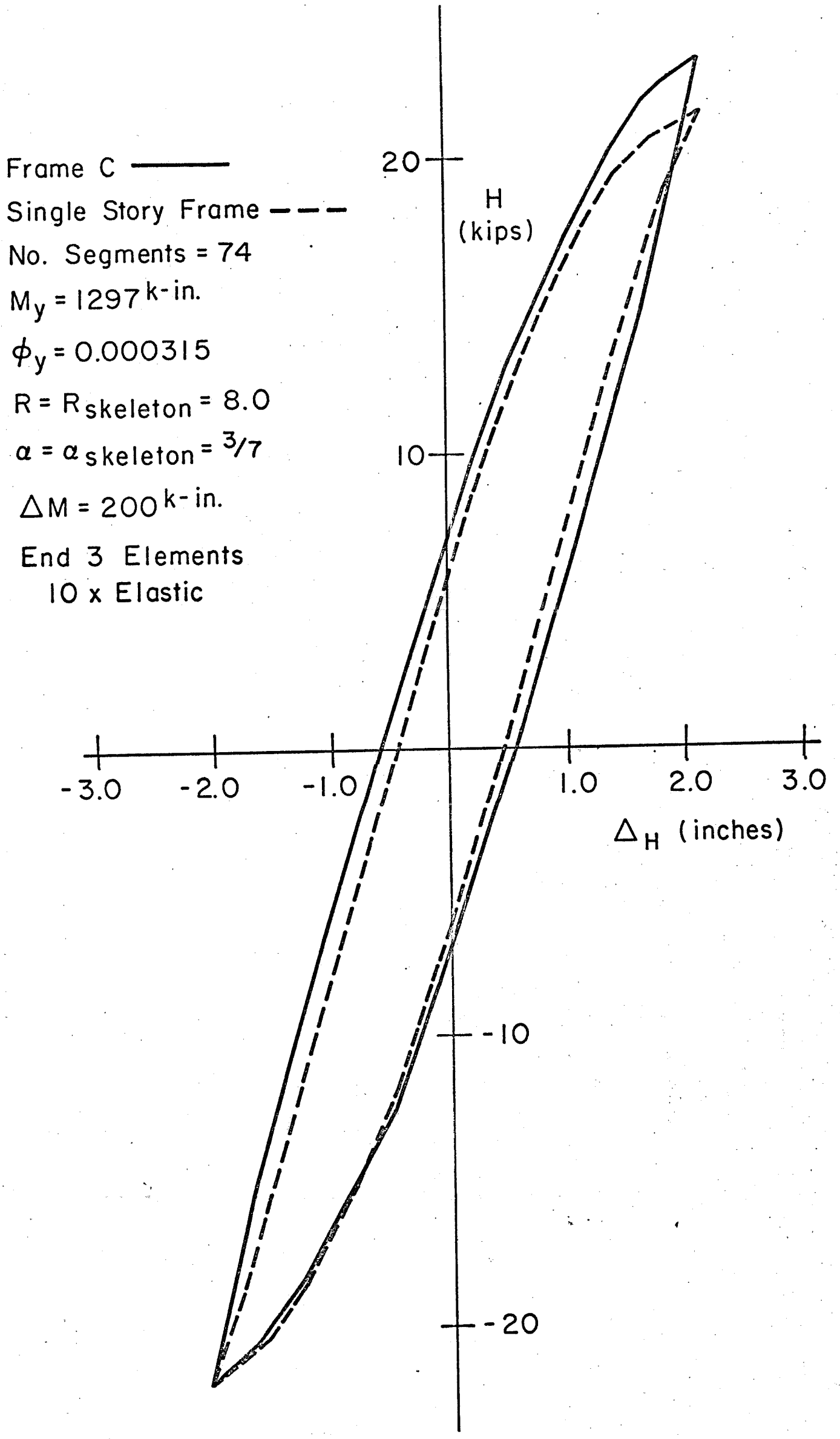

FIG. 6.10 COMPARISON OF EXPERIMENTAL (± 2.2 in.) AND PREDICTED HYSTERESIS LOOPS FOR FRAME C

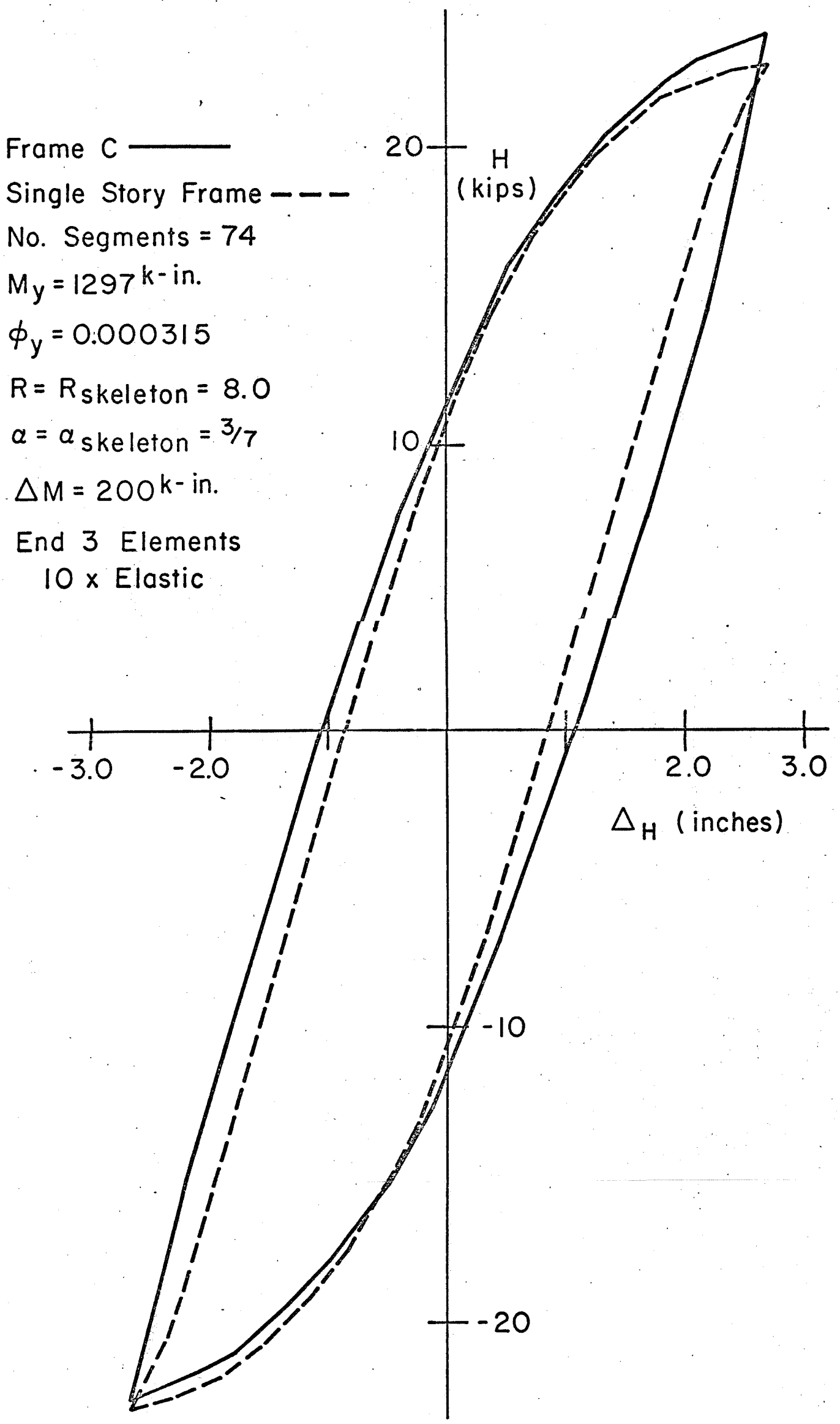

FIG. 6.11 COMPARISON OF EXPERIMENTAL (± 2.8 in.) AND PREDICTED HYSTERESIS LOOPS FOR FRAME C

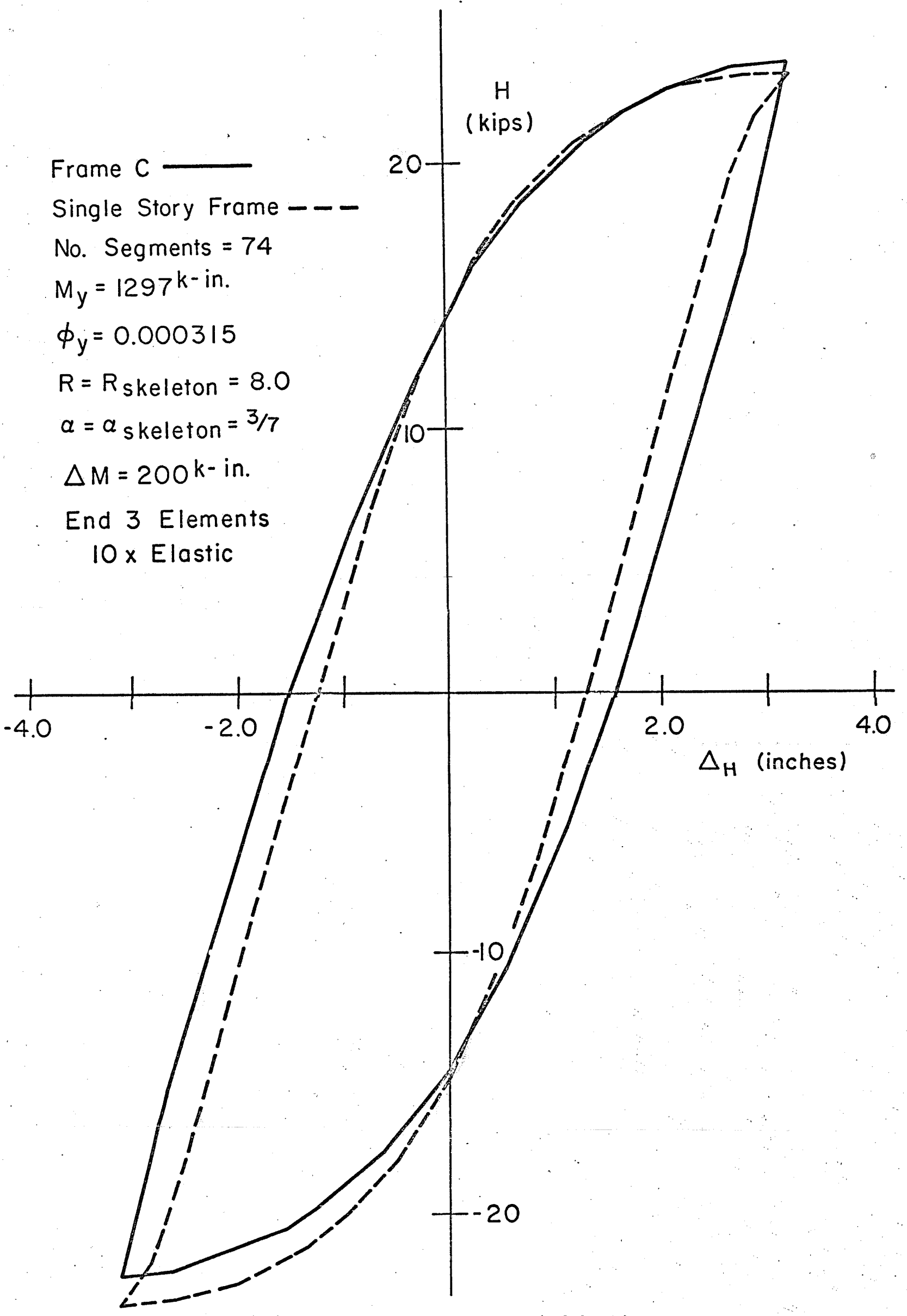

FIG. 6.12 COMPARISON OF EXPERIMENTAL (± 3.3 in.) AND PREDICTED HYSTERESIS LOOPS FOR FRAME C

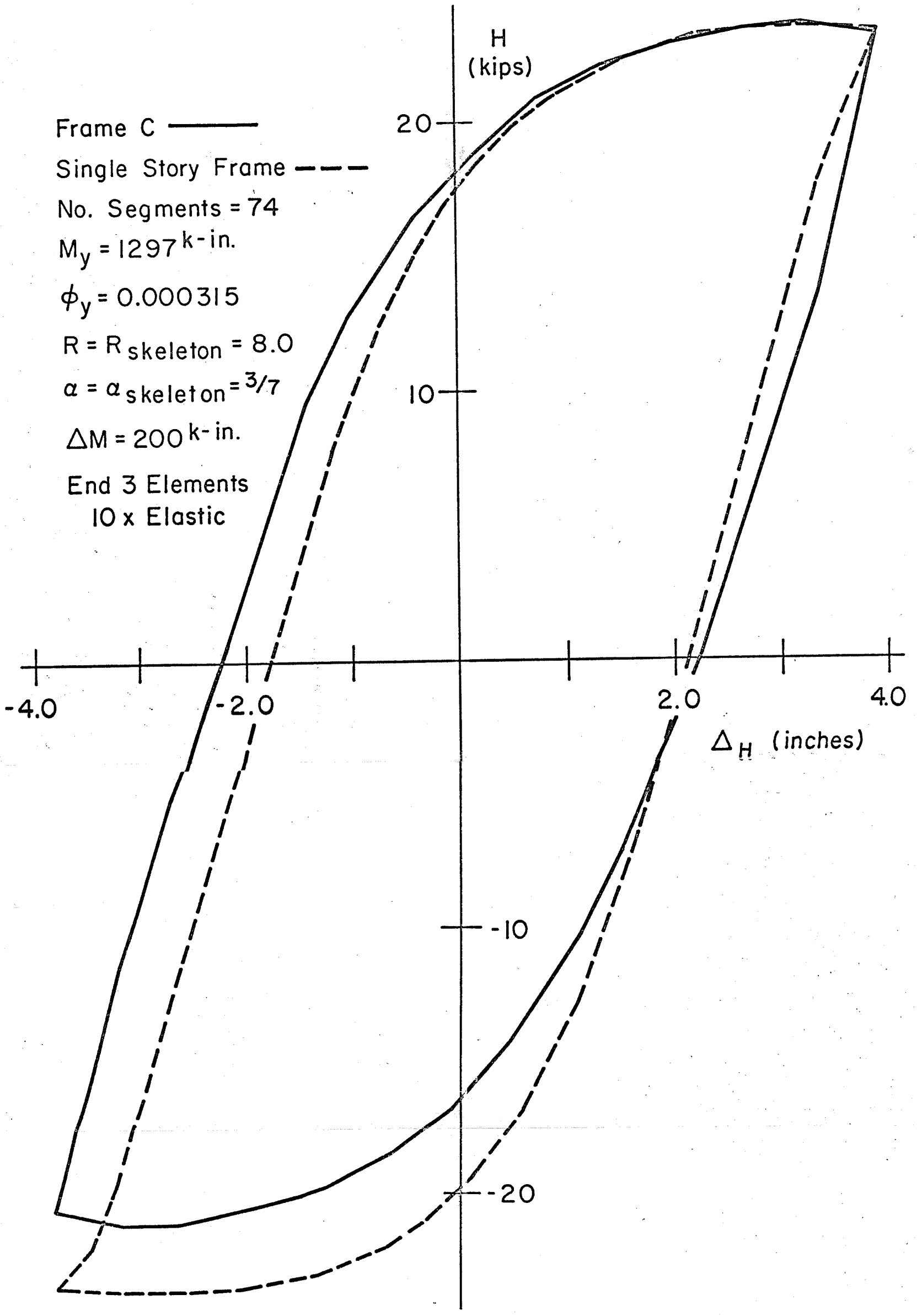

FIG. 6.13 COMPARISON OF EXPERIMENTAL (± 4.0 in.) AND PREDICTED HYSTERESIS LOOPS FOR FRAME C

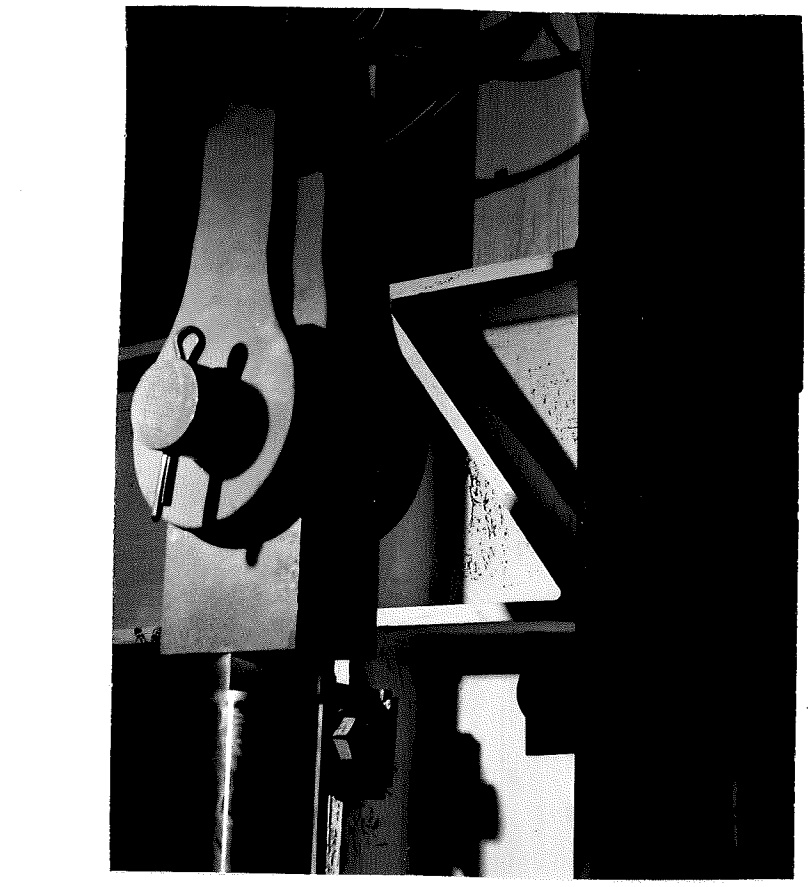

FIG. 6.14 YIELDING IN CONNECTIONS OF FRAME A

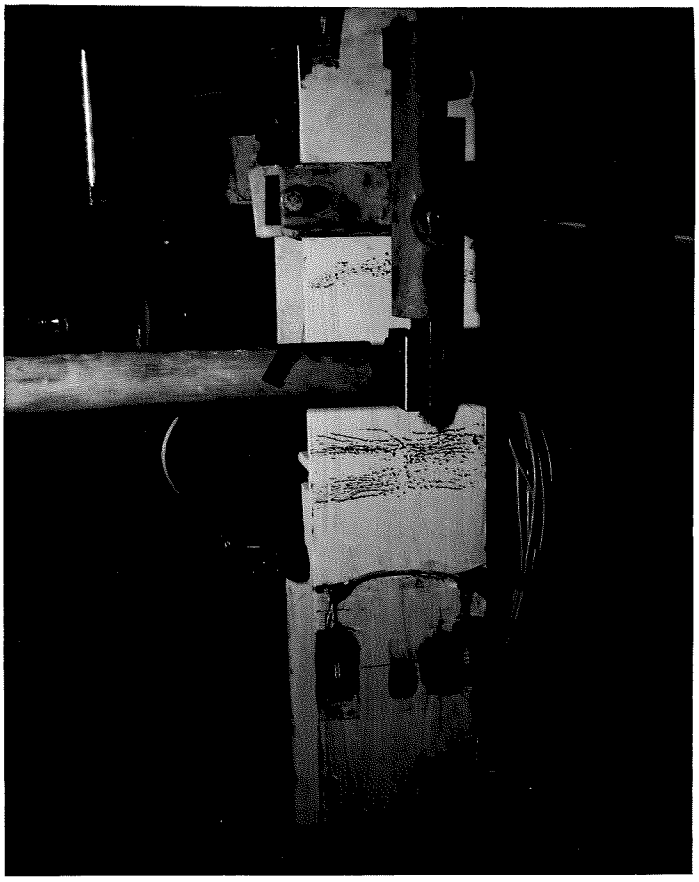

FIG. 6.15 YIELDING ABOVE AND BELOW CONNECTION IN FRAME A

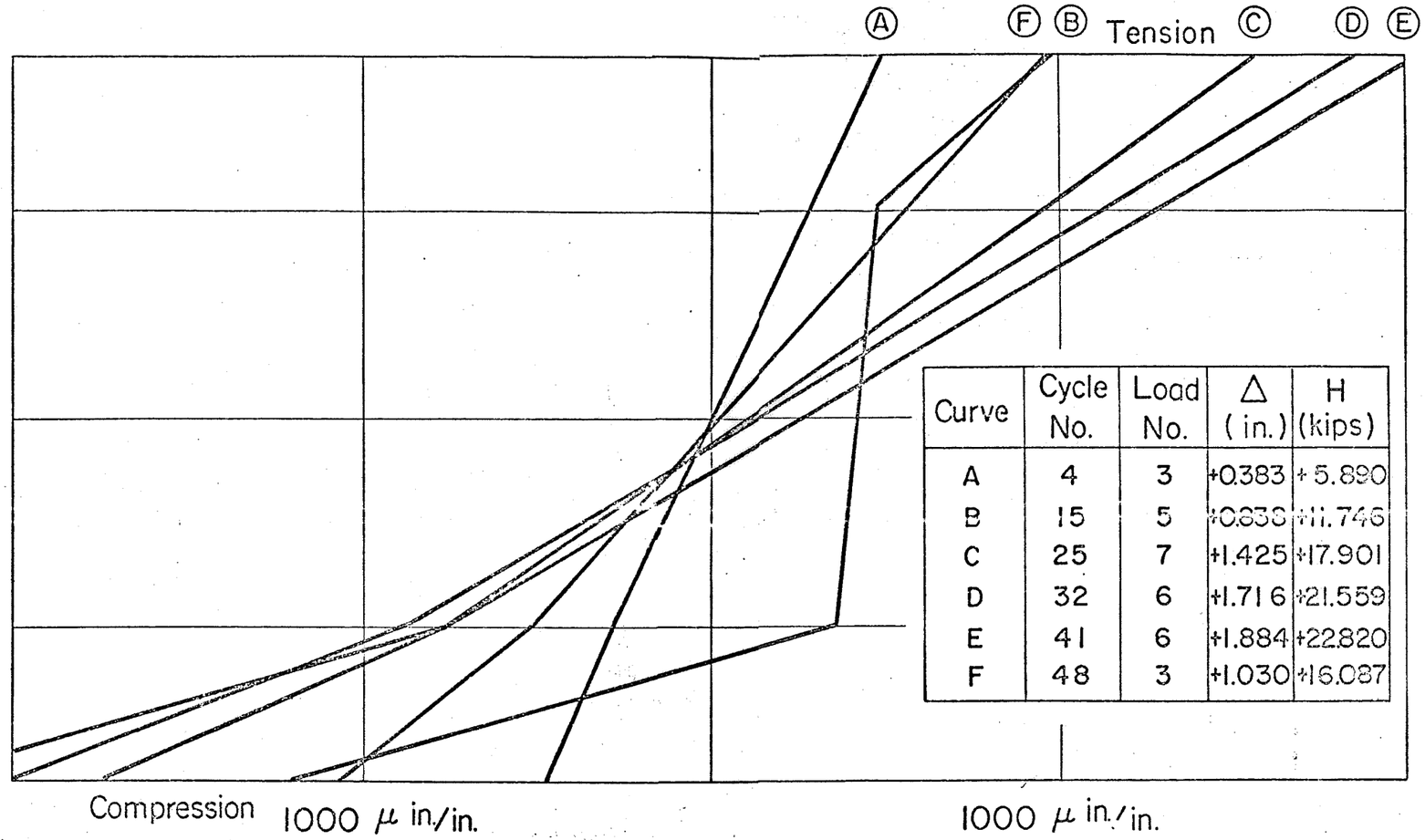

Curve	Cycle No.	Load No.	Δ (in.)	H (kips)
A	4	3	+0.383	+5.890
B	15	5	+0.838	+11.746
C	25	7	+1.425	+17.901
D	32	6	+1.716	+21.559
E	41	6	+1.884	+22.820
F	48	3	+1.030	+16.087

FIG. 6.16 STRAIN PROFILE IN FRAME C BEAM (EAST END)

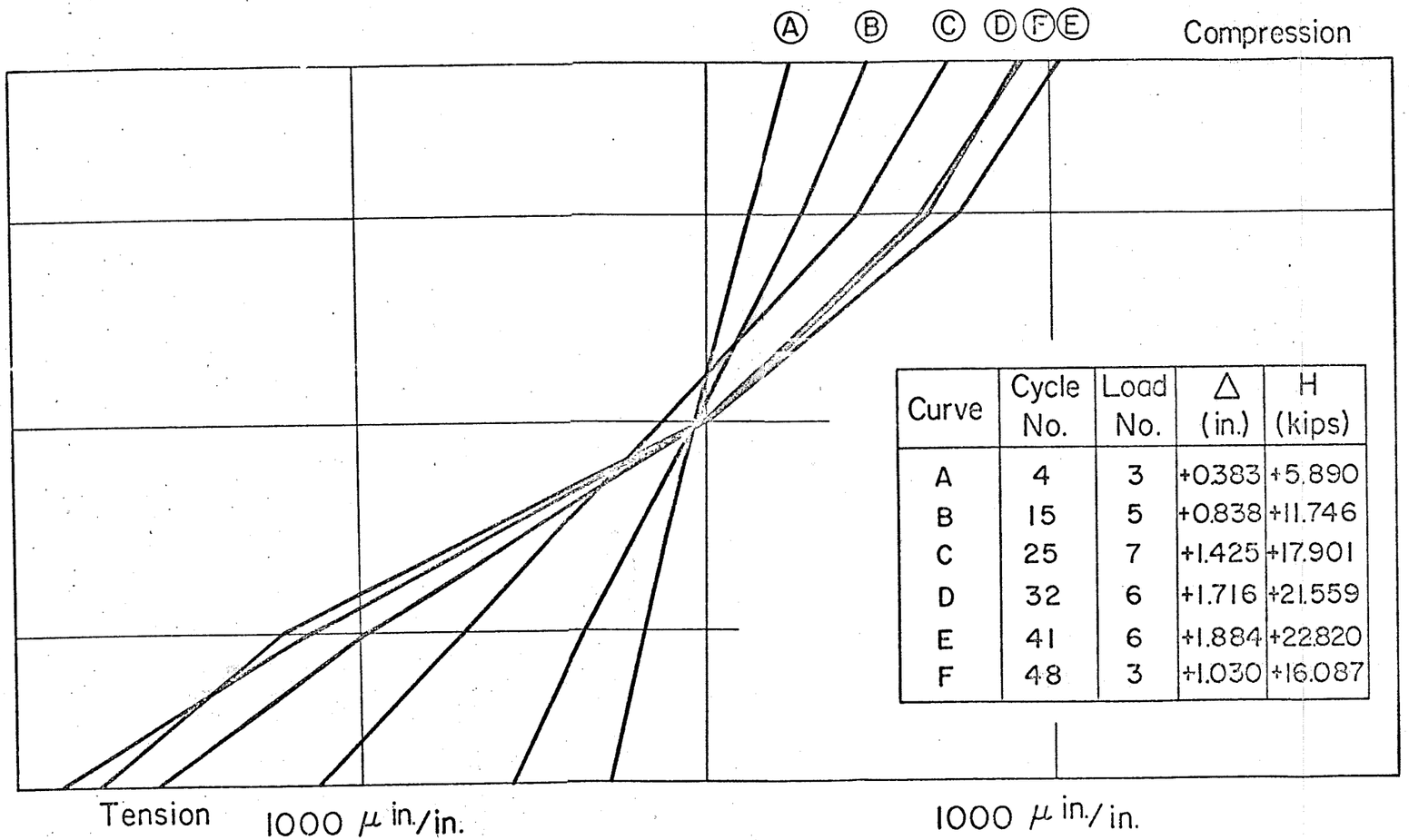

Curve	Cycle No.	Load No.	Δ (in.)	H (kips)
A	4	3	+0.383	+5.890
B	15	5	+0.838	+11.746
C	25	7	+1.425	+17.901
D	32	6	+1.716	+21.559
E	41	6	+1.884	+22.820
F	48	3	+1.030	+16.087

FIG. 6.17 STRAIN PROFILE IN FRAME C BEAM (WEST END)

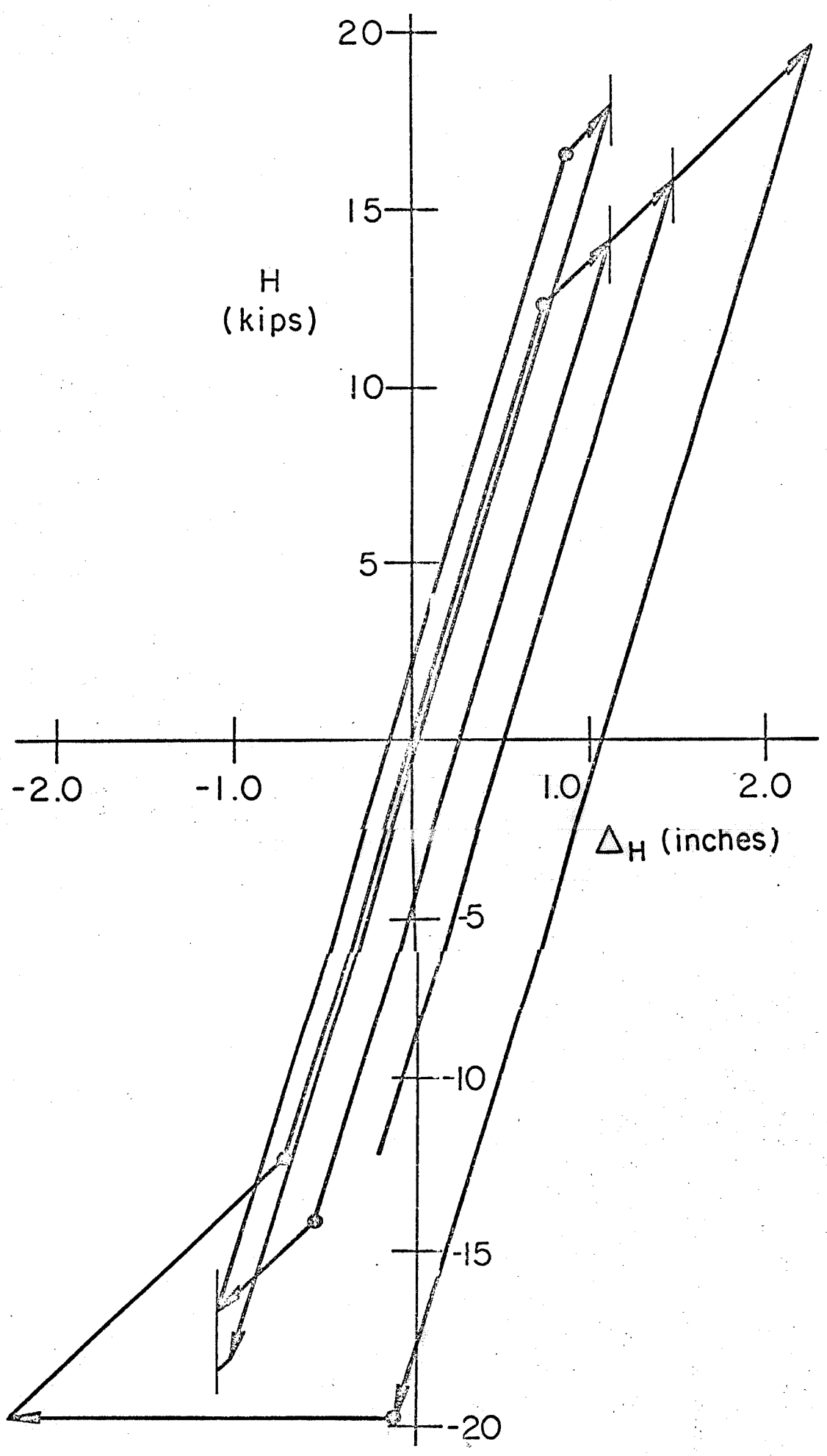

FIG. 6.18 PREDICTION OF FIRST ORDER ELASTIC-PLASTIC SHAKING DOWN OF SINGLE STORY FRAME

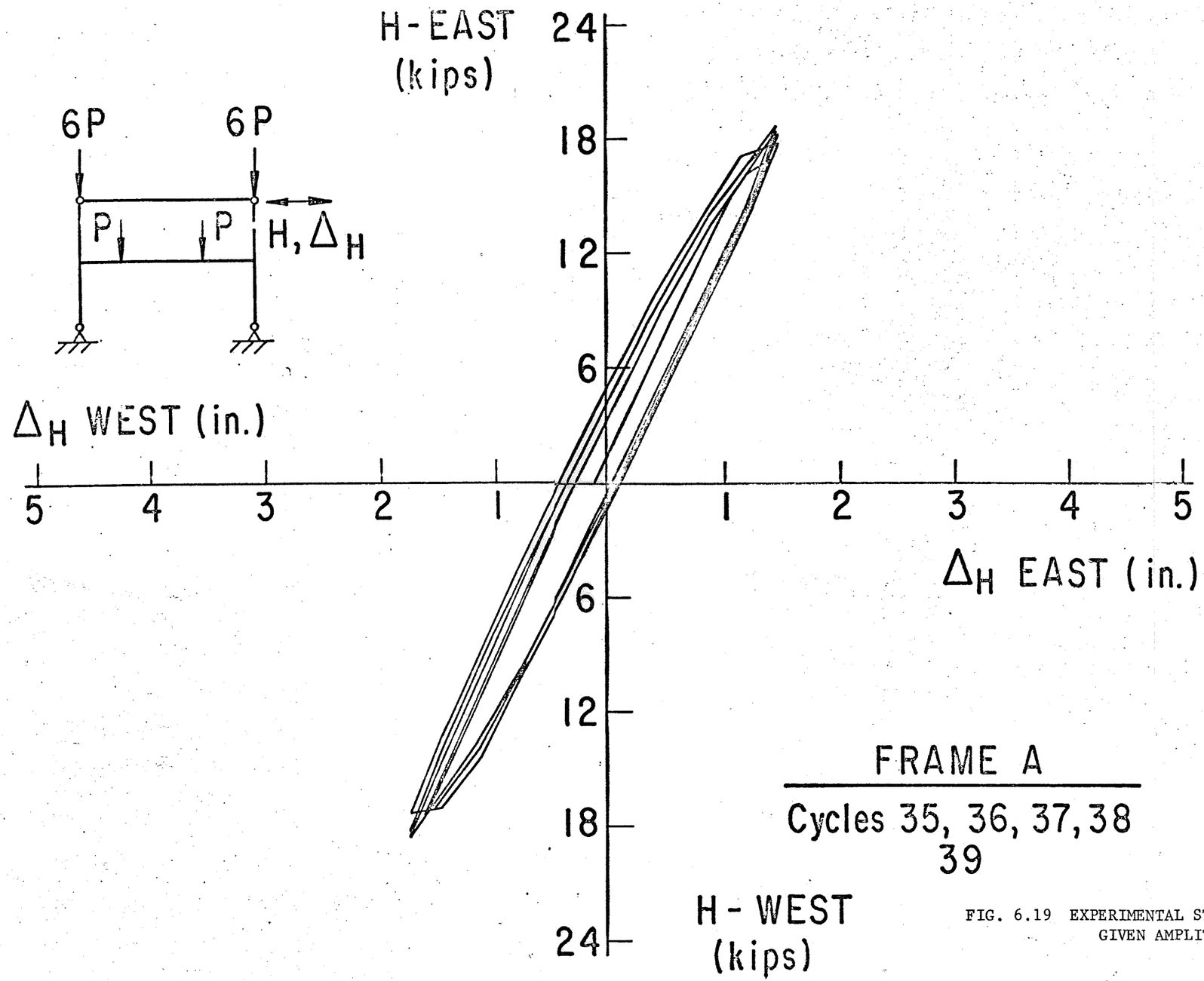

FIG. 6.19 EXPERIMENTAL STABILIZATION AT A GIVEN AMPLITUDE

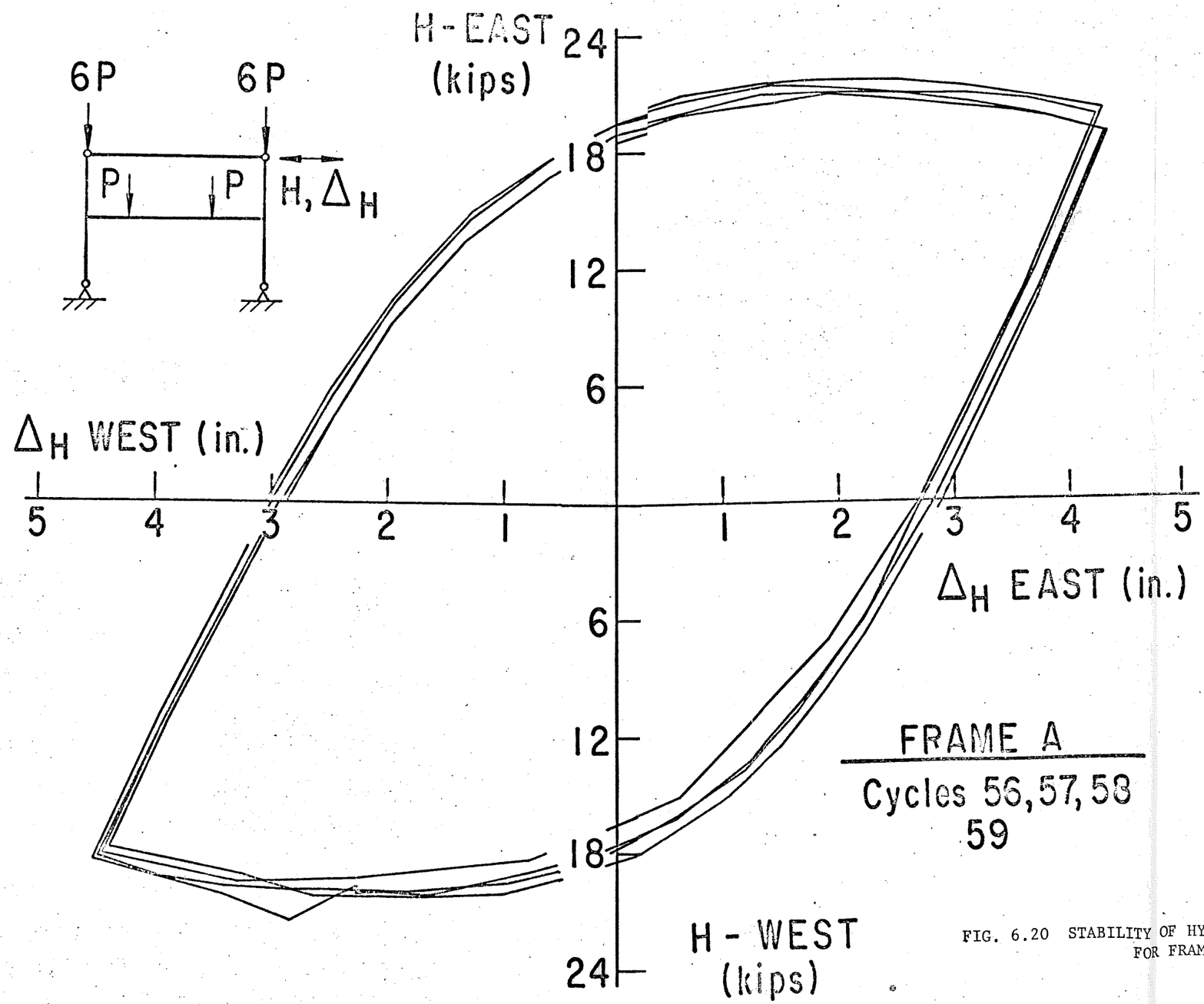

FIG. 6.20 STABILITY OF HYSTERESIS LOOPS FOR FRAME A

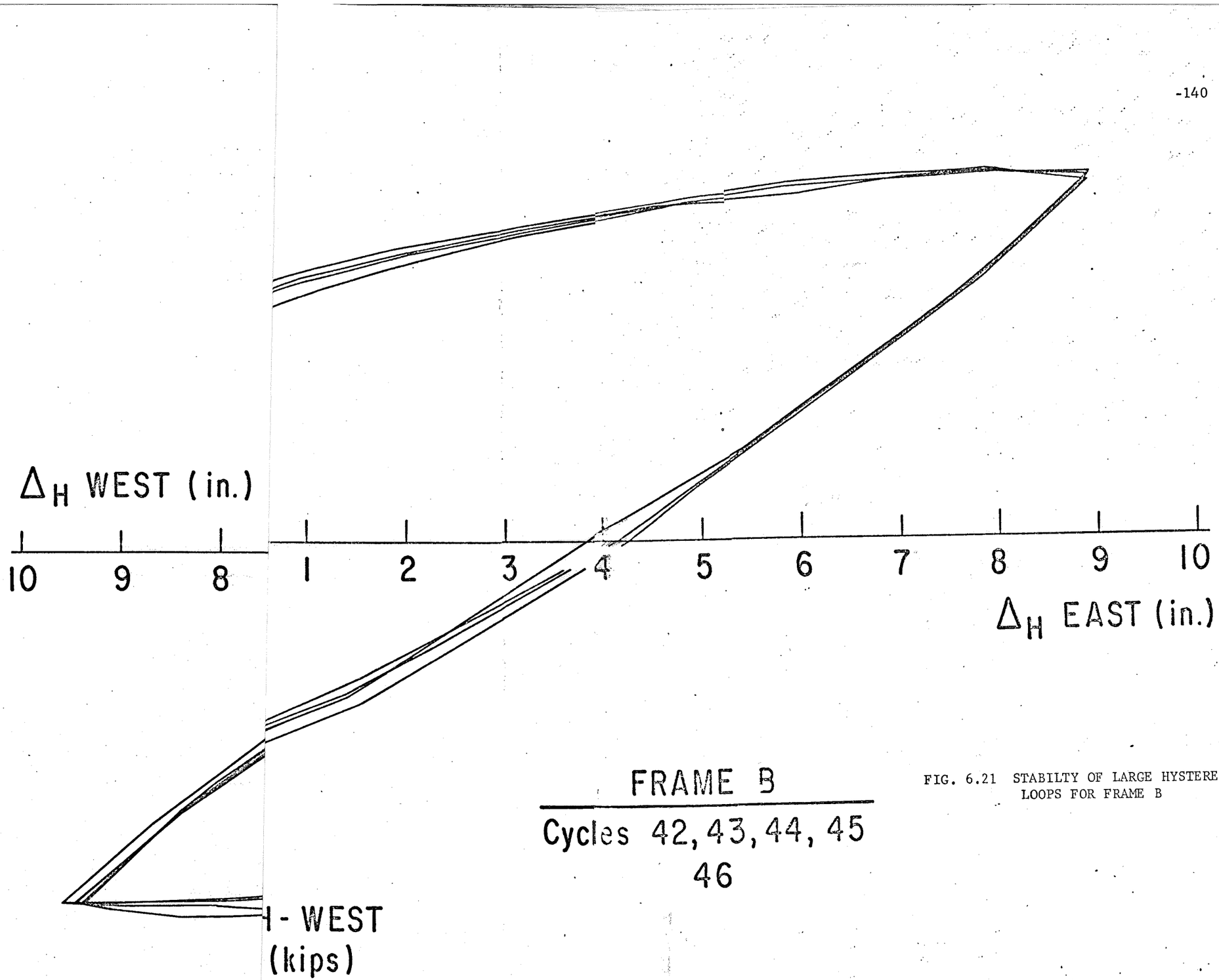

FIG. 6.21 STABILTY OF LARGE HYSTERESIS LOOPS FOR FRAME B

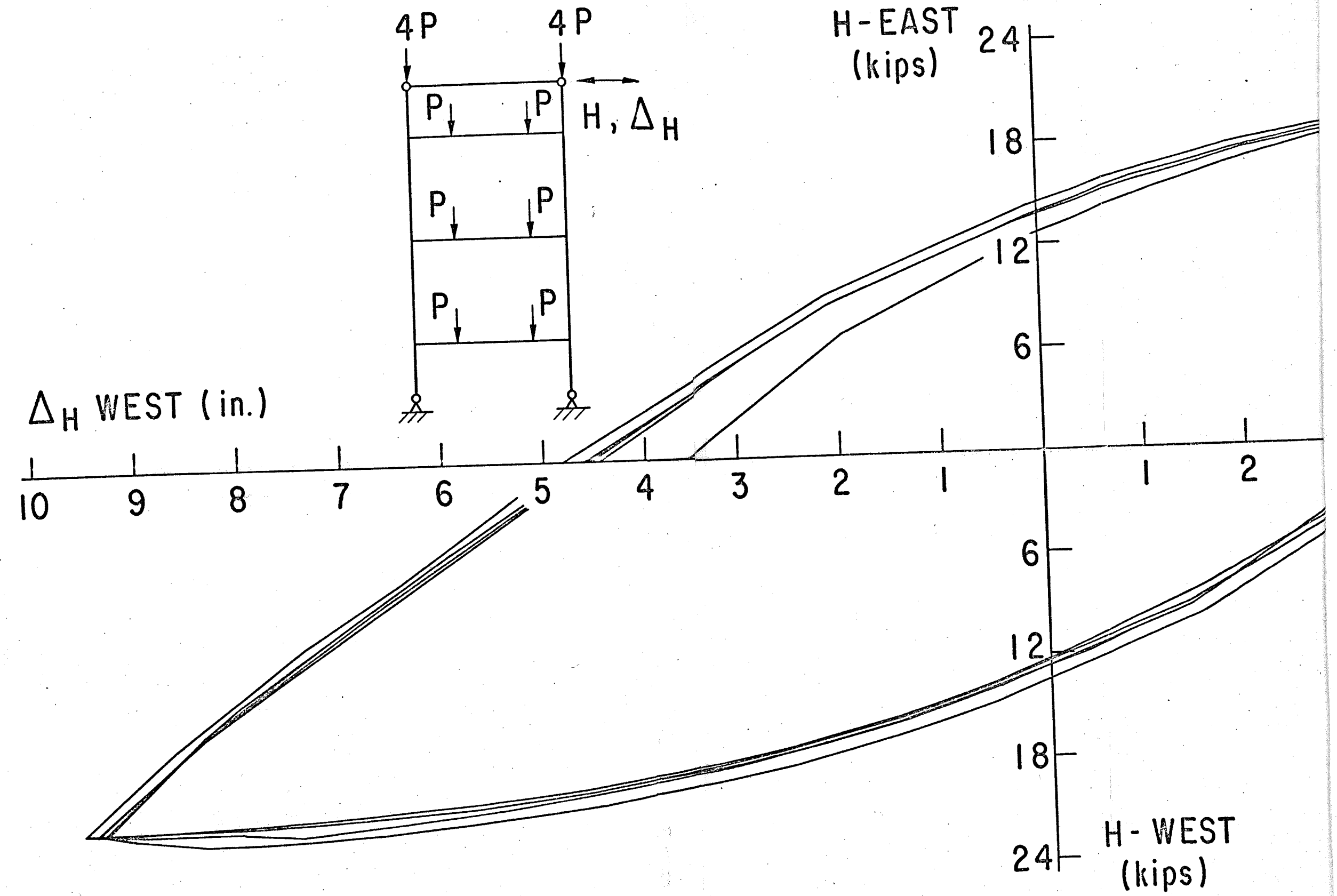
4P
4P
P
P
H, Δ_H
P
P
P
P
Δ_H WEST (in.)
10
9
8
7
6
5
4
3
2
1
H-EAST
(kips)
24
18
12
6
1
2
6
12
18
24
H-WEST
(kips)

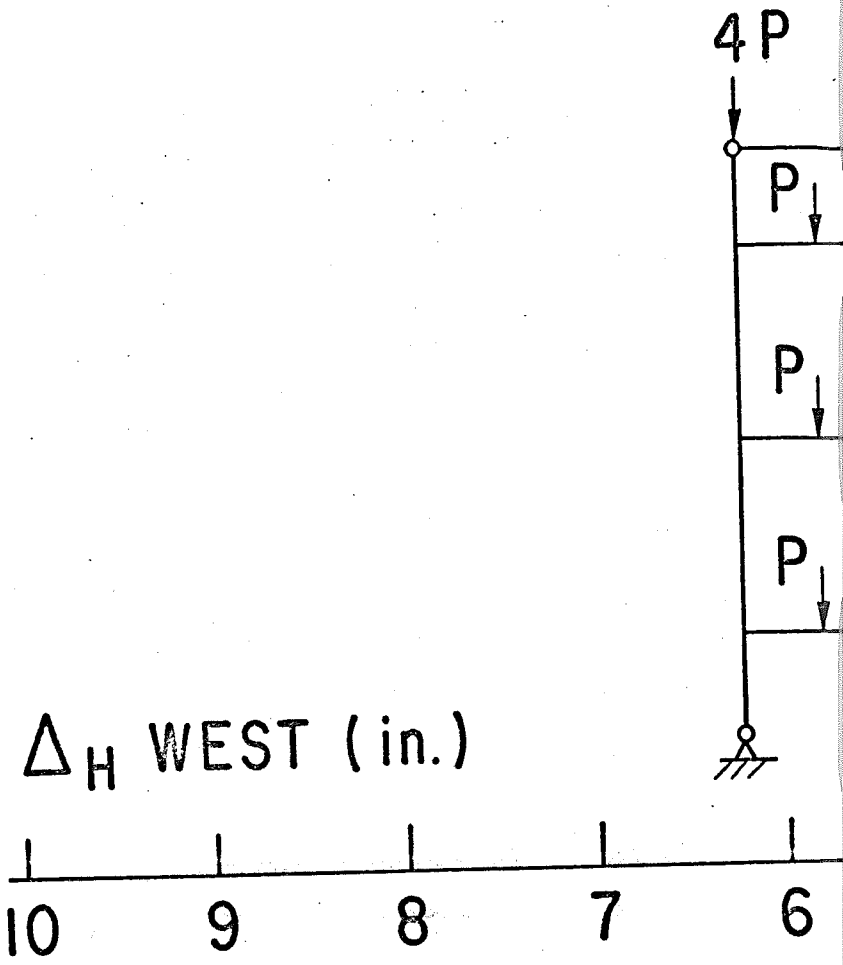

Δ_H WEST (in.)

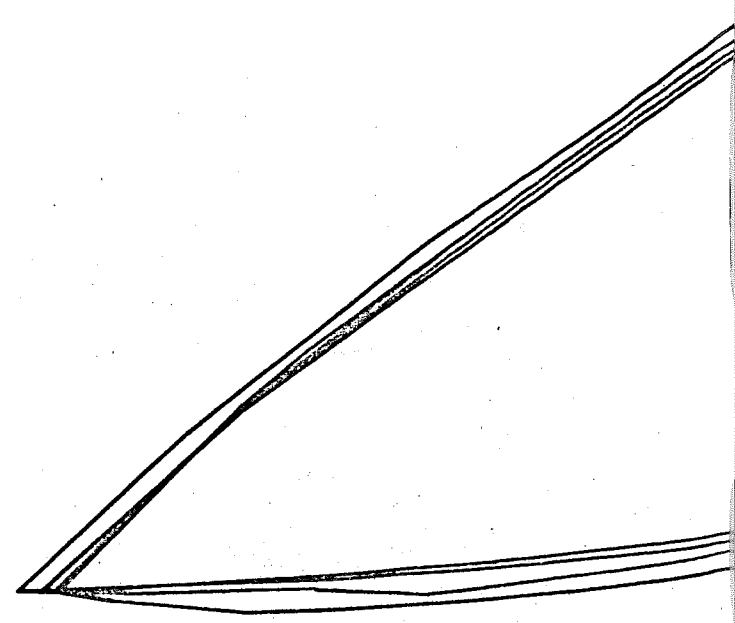

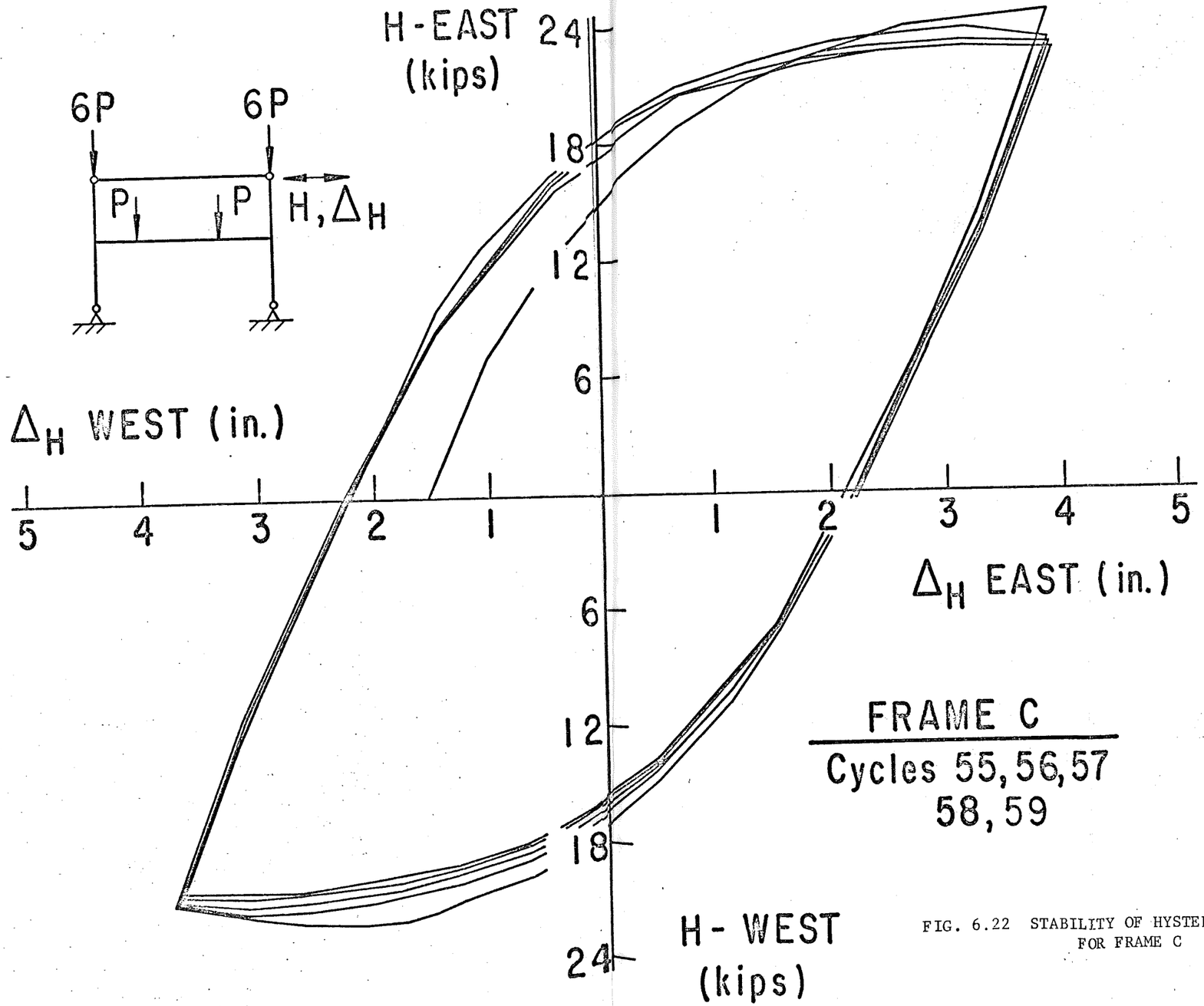

FIG. 6.22 STABILITY OF HYSTERESIS LOOPS FOR FRAME C

11. NOMENCLATURE

Terms and symbols were defined where they first appeared in the text and summarized below.

H	=	lateral loading on the frame
L, L_1, L_2, L_3	=	full length of beam and partial lengths
M_A, M_B	=	end moments on the beam
M_{x_i}	=	moment at point i on the beam
M_y	=	characteristic constant moment in the Ramberg-Osgood formulation
N	=	odd positive integer exponent in the Ramberg-Osgood formulation
P	=	typical working level of gravity load applied to the beam and in multiples to the tops of the columns (equal to 17.28 kips throughout)
P_L, P_R	=	concentrated loads, left and right
$P\text{-}\Delta$	=	denotes effect of gravity loads acting at the sway displacement
$R, R_{SKELETON}$	=	fractional exponent for Ramberg-Osgood formulation for hysteresis and skeleton curves, respectively.
V_A, V_B	=	end shears on the beam
$\alpha, \alpha_{SKELETON}$	=	constant coefficient for the exponential portion of Ramberg-Osgood formulation for hysteresis and skeleton curves, respectively.
φ_{x_i}	=	curvature at point i on the beam
φ_y	=	characteristic constant curvature in the Ramberg-Osgood formulation

Δ_H = deflection of top of frames, where the lateral load H was applied

Δ_M = incremental stiffness moment

θ_A, θ_B = end rotations of the beam

12. REFERENCES

1. International Conference of Building Officials
   UNIFORM BUILDING CODE (in particular sections 2314, 2722, 2723), Pasadena, California, 1970.

2. Sfintesco, D.
   DYNAMIC EFFECTS OF WIND AND EARTHQUAKE, Theme IIIc, Preliminary Publication of IABSE for Eighth Congress in New York in September of 1968 (Pub. June 1967).

3. Hanson, R. E.
   COMPARISON OF STATIC AND DYNAMIC HYSTERESIS CURVES, Journal of the Engineering Mechanics Division, ASCE, 92, (EM5) p. 87, (October 1966).

4. AlMuti, A. M.
   POST-ELASTIC RESPONSE OF MILD STEEL BEAMS TO STATIC AND DYNAMIC LOADING, Ph.D. Dissertation, The University of Michigan, June 1970.

5. Manjoine, M. J.
   INFLUENCE OF RATE OF STRAIN AND TEMPERATURE ON YIELD STRESSES OF MILD STEEL, Transactions, ASME, Vol. 66, 1944, pp. A211-18.

6. Rao, N. R. N., Lohrmann, M., and Tall, L.
   EFFECT OF STRAIN RATE ON THE YIELD STRESS OF STRUCTURAL STEELS, Journal of Materials, ASTM, Vol. 1, No. 1, March 1966.

7. Berg, G. V.
   A STUDY ON THE EARTHQUAKE RESPONSE OF INELASTIC SYSTEMS, Proceeding 34th Annual Convention Structural Engineering Association of California, October 1965.

8. Morrow, J.
   CYCLIC PLASTIC STRAIN ENERGY AND FATIGUE OF METALS, Special Technical Publication No. 378, ASTM, 1965.

9. Benham, P. P. and Ford, H.
   LOW ENDURANCE FATIGUE OF A MILD STEEL AND AN ALUMINUM ALLOW, Journal of Mechanical Engineering Science, 3 (2), (June 1961).

10. ASCE-WRC
    PLASTIC DESIGN IN STEEL, ASCE Manual of Engineering Practice No. 41, 1971.

11. Bertero, V. V. and Popov, E. P.
    EFFECT OF LARGE ALTERNATING STRAINS ON STEEL BEAMS, Journal of the Structural Division, ASCE, 91 (ST1), p. 1, (February 1965).

12. Popov, E. P. and Franklin, H. A.
STEEL BEAM-TO-COLUMN CONNECTIONS SUBJECTED TO CYCLICALLY REVERSED LOADING, Steel Research for Construction, AISI, February 1966.

13. Popov, E. P. and Pinkney, R. B.
BEHAVIOR OF STEEL BUILDING CONNECTIONS SUBJECTED TO REPEATED INELASTIC STRAIN REVERSAL - Experimental Data - Report No. 67-31, University of California at Berkeley, December 1967.

14. Popov, E. P. and Pinkney, R. B.
BEHAVIOR OF STEEL CONNECTIONS SUBJECTED TO REPEATED INELASTIC STRAIN REVERSAL, Report No. 67-30, University of California at Berkeley, December 1967.

15. Popov, E. P. and Pinkney, R. B.
RELIABILITY OF STEEL BEAM-TO-COLUMN CONNECTIONS UNDER CYCLIC LOADING, Proceedings Fourth World Conference on Earthquake Engineering, Santiago, Chile, January 1969.

16. Popov, E. P.
PERFORMANCE OF STEEL BEAMS AND THEIR CONNECTIONS TO COLUMNS DURING SEVERE CYCLIC LOADING, Contributions to expanded discussion, Eighth Congress of IABSE, Theme III, New York, September 1968.

17. Vann, W. P.
Discussion of "CYCLIC YIELD REVERSAL IN STEEL BUILDING CONNECTIONS by E. P. Popov and R. B. Pinkney," Journal of the Structural Division, ASCE, 96 (ST1), January 1970.

18. Popov, E. P.
BEHAVIOR OF STEEL BEAM-TO-COLUMN CONNECTIONS UNDER REPEATED AND REVERSED LOADING, Plastic Design of Multi-Story Frames - Guest Lectures, Fritz Engineering Laboratory Report No. 273.62, Lehigh University, July 1966.

19. Popov, E. P. and Pinkney, R. B.
CYCLIC YIELD REVERSAL IN STEEL BUILDING CONNECTIONS, Journal of the Structural Division, ASCE, 95, (ST3), p. 327, (March 1969).

20. Popov, E. P.
LOW-CYCLE FATIGUE OF STEEL BEAM-TO-COLUMN CONNECTIONS, RILEM International symposium on the Effects of Repeated Loading of Materials and Structural Elements, Mexico City, September 15-17.

21. Sherbourne, A. N.
SOME PRELIMINARY EXPERIMENTS ON THE BEHAVIOR OF DUCTILE STRUCTURES UNDER REPEATED LOADS, Experimental Mechanics, 3 (5), p. 119, (May 1963).

22. Krishnasamy, S. and Sherbourne, A. N.
RESPONSE OF A "PLASTIC HINGE" TO LOW CYCLE ALTERNATING DEFLECTIONS, Experimental Mechanics, 8 (2), p. 133, (1966).

23. Royles, R.
INCREMENTAL EXTENSION OF MILD STEEL BEAMS IN REVERSED BENDING, Journal of Strain Analysis, 1 (2), p. 133, (1966).

24. Hagura, H.
RESEARCH ON THE ELASTIC-PLASTIC ANALYSIS OF STEEL SECTIONS SUBJECTED TO ALTERNATIVE LOADS, Trans. of the Arch. Inst. of Japan No. 125, p. 8, (July 1966).

25. Naka, T., et al
ULTIMATE STRENGTH OF COLUMNS IN MULTI-STORY RIGID FRAMES, Yawata Technical Report No. 256, p. 82, September 1966.

26. Naka, T., Kato, B., and Watabe, M.
RESEARCH ON THE BEHAVIOR OF STEEL BEAM-TO-COLUMN CONNECTIONS, Laboratory for Steel Structures, 1966, University of Tokyo, Japan.

27. Wakabayashi, M., et al.
AN EXPERIMENTAL STUDY ON THE ELASTIC-PLASTIC STABILITY OF CROSS SHAPED STRUCTURAL SYSTEMS, Kinki Branach of the Arch. Inst. of Japan, 1967.

28. Wakabayashi, M.
THE RESTORING FORCE CHARACTERISTIC OF MULTI-STORY FRAMES, Bulletin of the Disaster Prevention Research Institute (Japan), 14, Part 2, February 1965.

29. Igarashi, S., et al.
PLASTIC BEHAVIOR OF STEEL FRAMES UNDER CYCLIC LOADING, Trans. of the Arch. Inst. of Japan, No. 130, December 1966.

30. Igarashi, N.
HYSTERESIS CHARACTERISTICS AND STRUCTURAL DAMPING OF STEEL STRUCTURES UNDER ALTERNATE LATERAL LOADING, Trans. of the Arch. Inst. of Japan, No. 120, February 1960.

31. Yokoo, Y., et al.
HORIZONTAL-FORCE-RESTRAINT PROPERTIES OF MULTI-STORY STEEL FRAMES, Yawata Technical Report No. 256, p. 43, September 1966.

32. Yarimci, E.
INCREMENTAL INELASTIC ANALYSIS OF FRAMED STRUCTURES AND SOME EXPERIMENTAL VERIFICATIONS, Ph.D. Dissertation, Lehigh University, 1966.

33. Arnold, P., Adams, P. F., and Lu, L. W.
THE EFFECT OF INSTABILITY ON THE CYCLIC BEHAVIOR OF A FRAME, Proceedings, RILEM Symposium on "Effects of Repeated Loading on Materials and Structures," Mexico City, September 1966.

34. Beedle, L. S.
REVERSED LOADING OF FRAMES - PRELIMINARY TESTS, Proceedings, Structural Engineers Association of California, p. 87, 1965.

35. Parikh, B. P.
ELASTIC-PLASTIC ANALYSIS AND DESIGN OF UNBRACED MULTI-STORY STEEL FRAMES, Ph.D. Dissertation, Lehigh University, 1966.

36. McNamee, B. M.
THE GENERAL BEHAVIOR AND STRENGTH OF UNBRACED MULTI-STORY FRAMES UNDER GRAVITY LOADING, Ph.D. Dissertation, Lehigh University, June 1967.

37. Korn, A. and Galambos, T. V.
BEHAVIOR OF ELASTIC-PLASTIC FRAMES, Journal of the Structural Division, ASCE, 94 (ST5), (May 1968).

38. Kaldjian, M. J.
MOMENT-CURVATURE OF BEAMS AS RAMBERG-OSGOOD FUNCTIONS, Journal of the Structural Division, ASCE, 93 (ST5), (May 1968).

39. Wright, E. W. and Gaylord, E. H.
ANALYSIS OF UNBRACED MULTI-STORY STEEL RIGID FRAMES, Journal of the Structural Division, ASCE, 94 (ST5), (May 1968).

40. Ramberg, W. and Osgood, W.R.
DESCRIPTION OF STRESS-STRAIN CURVES BY THREE PARAMETERS, Technical Note 902, NACA, July 1943.

41. Alvarez, R. J. and Birnstiel, C.
INELASTIC ANALYSIS OF MULTI-STORY FRAMES, Journal of the Structural Division, ASCE, 95 (ST11), (November 1969).

42. Tanabashi, R., et al
LOAD-DEFLECTION BEHAVIORS AND PLASTIC FATIGUE OF WIDE-FLANGED BEAMS SUBJECTED TO ALTERNATING PLASTIC BENDING, Trans. of the Arch. Inst. of Japan, I: No. 175, (September 1970), II: No. 176, (October 1970), III: No. 177, (November 1970).

43. Lazan, B. J.
DAMPING OF MATERIALS AND MEMBERS IN STRUCTURAL MECHANICS, Pergamon Press, 1968.

44. Jennings, P. C.
PERIODIC RESPONSE OF A GENERAL YIELDING STRUCTURE, Journal of the Engineering Mechanics Division, ASCE, 90 (EM2), (April 1964).

45. Goel, S. C.
INELASTIC BEHAVIOR OF MULTI-STORY BUILDING FRAMES SUBJECTED TO EARTHQUAKE MOTION, Ph.D. Dissertation, The University of Michigan December 1967.

46. Tavernelli, J. F. and Coffin, L. F., Jr.
EXPERIMENTAL SUPPORT FOR GENERALIZED EQUATION PREDICTING LOW CYCLE FATIGUE, Trans. ASME, Vol. 84, Series D, Journal, Basic Engineering, December 1962.

47. Kurobane, Y. and Shiraishi, M.
BEHAVIOR OF YIELD HINGE AT GIRDER END UNDER ALTERNATING BENDING, Arch. Inst. of Japan, Fukuoka, Japan, April 6, 1969.

48. Chipman, R. D.
DIMENSIONLESS INELASTIC BENDING RELATIONSHIPS, Experimental Mechanics, February 1963.

49. Giberson, M. F.
TWO NONLINEAR BEAMS WITH DEFINITIONS OF DUCTILITY, Journal of the Structural Division, ASCE, 95 (ST2), February 1969).

50. Carpenter, L. D. and Lu, L. W.
BEHAVIOR OF STEEL FRAMES SUBJECTED TO REPEATED AND REVERSED LOADS, Final Report of Eighth Congress of IABSE in New York, September 1968.

51. Carpenter, L. D. and Lu, L. W.
REPEATED AND REVERSED LOAD TESTS ON FULL-SCALE STEEL FRAMES, Proceedings, Fourth World Conference on Earthquake Engineering, Santiago, Chile, January 1969.

52. Driscoll, G. C., Jr., et al.
PLASTIC DESIGN OF MULTI-STORY FRAMES - LECTURE NOTES, Fritz Engineering Laboratory Report No. 273.20, Lehigh University, August 1965.

53. Masing, G.
EIGENSPANNUNGEN AND VERFESTIGUNG BEIM MESSING, Proceedings of the Second International Congress for Applied Mechanics, Zurich, September 1926.

54. Iwan, W. D.
ON A CLASS OF MODELS FOR THE YIELDING BEHAVIOR OF CONTINUOUS AND COMPOSITE SYSTEMS, Journal of Applied Mechanics, ASME, Vol. 34, No. 3, (September 1967).

55. Wilson, E. L.
Discussion, ANALYSIS OF FRAMES WITH NONLINEAR BEHAVIOR, Journal of the Engineering Mechanics Division, ASCE, 86, (EM6), (December 1960).

56. Ang, A. H. S.
ANALYSIS OF FRAMES WITH NONLINEAR BEHAVIOR, Journal of the Engineering Mechanics Division, ASCE, 86, (EM3), (June 1960).

57. Sheninger, E. and Lu, L. W.
EXPERIMENTS ON NON-SWAY STRUCTURAL SUBASSEMBLAGES, Journal of the Structural Division, ASCE, 96, (ST3), (March 1970).

58. Sidebottom, O. M. and Chang, C. T.
INFLUENCE OF THE BAUSCHINGER EFFECT ON INELASTIC BENDING OF BEAMS, Proceedings of First U.S. National Congress of Applied Mechanics, Vol. 1, 1952.

59. Younger, D. G.
THE CYCLIC STATE OF MATERIALS AND THE RELATIONSHIP TO MECHANICAL PROPERTIES AND FATIGUE, Tech. Dept. AFFDL-TR-66-125, Wright-Patterson Air Force Base, Dayton, Ohio, November 1966.

60. Carpenter, L. D. and Lu, L. W.
REVERSED AND REPEATED LOAD TESTS OF FULL-SCALE STEEL FRAMES, Fritz Engineering Laboratory Report No. 332.7, Lehigh University, April 1972.

13. VITA

The author was born in Passaic, New Jersey on December 24, 1941, and is the son of Byron and Phyllis Carpenter of Mentor, Ohio.

The author's primary and secondary education was in the Mentor school system. Prior collegiate education was at Ohio University where he graduated with a Bachelor of Science and Master of Science in Civil Engineering in June 1963 and August 1965, respectively. While attending Ohio University the author was employed as an undergraduate student assistant, graduate assistant, and acting instructor.

During the summer of 1963 the author was employed by the Army Corps of Engineers at Huntington, West Virginia as a Structural Engineer in the Masonry Design and Analysis Section.

While in residence at Lehigh University he was employed as a teaching assistant, research assistant and instructor in Civil Engineering.

Since November 1969 the author has been employed by Skidmore, Owings and Merrill in Chicago as Senior Structural Engineer.

The author has co-authored papers and given oral presentations concerning the research area of the dissertation. He has been an Associate Member of the American Society of Civil Engineers since 1963.

The author is married to the former Bobbie Ann Merriam of Mentor, Ohio and they have a son Lauren and two daughters Jenninfer and Shirley.